Materials Science

DOI: 10.1002/anie.201306129

Carbon Fibers: Precursor Systems, Processing, Structure, and Properties

*Erik Frank, Lisa M. Steudle, Denis Ingildeev, Johanna M. Spörl, and Michael R. Buchmeiser**

Keywords:
carbon fibers · cellulose · lignin · pitch · poly(acrylonitrile)

Dedicated to Professor Rolf Mülhaupt on the occasion of his 60th birthday

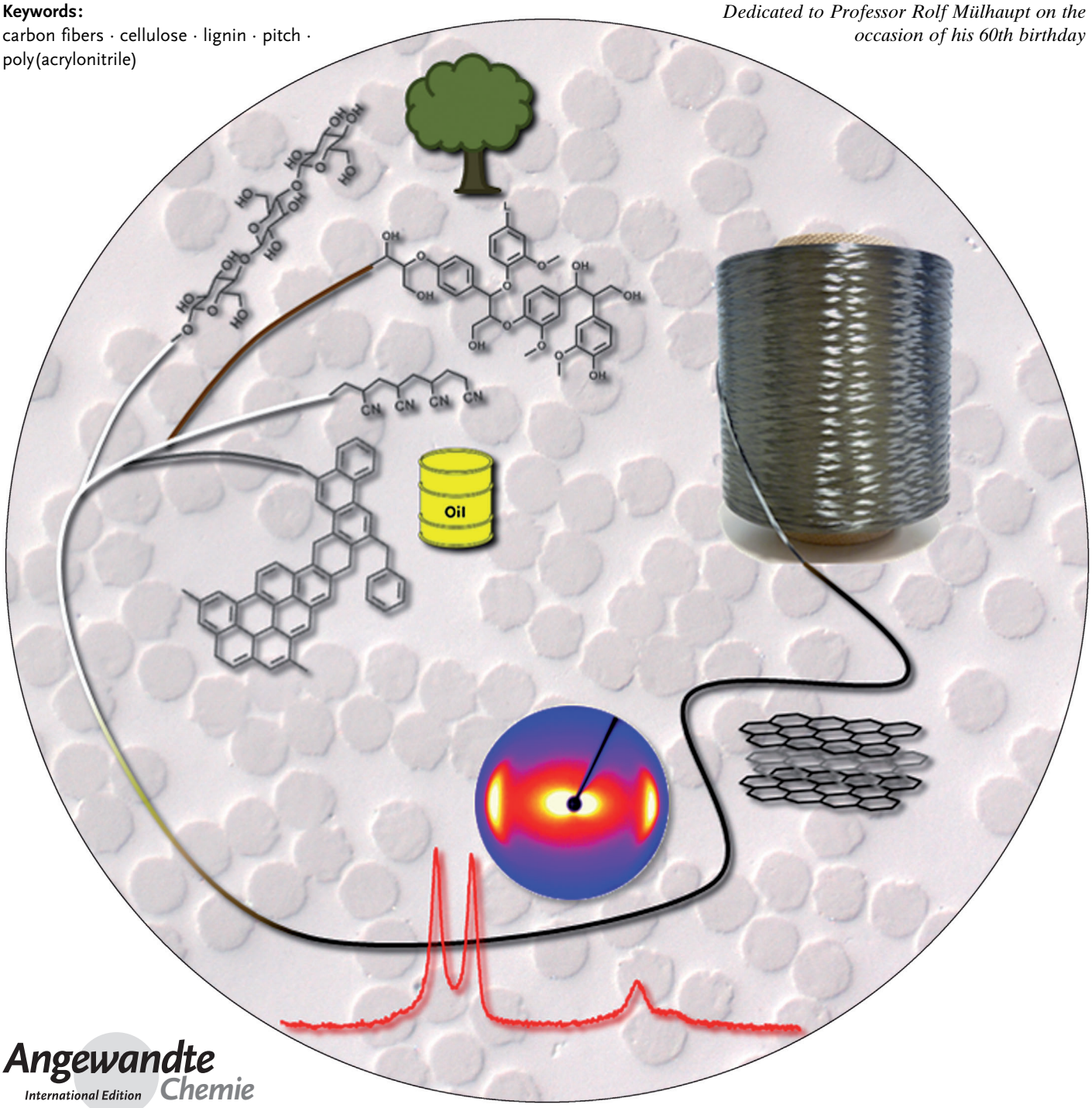

This Review gives an overview of precursor systems, their processing, and the final precursor-dependent structure of carbon fibers (CFs) including new developments in precursor systems for low-cost CFs. The following CF precursor systems are discussed: poly(acrylonitrile)-based copolymers, pitch, cellulose, lignin, poly(ethylene), and new synthetic polymeric precursors for high-end CFs. In addition, structure–property relationships and the different models for describing both the structure and morphology of CFs will be presented.

From the Contents

1. Introduction

1.1. Definitions and Market

The definition of CFs in the past was that of fibers made of at least 92 wt% of carbon and prepared from polymeric precursors.[1] However, this definition may have to be refined as in the last few years new fiber types with nearly 100% carbon have been generated, which were made only from carbon allotropes such as carbon nanotubes[2] or graphene.[3] Furthermore, carbon fibers can be made from carbon nanofibers (CNFs).[4] Thus, a new definition of CFs as fibers with a carbon content of at least 92 wt% made from a polymeric precursor or made from carbon allotrope building blocks might be more suitable.

CFs have high tensile strengths of up to 7 GPa with very good creep resistance, low densities ($\rho = 1.75$–$2.00\ g\,cm^{-3}$), and high moduli up to $E \leq 900$ GPa. They lack resistance to oxidizing agents such as hot air and flames, but they are resistant to all other chemical species. The good mechanical properties make CFs attractive for use in composites in the form of woven textiles as well as of continuous or chopped fibers. The composite parts can be produced through filament winding, tape winding, pultrusion, compression molding, vacuum bagging, liquid molding, and injection molding. The CF industry has been growing continuously, with a focus on aerospace, military, construction, as well as on medical and sporting goods.[5]

As a consequence of the increasing use of CFs for wind power and in the automotive sector, the demand for CFs in the coming five years is expected to at least double. To establish CFs in the mass market, the price of CFs has to be significantly reduced. In the medium term, alternative raw materials for CFs must be identified and implemented. Not only the automotive industry but also the construction industry, power industry, and mechanical engineering will require such novel, low-cost fibers when switching to new materials in price-sensitive products and renewable energies. Renewable raw materials such as biopolymers or polymers from biogenic sources are especially interesting sources for CFs. These polymers are available inexpensively from biogenic sources such as cellulose- and lignin-containing plants. Therefore, worldwide research projects for the investigation of biogenic CFs have been initiated.

2. Precursor Systems

2.1. Carbon Fibers Based on Poly(acrylonitrile) (PAN)[6]

2.1.1. Polymerization

Poly(acrylonitrile) (PAN) was first recognized as a suitable precursor material for CFs by Shindo in 1961.[7] It is currently the most important starting material for the preparation of CFs. The polymerization of acrylonitrile is of crucial importance, particularly since further steps in CF production such as spinning, stabilization, and carbonization of the precursor fiber, as well as the resulting CF properties strongly depend on the characteristics of the precursor polymer used.[1] Acrylonitrile (AN) can be polymerized in the bulk, in suspension, in solution, and in emulsion by applying free-radical, ionic, or atom-transfer radical polymerization.[1,8] Solution polymerization and suspension polymerization are currently the most widely used procedures for the preparation of PAN-based copolymers for the production of CFs (Scheme 1). However, for continuous processing, the solution

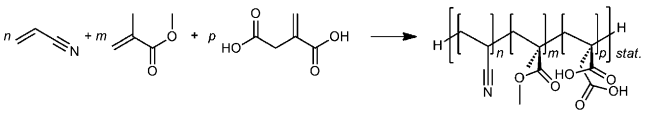

Scheme 1. Synthesis of a typical terpolymer consisting of acrylonitrile, methyl methacrylate, and itaconic acid (AN/MMA/IA).

polymerization of AN and related monomers is probably more satisfactory.[1,8e,o–ac] Solution polymerization can be carried out with solvents such as dimethylacetamide (DMAc), dimethylformamide (DMF), dimethylsulfoxide

[*] Dr. E. Frank, Dr. D. Ingildeev, Prof. M. R. Buchmeiser
Institut für Textilchemie und Chemiefasern (ITCF Denkendorf)
Körschtalstrasse 26, 73770 Denkendorf (Germany)
E-mail: michael.buchmeiser@itcf-denkendorf.de
Dipl.-Chem. L. M. Steudle, Dipl.-Chem. J. M. Spörl,
Prof. M. R. Buchmeiser
Lehrstuhl für Makromolekulare Stoffe und Faserchemie
Institut für Polymerchemie, Universität Stuttgart
Pfaffenwaldring 55, 70550 Stuttgart (Germany)

(DMSO), and aqueous sodium thiocyanate solutions, and thus allows the immediate manufacture of spinning dopes.[1,8a,9] Since the copolymers have a high molecular weight, the polymerization reaction is usually carried out in solution at rather low concentration. Two important drawbacks limit the application of this polymerization procedure. The conversion of the monomer into polymer reaches 50–70%, so the resulting solutions may be processed only after complete recovery of the remaining acrylonitrile from the spinning dope. Usually, the spinning dope still contains 0.2–0.3 wt% of this toxic and carcinogenic monomer.[8a] Another important drawback is that conventional solvent systems used for the polymerization process are usually characterized by high transfer constants. In contrast, the suspension polymerization of acrylonitrile has the advantage that almost no by-products are produced and that it can be carried out under controlled conditions, so that both branching and cross-linking are avoided.[8a–n] Further advantages of this setup are the simple removal of the polymer by filtration and drying, adjustment of the molecular weights over a very wide range, and control of the particle size. Particularly on a large scale, this discontinuous process permits good control over the exothermic nature of the polymerization, thus allowing a polymer yield of up to 90%.

Persulfate salts, especially potassium persulfate, ammonium persulfate, sodium metabisulfite, and iron(III) salts belong to the most important initiators used for polymerization. Today, special attention focuses on reducing the defects in the CFs generated by the residues of the initiator system. Efforts involve, but are not limited to, the application of modified initiator systems that replace conventional alkali metals and thereby reduce the amount of transition metals

Michael R. Buchmeiser completed his PhD in 1993 at the University of Innsbruck/Austria and then spent a year at MIT/USA with Prof. R. R. Schrock. In 1998 he completed his habilitation at the University of Innsbruck. 2004–2009 he was Associate Professor for Chemical Technology of Polymers at the University of Leipzig/Germany, and 2005–2009 Vice-Director of the Leibniz Institute of Surface Modification. Since 2009 he has held a Chair at the University of Stuttgart/Germany and been Director of the ITFC Denkendorf. He has received the Prof. Ernst Brandl Prize, START Prize, Novartis Research Prize, and Otto Roelen Medal.

Erik Frank received his PhD in Chemical Technology working on heterogeneous catalysis in 2002 from the University of Karlsruhe (TH), which was renamed KIT (Karlsruhe Institute of Technology) by merging with the Forschungszentrum Karlsruhe in 2009. Since 2003 he has been a senior scientist at the Institute of Textile Chemistry and Chemical Fibers (ITCF) Denkendorf, focusing on carbon fibers and conducting polymers. Currently, lignin- and polyethylene-based carbon fibers are developed under his leadership at the new high-performance fiber research center of the ITCF.

Denis Ingildeev studied Chemistry at the University of Stuttgart and completed his PhD on the manufacturing and characterization of cellulosic fibers and cellulose/polymer blends in the group of Prof. Franz Effenberger. In 2010 he became a senior scientist at the Institute of Textile Chemistry and Chemical Fibers (ITCF) Denkendorf, focusing on the synthesis and processing of poly(acrylonitrile)-based precursors for the manufacture of carbon fibers obtained by wet spinning as well as developing sustainable processing technologies for natural polymers such as cellulose, cellulose derivatives, and chitin.

Johanna M. Spörl is a PhD student in the group of Prof. Michael R. Buchmeiser at the University of Stuttgart. She received her diploma in chemistry in 2011 from the same institution. In her diploma thesis, supervised by Prof. Michael R. Buchmeiser, she focused on the controlled radical polymerization of acrylonitrile. The topic of her PhD is the development of carbon fibers from renewable resources (especially cellulose), and covers the entire process chain from polymer synthesis and characterization to fiber formation by wet spinning to, finally, the formation of carbon fibers.

Lisa M. Steudle received her diploma in Chemistry at the University of Stuttgart in 2010. She carried out her diploma thesis at the Inorganic Department of the University of Stuttgart in the group of Prof. Wolfgang Kaim. She is currently carrying out PhD research under the guidance of Prof. Michael R. Buchmeiser, focusing on the development of new precursors for lignin-based carbon fibers. Her research fields are polymer synthesis and analysis, as well as the manufacturing and characterization of fibers, particularly of carbon fibers.

such as iron so that impurities at all steps of the CF production chain can be avoided.[10]

Typically, PAN-based copolymers used for the preparation of CFs have molecular weights in the range 70000–260000 $g\,mol^{-1}$ and a polydispersity index (PDI) of 1.5–3.5.[1,11] The mechanical properties of CFs obtained using textile PAN with a specific co-monomer content of more than 5 mol% are very limited by the non-optimized chemistry, cyclization behavior, and purity. Usually, PAN-based precursors contain a minimum of 95 mol% AN and a maximum of 5 mol% co-monomers.[5a,10] These co-monomers have a large impact on polymer processing as well as on the kinetics and physics of the stabilization and carbonization; consequently, polymer composition moved to the center of interest.[1,5a,12] Commercial PAN-based precursor materials are commonly produced by using polymerization mixtures of AN with more than one co-monomer, for example, with methyl acrylate and itaconic acid. For these purposes, the monomers should all have similar reactivity, that is, copolymerization parameters. Only in that case will the composition of the terpolymer be comparable to the one of the reaction mixture and the co-monomers will be homogeneously distributed along the chain.[1] Although the open literature provides a good base for the selection of the monomers and the composition of the precursor polymer,[12,13] the identification of the optimum composition of the precursor polymer (and of the processing parameters) for the achievement of certain properties is still a challenging task.[14] In other words, to obtain high-performance fibers in terms of tensile strength and modulus, all process parameters including copolymer composition, molecular weights, molecular-weight distribution, as well as spinning, drawing, stabilization, and carbonization parameters must be taken into account. Unfortunately, a stringent and widely applicable model that allows the fiber properties to be correlated with process and polymer parameters is still missing. In fact, despite the tremendous progress in the field of CF research, even the correlation between CF structure and CF properties is not fully developed. In addition, an idea of how the polymer structure, orientation, and crystallinity are transformed into the final carbonaceous structure needs to be developed.

2.1.2. *Processing*

PAN-based polymers undergo a thermally induced cyclization reaction below their melting points and can, therefore, not be processed in the melt with conventional spinning techniques. Consequently, melt spinning of pure PAN is impossible unless large amounts of solvent and plasticizers are added. In such a melt-assisted spinning process, additives are used to reduce the interaction between the nitrile groups of the polymer chains. This way, the melting point of the plasticized PAN is reduced to an appropriate range for melt spinning.[15] However, to date, the CF qualities that can be accessed from wet-spun precursor fibers have not yet been reached with melt-spun PAN-based precursor fibers. This is why wet spinning is still the preferred method for the manufacture of CF precursors.

The choice of the solvents for PAN-based copolymers is significantly important in the production of precursor fibers by wet-spinning processes. As already mentioned, the highly polar nitrile groups of PAN experience strong dipole–dipole interactions, thus making the polymer soluble only in highly polar solvents such as DMAc, DMF, DMSO, and solutions of $ZnCl_2$ or NaSCN,[1,9] as well as in ionic liquids.[16] Schildknecht listed a variety of solvent systems in which PAN is soluble.[8z]

The conventional wet-spinning technique entails extrusion of the copolymer solution into a precipitation bath, where jets of the spinning dope leaving the spinneret come into contact with substances miscible with the solvent but which do not dissolve the polymer. In wet spinning, the solution concentration of 15–25 wt% ($10 \leq |\eta_0^*| \leq 200\ Pa\,s^{-1}$) strongly depends on the polymer properties such as co-monomer content, molecular weight, and PDI, and is adjusted to obtain a viscoelastic behavior of the polymer solution that is optimal for spinning at pressures of 5–20 bar. The polymer solutions are spun through a spinneret with multiple holes, a total of 100–500000, each having a diameter in the range 40–100 μm. The line speeds at the coagulation step of the wet spinning are rarely higher than 20 $m\,min^{-1}$.[1]

There are many possible technical designs of wet-spinning processes (Figure 1). The precipitation bath can be situated horizontally or vertically, different baths for washing and

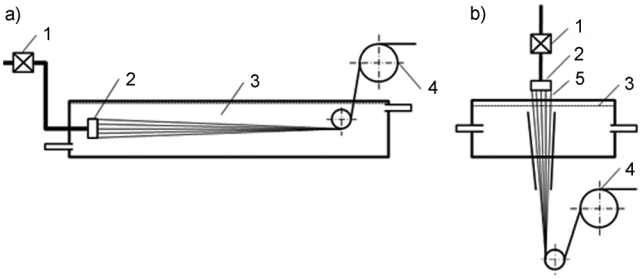

Figure 1. a) Wet and b) dry jet spinning techniques. 1: metering pump, 2: spinneret, 3: precipitation bath, 4: take-up godet, 5: air gap.

drawing can be applied, followed by further manufacturing operations such as the application of lubricants, drying, or heat-setting. The most important issue is to obtain fibers with the optimum morphological structure, which is very sensitive to the composition and conditions within the coagulation bath. Thus, the coagulation bath is not stationary but circulates with a finite velocity. The flow pattern in the bath is rather complex: the stream lines are usually not parallel to the axis of the spinning line, which creates unequal flow and solidification conditions for the individual filaments. Modern systems used for wet spinning often involve directed flow of the spinning bath. The aim of this modification is to make the flow pattern in the bath symmetrical and to equalize the conditions experienced by the individual filaments, so as to promote homogeneous penetration of the nonsolvent into the bundle of filaments.

The other fundamental method of wet spinning, dry jet or air gap spinning, can be applied to highly viscous spinning

dopes with polymer contents of up to 30 wt% and corresponding zero-shear viscosities in the range between 300 and 20000 Pa s.[17] This procedure entails the extrusion of spinning dopes into an air gap of 10–200 mm, where the filaments undergo jet stretch, which produces a high degree of molecular orientation, before entering a liquid coagulation bath. Further processing stages correspond to those of the conventional wet-spinning technique. This allows the spinning dope and coagulation bath to be at different temperatures and, therefore, high diffusion rates can be avoided during the phase-inversion process in the coagulation bath. The process is limited by the number of holes in the spinneret and usually cannot be used for fiber tows with more than 12000 individual filaments.

Solidification and coagulation of a polymer during fiber formation is specific for the chosen spinning procedure. In jet spinning it is due to dry stretching of the filaments in an air gap, accompanied by heat transfer, followed by solvent extraction in a precipitation bath; in wet spinning the solvent is directly extracted from the polymer solution into the coagulation bath, and diffusion-controlled phase transitions play a determining role.

The present state of theory of wet spinning does not enable the formulation of fundamental equations describing the process in quantitative terms. There is still some uncertainty about the deformation of a non-uniform system provided by the partially solidified fiber tow, and the mechanism of mass transfer is affected by temperature and the concentration fields in both the spinning dope and the coagulation bath. Phase equilibria and the kinetics of phase separation are ambiguous, although undoubtedly play a decisive role in the formation of fiber structure and physical properties. The chemical structure of the polymer, solvent, and nonsolvent affect both the phase diagram and the transport rates. Additionally, the dynamics of the coagulation process are influenced by external tension, surface tension, mass exchange, and rheological effects. The only phase equilibrium data available are the so-called "coagulation values", that is, volumes of nonsolvent required for turbidimetric titration of a standard, dilute polymer solution.[18] These data are specific for different co-monomer systems, and thus information about phase equilibria at the higher polymer contents involved in fiber spinning is still lacking.

Very important, controllable factors in wet spinning are the temperature and the concentration gradients in the spinning bath and dope, which influence to a large extent the kinetics of mass transfer. Generally, an increase in the solvent content and a decrease in the temperature of the bath reduces the driving force for diffusion and, consequently, the fluxes of solvent out of the filaments and nonsolvent directed inwards. Furthermore, the cross-sectional shape of the filaments relate to the diffusion rate of the liquids of the coagulation bath into the filaments and the transfer of the polymer solvent to the coagulation bath.[1,9,19]

High coagulation rates in the spinning bath are usually accompanied by the formation of a rigid "skin" on the surface of the filaments. The skin is separated by a distinct boundary from the fluid "core", and the resulting radial gradients of viscosity, modulus, etc., are extremely high. Furthermore, diffusion-controlled solidification of the filaments instead involves the growth of the skin layer at the expense of the core rather than a continuous change in the physical characteristics at all points of the cross-section. The undesirable rigid skin of the precursor fiber leads to the collapse of the cross-section and, therefore, to kidney-shaped fiber cross-sections (Figure 2).[1,9,11,20] The deviation from circularity associated

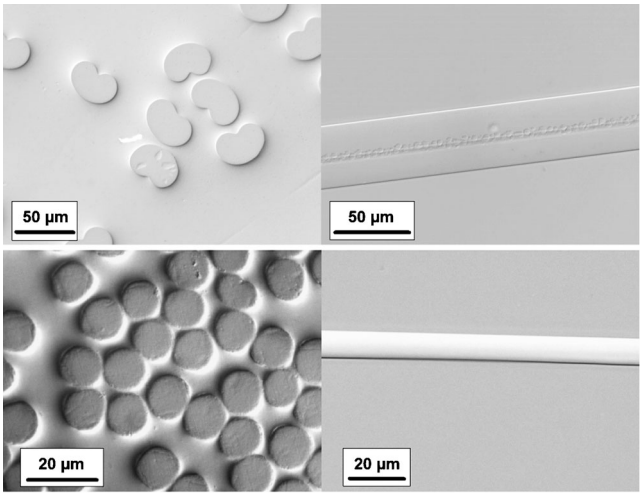

Figure 2. Effect of spinning conditions on the morphology of wet-spun undrawn acrylic fibers: Top: Effect of high coagulation rate on the cross-section and fiber structure; bottom: effect of low coagulation rate on the cross-section and fiber structure.

with solidification conditions affect the luster, sorption ability, the mechanical and physical properties, as well as the subsequent oxidation and carbonization steps. The formation of dense precursor fibers with preferred circular cross-sections is accomplished with low diffusion rates by using highly concentrated spinning dopes at elevated temperatures, high solvent contents in the spinning bath,[21] and low temperatures of the spinning bath.[21a,c,22] As noted above, noncircular cross-sections can usually be attributed to high diffusion rates outwards from the thread. The diffusion of the solvent is dependent on the rigidity of the solid layer as well as the osmotic pressure. Additionally, rapidly acting coagulation baths promote the formation of voids and capillaries with dimensions up to several micrometers, thereby leading to poor mechanical properties of the resultant CFs.

Further important structural characteristics of the resultant precursor fibers depend on the supramolecular structure formed, namely, degree of crystallinity, crystallite orientation, crystallite size etc., after the coagulation bath. These characteristics are very sensitive to the spinning conditions, and strongly affect the behavior in terms of drawing and further processing operations as well as the mechanical properties of both the precursor and the final CFs.

Once the fiber has been spun, the subsequent processing steps are basically similar, irrespective of the initial spinning technique, although handling procedures depend very much on the polymer composition. Further processing steps of wet

spinning entail washing, drawing, application of a finish, drying, relaxation processes and, finally, collection. To remove excess solvent from the fibers and to increase the molecular orientation of the molecular chains, the coagulated fiber bundle is washed with hot water and/or water steam in conjunction with fiber drawing. Fibers can be drawn at elevated temperatures, typically at 120–180 °C, for example, by using ethylene glycol or glycerol as a drawing medium.[11,13g,23] A further increase in the tensile properties is observed as the orientation increases during the high-temperature drawing process. Before drying, a finish is usually applied as an aqueous emulsion to act as a lubricant and antistatic. Typical finishes include sorbitan esters of long-chain fatty acids, poly(oxyethylene) derivatives, and modified poly(siloxane)s.[24] Drying and relaxation processes are necessary to remove water and to reduce the tension in the supramolecular structure of the precursor fiber after drawing. The resultant wet-spun precursor fiber tows have a relatively low fiber count of approximately 1.2 dtex. Large tows, above 40 000 individual filaments, are plaited into cardboard packages by using a controlled longitudinal placement, which permits the easy unloading of the tow for further processing. Lower filament counts, such as 3000 and 12 000 filaments, can be wound directly on a spool by using precision winders.

2.1.3. Heat Treatment of Carbon Fiber Precursors

Generally, the heat treatment of PAN-based precursor fibers entails three steps, that is, oxidation, carbonization, and graphitization (Scheme 2). The precursor fiber is first oxidized at a temperature between 200 and 300 °C, which results in the formation of N-containing ladder-type polymers. This allows further processing at higher temperatures. After oxidation, the fibers are carbonized at temperatures up to 1200–1600 °C in an inert atmosphere to obtain a turbostratic carbon structure. Then, to improve the ordering and orientation of the basal planes in the direction of the fiber axis, the fiber can be graphitized at up to 3000 °C, depending upon the required tensile modulus of the resultant CF. The entire procedure will be outlined in more detail below.

2.1.4. Oxidation of PAN-Based Precursors

PAN-based precursor fibers are treated in an oxidizing atmosphere at temperatures between 200 and 300 °C. Generally, the oxidation reactions of the homopolymer PAN that occur during this thermal treatment are very difficult to control. The rapid evolution of heat, as a result of the highly exothermic kinetics of the oxidation step, can cause defects inside the fiber and on the surface of the filaments, particularly in larger fiber tows. However, the exothermic reaction can be influenced by the specific composition of a co-monomer whose presence has a significant effect on the oxidation process.[12] The functional groups present in the copolymer can cause side reactions, which depend on the nature of the co-monomers, the co-monomer content, the co-monomer distribution, the supramolecular structure of the precursor fiber, the by-products, and on any traces of chemical compounds, which may have been introduced

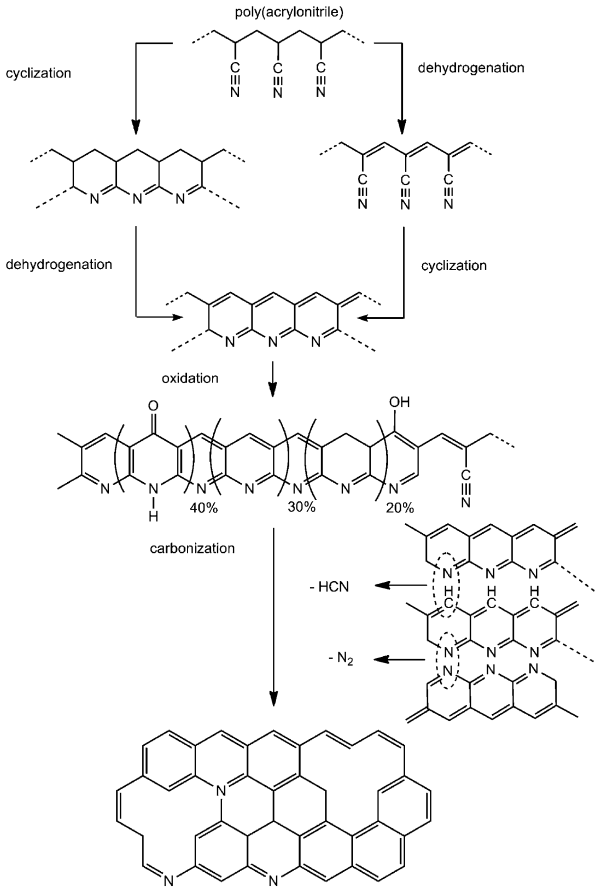

Scheme 2. Model reaction paths from PAN to a carbon phase.[10,25]

during both polymerization and spinning, as well as on the heat treatment.

The oxidation of the precursor fibers is accomplished by passing them through an oven, which has a series of different air-heated zones that gradually increase in temperature. A significant increase in line speed can be realized by providing additional heating zones. Strict control of the exothermic reaction in the oven is achieved by maintaining a uniform temperature distribution within the oven and the single filaments, thereby avoiding any overheating. The optimum air flow heats the fiber, provides oxygen for the reaction, and removes exhaust components and excess reaction heat from the fibers. Furthermore, the procedure is carried out under tension or even by applying drawing to prevent shrinkage of the filaments.[1,5a] During the oxidation stage, the PAN-based fiber increases in density from 1.18 to 1.36–1.38 $g\,cm^{-3}$, and the oxidized fibers then contain 62–70 wt% carbon, 20–24 wt% nitrogen, 5–10 wt% oxygen, and 2–4 wt% hydrogen.[8e]

During the oxidation process, the polymer chains are converted into a heteroaromatic structure, similar in some aspects to the later carbon phase. Different models have been proposed for the cyclization of PAN, and the mechanism of formation of the ladder structure is a very complex cascade of chemical reactions, which has been investigated intensively in the last few decades.[23a,26] However, the different reactions depend heavily on the nature of the copolymers.[27] These

copolymers participate in the initial cyclization reaction and considerably influence the rate of the cyclization process. Thus, the onset temperature in the presence of carboxylic acids is significantly lowered compared to that of a PAN homopolymer (Figure 3).

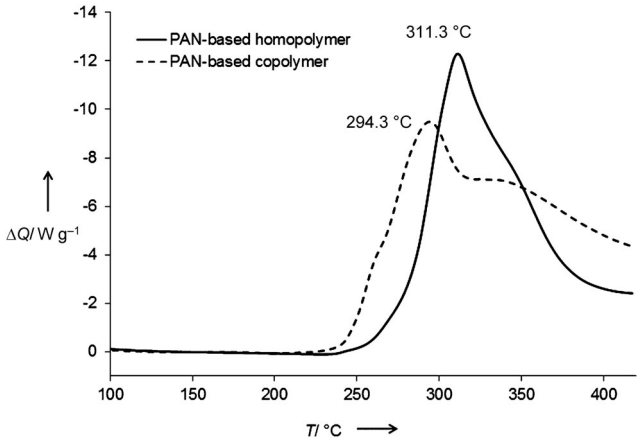

Figure 3. DSC of PAN-based homo- and terpolymers (AN/MMA/IA) in air at a heating rate of 10 K min^{-1}.

The difference in the oxidation behavior of PAN-based homo- and copolymers is that the cyclization reaction of the copolymer is initiated by stabilization accelerators formed by the degradation of the copolymer compound, while the cyclization of the homopolymer is initiated by radicals. Both reactions occur at elevated temperatures and result in a thermally stable cyclized structure. The chemical composition of the resultant ladder polymer, however, strongly depends upon the atmosphere in which the heat treatment is carried out. The rate of cyclization in an oxidizing atmosphere is higher and the final CF is produced in higher yields with improved mechanical properties compared to in an inert atmosphere. Co-monomers such as methyl acrylate facilitate the subsequent drawing of the fiber during the oxidation treatment. Heat treatment of PAN-based precursors under tension in an oxidizing atmosphere at temperatures over 200 °C causes initiation of several thermally activated processes, which result in considerable reorganization of the polymer chains and cross-linking of the molecular chains by oxygen.[28] Thus, the oriented supramolecular structure is preserved for the following processing steps, even after release of the tension. The optimum uptake of oxygen during the oxidation treatment is in the range of 8 to 10 %.[29]

Alternative stabilization methods such as plasma treatment,[30] electron-beam-assisted cyclization,[31] and microwave-assisted processing[32] are under investigation to reduce both the stabilization times and energy consumption.

2.1.5. *Carbonization and Graphitization of PAN-Based Precursors*

In the next step of the process, the stabilized precursor fiber tows, which are capable of withstanding the high temperatures, are subjected to thermal pyrolysis in an inert atmosphere and are thereby converted into CFs. The volatile compounds are removed to give CFs with a carbon yield of about 50 wt % with respect to the original precursor. These CFs contain > 98 wt % carbon, 1–2 wt % nitrogen, and 0.5 wt % hydrogen.[8e] During the early stages of the carbonization process, the rate of heating is generally low so that the formation of gaseous decomposition compounds does not damage the fiber. Between 400 and 500 °C, the hydroxy groups present in the oxidized PAN fibers undergo cross-linking condensation reactions, thereby resulting in reorganization and coalescence of the cyclized sections. Goodhew et al. have found that the cyclized structures undergo dehydrogenation reaction and produce a graphite-like structure bound by nitrogen atoms.[26f] Intermolecular dehydrogenation occurs between 400 °C and 600 °C, followed by denitrogenation and formation of plain graphite layers at higher temperatures. The effect of nitrogen on the structure and properties of PAN-based fibers has been shown by Tsai.[33] High heating rates during carbonization introduce defects in the CFs, while low carbonization rates result in the loss of large amounts of nitrogen at early stages of the carbonization process, which is in fact preferred to obtain CFs with high tensile strength. Most of the volatile products are evolved in the temperature range 200–1000 °C.[34] The evolved gases include HCN, H_2O, O_2, H_2, CO, NH_3, CH_4, higher molecular weight compounds, miscellaneous tars, and finish.[1,26k,l,n,35] As already mentioned, the ribbon polymer structure forms cross-links in the low temperature range, and subsequently additional condensation reactions ensue up to 1600 °C, thereby forming a turbostratic carbon phase.[10,26a,36] This phase is highly oriented in the fiber direction, but still contains many tetrahedral carbon-based cross-links between the graphite-type carbon layers. This particular structure is responsible for the typically high tensile strength of CFs. Although the chemistry of the oxidative stabilization, which results in the formation of acridone, naphthyridine, hydronaphthyridine, and other substructures as intermediates,[37] has been elucidated to some extent by XPS and FTIR studies[38] with the aid of model compounds,[39] the processes that lead to the cross-linking of the intermediate ribbon structures and the concomitant formation of a 3D structure during the removal of nitrogen are still mostly obscure.

The final step in the heat treatment of CFs at temperatures of up to 3000 °C is called graphitization. At these temperatures, the ordering and orientation of the small turbostratic crystallites in the direction of the fiber axis takes place. This results in a higher Young's modulus, but simultaneously leads to lower tensile strengths of the final CFs. The high-modulus furnace uses a graphite muffle that operates in a carefully controlled inert atmosphere, since even a low-volume air flow over the hot graphite element is sufficient to continually remove a molecular layer of graphite and cause severe erosion, which leads to premature failure.[1]

To improve the adhesion of CFs to matrix polymers, the final step of CF production involves both oxidative surface treatment and sizing, by applying, for example, solvent-based systems or emulsions, preferably with the same chemical

composition as the ultimate matrix resin. The oxidative surface treatment involves the application of electrochemical or electrolytic bathes. During this procedure, the surface of the CFs is etched and roughened, thereby increasing the surface area available for interfacial fiber/matrix interaction and generating reactive chemical groups on the fiber surface. The application of 0.1 to 5 wt% thermoplastic resins, thermosetting plastics, and water-based coatings with respect to the fiber weight improves the processability of the CF to fabrics and preimpregnated fibers (prepregs) by increasing the interfacial shear strength between the fiber and matrix resin.

Finally, small CF tows are collected using online winders and larger tows can be collected in tubes or plated into cardboards boxes. The resultant CFs have a relatively low fiber count of approximately 0.8 dtex, a density of 1.8 $g\,cm^{-3}$, and are available with low modulus, standard modulus, intermediate modulus, high modulus, and ultrahigh modulus according to the required mechanical properties.

2.2. Pitch-Based Carbon Fibers

Pitch is the name for tarry substances that are almost solid, that is, highly viscous at room temperature, and have a very high carbon content. It can be derived from natural resources (petroleum fraction, coal hydration, asphalt) or from synthetic materials (pyrolysis of polyaromatic compounds and polymers).

Pitch is a low-molecular-weight, inhomogeneous substance (a typical pitch precursor molecule is shown in Figure 4) with molecular weights around 1000 $g\,mol^{-1}$. Pitch is composed of hundreds of different species, mostly polyaromatic, with some methyl side groups. Generally, an increase in aromaticity increases the quality of the resulting CFs.[40]

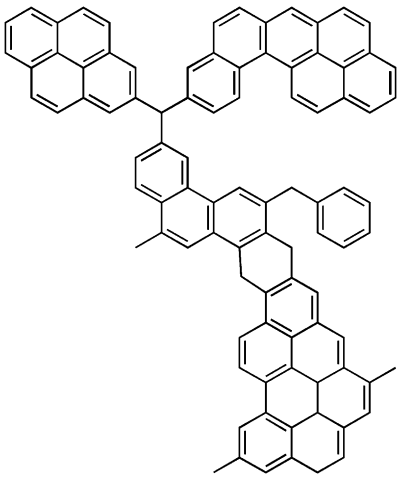

Figure 4. Typical pitch precusor in mesophase pitch.

A series of chemical and physical treatment steps typically have to be applied to obtain CFs from pitch (Figure 5).

In a first step, the raw material will be pretreated to achieve cleaner and higher molecular weight phases, which will be processable by melt spinning. For high-performance CFs with tensile strengths greater than 2 GPa and high to very high Young's moduli greater than 350 GPa, the anisotropic pitch route outlined in Figure 5 is preferred and will be discussed below. Generally speaking, the processing of monophasic pitches is a complex problem. Only the investigation of all processing steps results in high quality, modern pitch-based CFs.

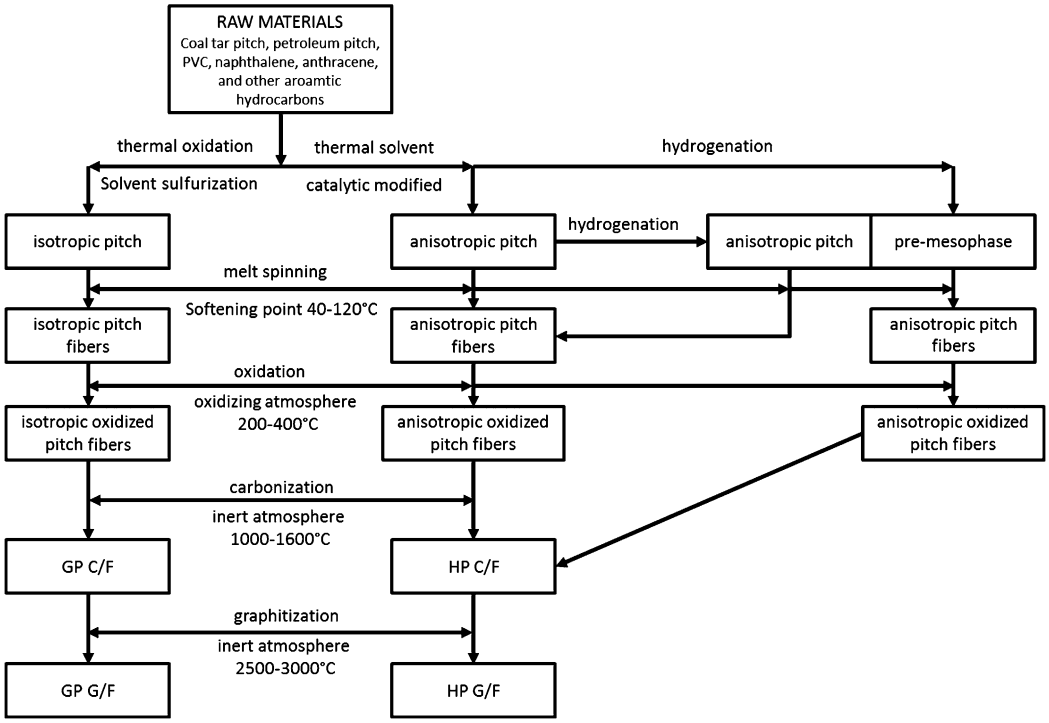

Figure 5. Processing steps for CFs starting from pitch as the precursor material. Redrawn from Ref. [41].

2.2.1. *Preparation of Anisotropic Pitches*

Anisotropic pitch, also called mesophase pitch, has to fulfill some requirements:[42]

- Cleanness: The material has to be free of particles and the ash content must be well below 1000 ppm.
- Orientation: The material must be orientable during the course of the spinning process.
- The pitch must display high reactivity on stabilization to prevent the filaments from fusing.
- The temperature for stabilization under oxidizing conditions must be below the melting point.
- High carbon yields must be achievable.

Typical procedures for the preparation of mesophase pitch are summarized in Figure 6:

Over the years, the following methods have been investigated for the preparation of mesophase pitch:

- Pyrolysis of pitch.
- Solvent extraction.
- Catalytic modification.

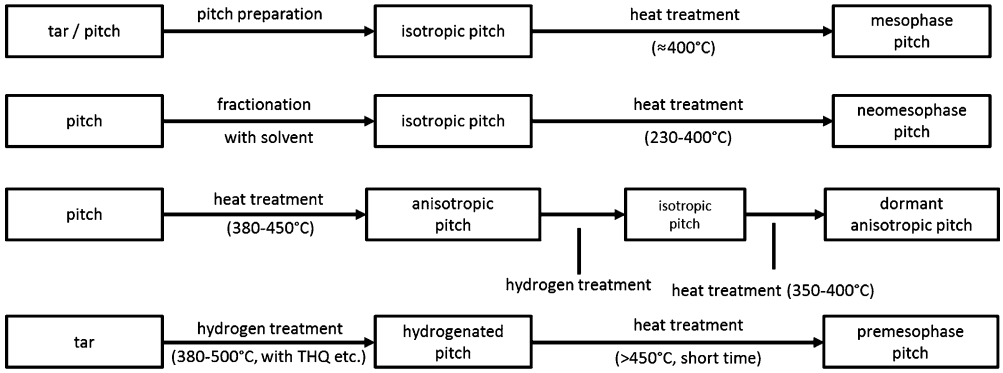

Figure 6. Typical procedures for the preparation of mesophase pitches. Redrawn from Ref. [43].

The last method (catalytic modification) is preferred in the pretreatment of pitch for the best control of the processing parameters and the quality of the pitch.

2.2.2. *Melt Spinning of Pitch*

Melt spinning of pitch is very difficult because of the rheological properties of molten pitch and the subtle processing conditions required. Figure 7 shows the extreme sensitivity of the texture of the precursor fibers of mesophase pitch to changes in the spinning temperature. Very small changes in temperature at the spinning nozzle can significantly change the entire texture of the pitch-based precursor fibers.

Clearly, the design of a melt-spinning plant for pitch-based precursor fibers is a complex task that requires a careful adjustment of the spinning head. A simplified melt-spinning device for mesophase precursor fibers is shown in Figure 8. As can be seen, pre-processed raw material is molten and densified in an extruder screw. At the end of the screw, the

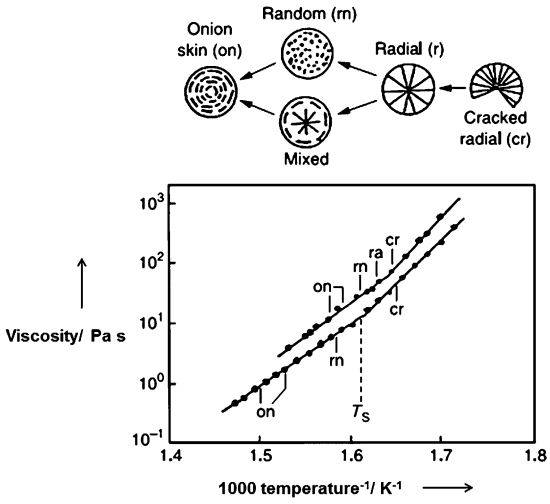

Figure 7. Variation of the mesophase texture with varying melt spinning temperature for two different types of pitch.[44] Reproduced with permission from the American Chemical Society.

pressure is increased to reach the level that is necessary to extrude the melt out of the nozzle holes. The molten pitch cools down under air and the resulting fibers are wound onto spools. The technical difficulty is to adjust the spinning temperature to meet the requirements for the viscosity of such low-molecular-weight systems. The spun fibers have a very limited tensile strength of around

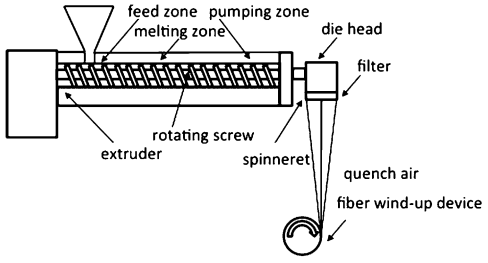

Figure 8. Simplified process for melt spinning a mesophase pitch-based precusor fiber. Redrawn from Ref. [45].

0.04 GPa (Table 1) and are difficult to handle in the following oxidation and carbonization processes.

Since any ordered structure of the pitch molecules orthogonal to the fiber direction in pitch-based CFs induce cracks (fiber type (cr) in Figure 7) and lower the strength of the pitch-based CFs, a laminar flow at the spinneret has to be avoided. Investigations with altered spinneret shapes[47] and different stirrer designs (Figure 9) resulted in a turbulent

Table 1: Comparison of the mechanical data from as-spun mesophase fibers and carbonized mesophase fibers.[46]

Processing stage	Tensile strength [GPa]	Tensile modulus [GPa]	Elongation [%]
as-spun	0.04	4.7	0.85
carbonized	2.06	216	0.95

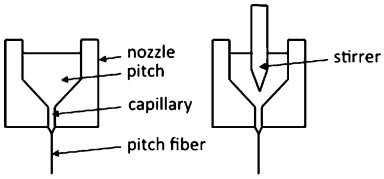

Figure 9. Melt spinning without (a) and with stirring (b). The use of shaped stirrers in the melt-spinning nozzles results in different microstructures. Redrawn from Ref. [48].

instead of a laminar flow being achieved in the melt-spinning process.

Ready-spun mesophase pitch precursor fibers have a microstructure consisting of well-oriented polyaromatic molecules in microdomains. These microstructures can be described as discotic nematic liquid crystals (Figure 10).

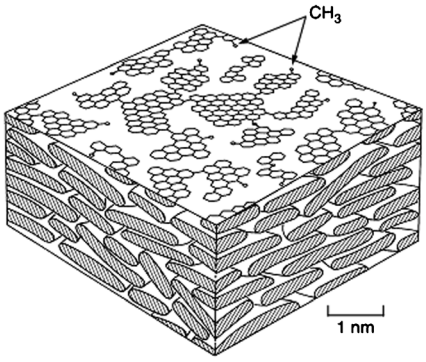

Figure 10. Model of the mesophase of pitch, showing a discotic nematic liquid crystal. Reproduced with permission from Elsevier.[49]

2.2.3. *Carbonization of Pitch-Based Carbon Fibers*

The conversion of mesophase pitch precursor fibers into CFs is accomplished by a stabilization step in an oxidizing atmosphere followed by a carbonization/graphitization step. To achieve acceptable tensile strengths and high Young's moduli, the temperature during the final heat treatment is typically between 2000 and 3000 °C. For such temperatures, furnaces have to be designed to eliminate turbulent flow of the protecting argon gas to avoid sublimation of the graphite materials in the furnace, which becomes a serious problem at temperatures above 2400 °C (Figure 11).

The fundamental carbonization reaction of pitch is shown in Figure 12. At temperatures over 350 °C, a condensation reaction based on the elimination of hydrogen establishes additional covalent bonds. Above 1500 °C, the structure

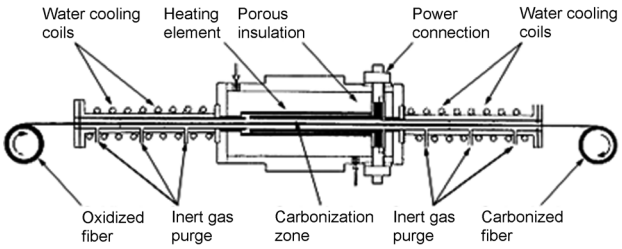

Figure 11. A hairpin element furnace for the carbonization of mesophase pitch fibers.[50] Reproduced with permission from William Andrew Publishing.

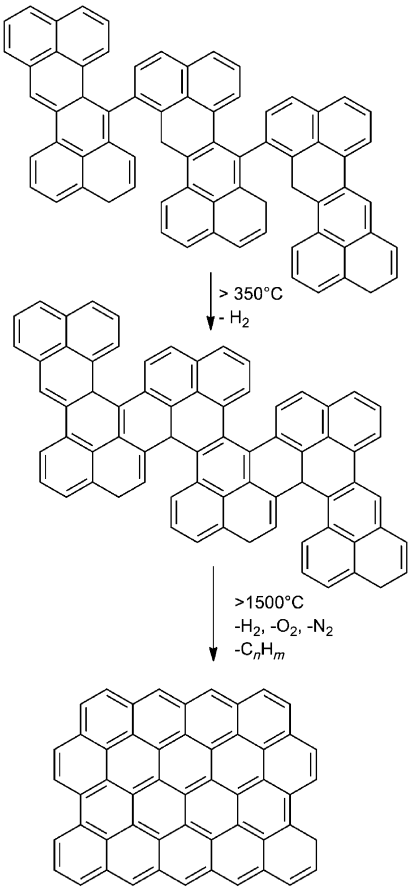

Figure 12. Fundamental reaction path for the carbonization of a polyaromatic mesophase pitch precursor. Redrawn from Ref. [1].

eliminates further hydrogen, and in the case of pitch from natural resources also nitrogen and oxygen. Some carbon is lost in the form of alk(en)yl fragments; nonetheless, the carbon yield of the polyaromatic pitch system is very high, typically between 80 and 85 %.[51]

2.3. *Cellulose-Based Carbon Fibers*

2.3.1. *Introduction*

The first CFs from a cellulose precursor were produced from vegetable fibers such as a simple cotton thread and served as the filament of electric lamps. This invention was

patented by Thomas Edison in 1880.[52] In 1959, Ford and Mitchell[53] (Union Carbide) developed a process for CFs and cloth made from rayon. Shortly after, in 1965, the first high-modulus CFs based on rayon became commercially available as the Thornel range from Union Carbide. Their production was based on a hot stretching process.[54]

Numerous books and reviews deal with the production of CFs from cellulose. Research activities on cellulosic precursors were substantial in the 1950s–1970s, but difficulties such as low yields and high production costs as well as the more promising results with PAN-based precursors were the most important drawbacks for this technology, which ultimately resulted in research in that area ceasing.[1,55] Nowadays, interest in producing CFs from renewable resources such as cellulose has arisen again. In an attempt to achieve a turnaround for energy systems and resources, the dependence on oil for state-of-the-art-precursors becomes increasingly undesirable. Another motivation is to overcome the high costs and low availability of PAN-based CFs and to effectively enter new markets such as the automotive industry as well as any other area concerned with the construction of lightweight materials.

2.3.2. *Possible Precursor Materials*

Natural cellulose fibers cannot be used as precursors for high-performance CFs because of their discontinuous character.[55c] Moreover, they have a low degree of orientation, a porous structure, and usually contain impurities such as lignin and hemicelluloses. However, possible precursor materials are regenerated cellulose fibers. These man-made cellulosics are endless filaments of well-defined dimension and high purity. The fiber morphology and fine structure are the key factors for any cellulosic CF precursor. The concept of the fringed fibril[56] is commonly used to describe the alignment of cellulose chains forming the fiber fine structure. Here, crystallites or ordered regions are connected to each other through less-ordered or amorphous regions (Figure 13).

The unit cell of natural cellulose is cellulose I, whereas in regenerated cellulose it is the allotropic modification cellulose II (Figure 14). In both cases, the elementary fibril consists of a monoclinic unit cell, which contains two cellobiose segments from two neighboring chains. In cellulose I, the chains are arranged in a parallel manner, while in cellulose II there are indications of an antiparallel arrangement. Moreover, in cellulose I there are two intramolecular hydrogen bonds formed between O3-H···O5′ and O2 H···O6′ of two adjacent anhydroglucose units (AGU). In cellulose II there is only one bifurcated hydrogen bond, O3-H···O5′,O6′.[57]

The fact that cellulose II is formed during regeneration can be explained by the fast crystallization process and a certain hindrance as a result of the entanglement present in solution, whereas in nature the formation of the denser cellulose I structure occurs very slowly.[58] Thus, cellulose I has a higher modulus than cellulose II.[59] A short overview of their production processes is given for regenerated cellulose, that is, for viscose and lyocell. The mechanical and structural properties for some cellulosic fibers are summarized in Table 2.

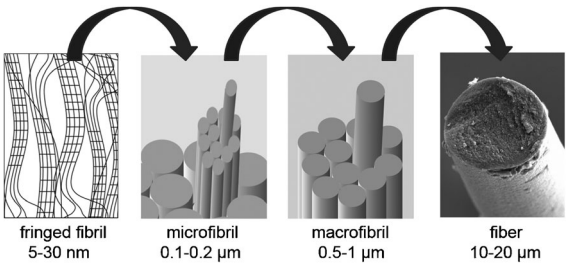

Figure 13. Supramolecular structure in cellulose—from fibril to fiber. The dimensions depend on the fiber type.

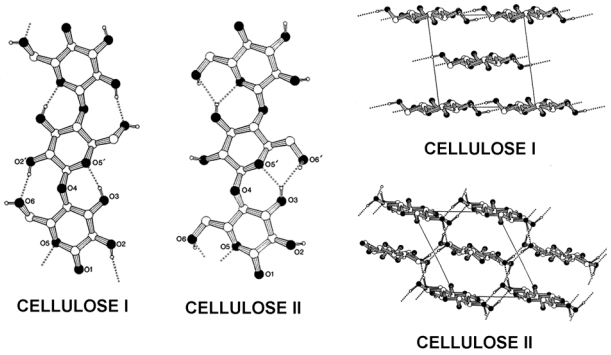

Figure 14. Chain conformation of cellulose I and II (left), crystal structure of cellulose I and II viewed along the chain axis (right). Reproduced with permission from Elsevier.[57b]

For the production of viscose rayon, the xanthation of alkali cellulose with carbon disulfide is required to dissolve cellulose in aqueous sodium hydroxide. The viscous solution containing about 8 wt% cellulose is spun into a coagulation bath (containing sulfuric acid, sodium sulfate, and zinc salts), where carbon disulfide is eliminated.[57a] The presence of zinc salts in the coagulation bath enables skin/core structures to be formed, whereby the thickness of the skin depends on the diffusion of zinc ions into the fiber. The skin contains many small crystallites and imparts strength, whereas the core contains fewer but larger crystallites. These rayon fibers are used technically as tire cords.[58,61] Nowadays, the viscose process has the highest technical significance in the production of rayon.

In the lyocell process, an air gap spinning process, nontoxic *N*-methylmorpholine *N*-oxide (NMMO) is used as a direct solvent for cellulose, with 10–14 wt% cellulose solutions used for spinning. The spinning dope has to be stabilized by additives such as isopropyl gallate to prevent side reactions.[57a,62] Lyocell fibers have a higher crystallinity than viscose (Table 2). The elementary fibril data show that very long and thin crystallites align in a highly oriented manner along the fiber axis in lyocell. The same occurs in the amorphous parts (Figure 13). There is little lateral interaction between the macrofibrils, which leads, in the wet state, to a high tendency to fibrillate.[57a] This characteristic is in fact problematic and can well be expected to be disadvantageous when lyocell-cellulose is to be used for the production of CFs.

Figure 15 shows typical scanning electron micrographs of cross-sections and surface structures of single filaments of

Table 2: Mechanical and structural properties of selected cellulosic fibers.

Fiber material	Titre [dtex]	Tenacity [cN/tex]	Elongation [%]	DP	Crystallinity [%]	Chain orientation[a]	Elementary fibril dimensions[b] [nm]	Ref.
viscose rayon	1.4	23.9	20.1	200–250	38	0.58/0.41	4.3/8/7	[57a, 60]
lyocell	1.3	40.2	13.0	600–800	62	0.85/0.59	3.9/21/2	[57a, 60]
tire cord	1.9	52.3	15.1	–	59	0.71/–		[57a, 60]
cotton	-				78	-	4.8/40-90/-	[57a, 60]
Fortisan[c]	0.7	23.9	3.2					[60]
Cupro[d]	2.5	22.3	24.3					ref. [60]
Bocell[e]	1.8	38.2	9.7					[60]

[a] Factor for the orientation of the crystallites/factor for total fiber orientation. [b] Crystallite width/crystallite length/amorphous length. [c] Saponified cellulose acetate fiber. [d] Fiber regenerated from an aqueous solution in $[Cu(NH_3)_4](OH)_2$. [e] Fiber regenerated from a phosphoric acid solution and spun by an air-gap spinning process.

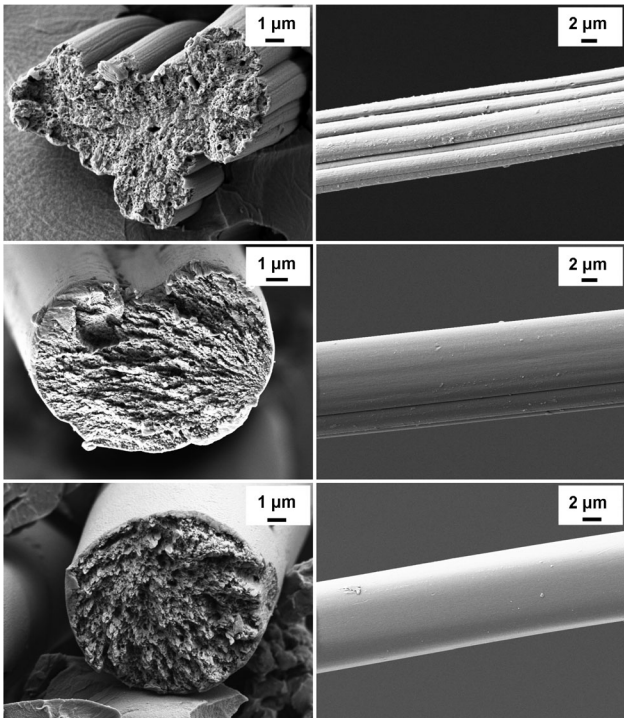

Figure 15. Scanning electron micrographs of single filaments of: viscose rayon (top), tire cord (middle), lyocell (bottom); left: cross-section, right: surface of a single filament.

viscose rayon, tire cord, and lyocell. Viscose fibers show a porous morphology with contractions along the fiber axis leading to an irregular cross-section. Moreover, the surface contains transversal grooves. All these defects give rise to predetermined breaking points and voids in the CF, thus resulting in low modulus, breaking elongation, and tenacity. Tire cord filaments have a smooth surface, with a cross-section that is almost round, but slightly kidney shaped. Lyocell fibers show a round cross-section and the surface is very smooth, with few defects. This is, despite their propensity to fibrillate, a clear benefit of using lyocell fibers as precursors for CFs, since a fiber morphology without or with only a few imperfections can be achieved.[63]

A new type of cellulosic fibers can be obtained by the ionic liquid (IL) approach.[64] Cellulose is dissolved directly in imidazolium-based ILs without the addition of any stabilizers and is spun into an aqueous coagulation bath. The resulting fibers have very promising characteristics with regard to the preparation of CFs, such as a high orientation, a compact morphology, and a very low fibrillation propensity.[62,65]

2.3.3. *Cellulose Pyrolysis Mechanism*

In general, the properties of CFs strongly depend on a controlled pyrolysis process and carbonization. A lot of effort has been made to understand the rather complex mechanism of cellulose pyrolysis. Besides the investigation of cellulose-based CFs, knowledge on cellulose pyrolysis is mainly connected with research on flame-resistant textiles[66] and the conversion of biomass into fuels,[67] chemicals, and energy.

Formally, the loss of 5 moles of water per AGU during dehydration corresponds to a mass loss of 55.6%. The maximum carbon yield is accordingly 44.4%, which represents a residual 6 carbon atoms per AGU. However, besides dehydration, cellulose pyrolysis is accompanied by degradation reactions, which result in the formation of CO_2, CO, alcohols, ketones, and other carbon-containing low-molecular-weight substances, which lead to a mass loss of up to 70–90%.[55c] Figure 16 shows a typical TGA curve for rayon fiber in an inert gas atmosphere. The onset temperature of the TG

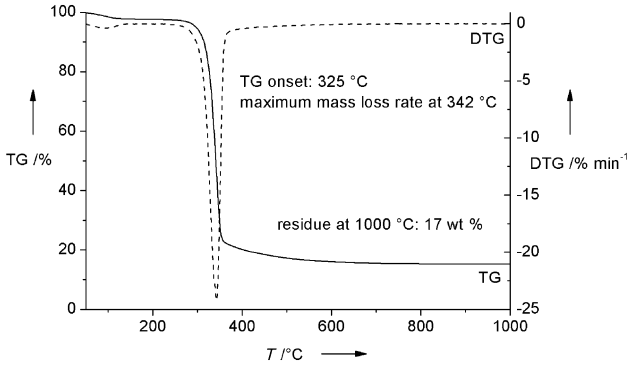

Figure 16. Typical TGA curve for rayon fibers in an inert atmosphere.

curve is 325 °C, while the rate of mass loss reaches its maximum at 342 °C. At 1000 °C a solid residue remains with 17 wt % of the mass of the initial amount of cellulose.

Tang and Bacon[68] studied the pyrolysis of different cellulose samples by TGA and IR measurements and proposed a mechanism that can be divided into four steps (Scheme 3). In the first step at temperatures up to 150 °C,

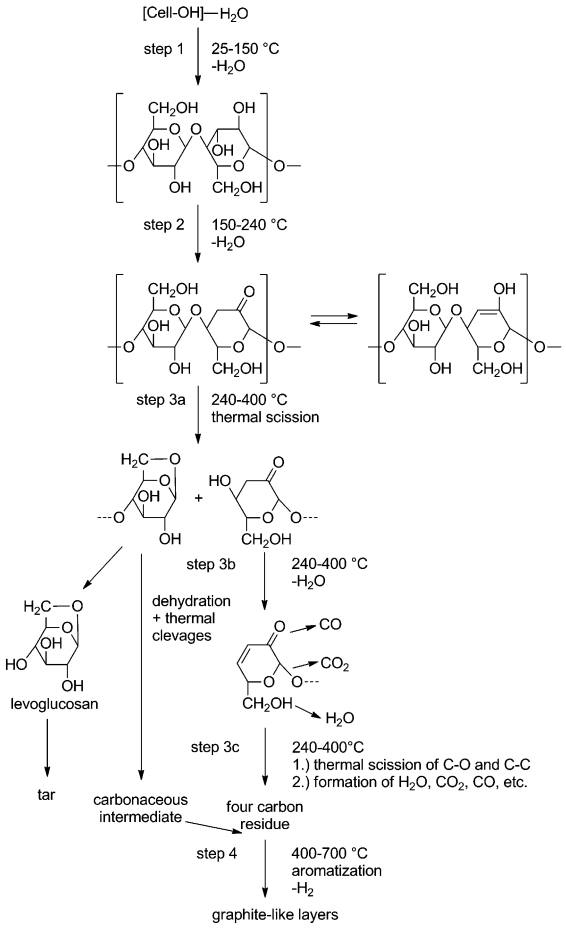

Scheme 3. Pyrolysis mechanism according to Tang and Bacon (redrawn from Ref. [68]).

physically adsorbed water is desorbed. In the second step between 150 °C to 240 °C, the AGU is dehydrated. Up to 400 °C, cellulose is decomposed by cleavage of glycosidic and other C–O bonds as well as of C–C-bonds. In the last step above 400 °C, aromatization of the remaining residue with four carbon atoms occurs.

Kilzer and Broido[69] proposed a reaction scheme (Scheme 4) in which the processes of dehydration to "dehydrocellulose" and depolymerization to tarry products occur simultaneously. However, the term "dehydrocellulose" was omitted later.[70]

The pathways that have been proposed to explain dehydration are both intra- and intermolecular: thus, double bonds or ether bonds are created along the chain by β-elimination or nucleophilic substitution within the AGU. The formation of ether bonds between two neighboring polymer

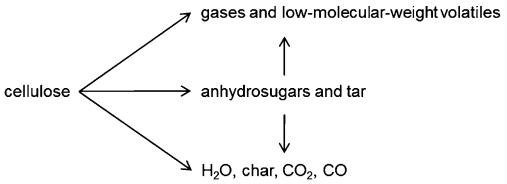

Scheme 4. Model for the pyrolysis of cellulose by Kilzer and Broido (redrawn from Ref. [69]).

chains leads to polymer networks with high thermal stability.[55d,69] Fairbridge et al.[71] observed that water was the only volatile product during thermal degradation at temperatures up to 250 °C. Tang and Bacon[68] are in favor of intramolecular reactions, whereas Kilzer and Broido[69] hold to the formation of intermolecular ether bonds. The formation of double bonds and, subsequently, of conjugated double bonds and aromatic structures stabilizes the residue and makes it less accessible to cleavage than the original cellulose.[72] The enol formed by intramolecular dehydration can rearrange to the tautomeric ketone, thereby leading to increased chain-degradation reactions and loss of carbon.[73] Depolymerization occurs within the same temperature regime as dehydration, although pyrolysis starts at higher temperatures. The primary hydroxy group at C6 of AGU acts as a nucleophile that cleaves the glycosidic bond, which leads to a gradual unzipping of the polymer chain and the formation of levoglucosan.[69]

Bradbury and Shafizadeh[74] extended the model of Kilzer and Broido by a preliminary step in which activated cellulose (activation energy 242.8 kJ mol^{-1}) is formed, which enables the formation of char and gas (activation energy 153.1 kJ mol^{-1}) or primary volatiles (197.9 kJ mol^{-1}) at low temperatures. The activation step is associated with depolymerization down to a degree of polymerization of around 200. No initial activation step was found at low temperatures.[74a] This mechanism is referred to as the Broido–Shafizadeh model and is most widely accepted to describe the pyrolysis of cellulose or biomass,[75] although it is not capable of describing the decomposition reactions in detail. The pyrolysis of levoglucosan gives char, thus indicating that chars may also result from primary volatiles that are formed upon the pyrolysis of cellulose during depolymerization reactions.[74a,76]

Shafizadeh also studied charring reactions of different carbohydrates as model compounds and found that unsaturated products generated by dehydration of the carbohydrate units undergo condensation to form higher molecular weight products.[73] Moreover, cleavage of carbon substituents leads to the formation of free radicals, which are able to condense and cross-link to form a stable residue. The addition of zinc chloride did not only catalyze the dehydration but also helped to condense the intermediates to form char by creating ether bonds. ESR investigations on the condensation of 3-deoxy-D-erytro-hexosulose or levoglucosan revealed that the charring reactions where accompanied by the formation of stable free radicals.[73,76] The general pathways for the pyrolysis of cellulose are depicted in Scheme 5.

Brunner and Roberts assumed that dehydration is the rate-determining step at low temperatures, while decomposition has the higher reaction rate at $T > 240$ °C. If dehydra-

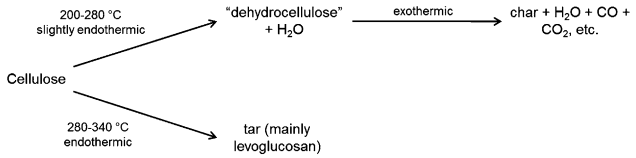

Scheme 5. Competitive pathways in cellulose pyrolysis (redrawn from Ref. [77]).

tion is completed at low temperatures, the material is less susceptible to decomposition at high temperatures. Thus, the char yield can be increased by applying slow heating rates. However, the authors also found that the micropore volumes and surface areas increased in the char structure as the heating rates decreased.[72]

Mechanistic insight has also been gained by studying the pyrolysis products, for example, by pyrolysis-GC-MS. A multitude of compounds have been found by different pyrolysis techniques.[73,78] It should be noted that the product distribution is also determined by both the cellulose source and the pyrolysis conditions such as heating rate and atmosphere. Vacuum pyrolysis, for example, enhances the formation of tar compared to pyrolysis under nitrogen.[73] A selection of the pyrolysis products of cellulose is given in Table 3.

Table 3: Selected pyrolysis products of cellulose.

Mass [g mol^{-1}]	Pyrolysis product
2	H_2
14	CH_2
16	CH_4, O
18	H_2O
24	C_2^+
28	CO, C_2H_4
44	CO_2
162	levoglucosan
126	levoglucosenone
144	1,4:3,6-dianhydro-α-D-glucopyranose
60	hydroxyacetaldehyde
60	acidic acid
162	1,6-anhydro-β-D-glucofuranose
90	glyceraldehyde
96	furfural
126	5-hydroxymethylfurfural
74	1-hydroxy-2-pronanone
98	furfural alcohol
60	propanol
58	propanal
72	2-butanone
82	2-methylfuran
102	methyl-2-oxopropanoate
116	2-ethyl-4-methyl-1,3-dioxolane
114	2-methyl-5-vinyl-1,3-dioxolane

2.3.4. *Process Steps towards Cellulose-Based Carbon Fibers*

2.3.4.1. *Step 1: Stabilization*

To produce CFs from cellulose fibers with high carbon yield and thus high density and little defects—the major targets for good CFs—the pyrolysis of cellulose needs to be regulated in a way that the fraction of carbon lost by depolymerization and degradation reactions remains as small as possible. In this way, both the properties of the CF are improved as well as the efficiency of the entire process, which makes it possible to produce CFs at lower cost.

The first aim should, therefore, be to promote dehydration reactions to prevent the formation of levoglucosan. Three general options exist for this purpose:

- application of slow heating rates
- use of flame retardants
- pyrolysis in a reactive atmosphere.

Usually, a combination of at least two of these options is employed.

Slow Heating Rates

Ford and Mitchel applied heating rates between 10 and 50 °C h^{-1} in a temperature range of 100 to 400 °C. Between 400 to 900 °C, the rate was increased to 100 °C h^{-1}.[53b] Cross et al. subjected cellulosic material to an extensive drying step at 125 °C. The oven was then opened to cover the fiber surface with a protective layer of coke. Further heating to 400 °C was then carried out at 5 °C h^{-1}.[79] Brunner and Roberts studied the influence of the heating rate on the carbon yield of pyrolyzed cellulose.[72] The yield increased from 11 to 28 % at 900 °C when the heating rate was decreased from 70 °C h^{-1} to 0.03 °C h^{-1}. For the low heating rate, the carbon yield was consistent with the four-carbon residue predicted by Tang and Bacon.[68,80] Above 700 °C, cellulose pyrolyzed at a slow heating rate did not show any weight loss, while rapidly charred samples gradually decreased in weight. Brunner and Roberts also studied the properties of the chars and found smaller O/C ratios when slow heating was applied. The micropore volume, surface area, and densities were higher for slow heating rates. The micropore volume increased by a factor of four at 0.03 °C h^{-1} compared to chars pyrolyzed at 70 °C h^{-1}.[72] However, such extremely slow heating rates are uneconomical.

Oxidation

An oxidative pretreatment step is often performed prior to the final carbonization of a cellulosic precursor. At a first glance this appears somewhat contradictory because it is not an indispensable step such as in the stabilization of a PAN precursor. However, a larger amount of char remained after carbonization of preoxidized cellulose.[55a,d,81] A comparison of the pyrolysis results obtained in air or in an inert atmosphere turned out to be of great importance to find suitable conditions for stabilization and carbonization. Thus, oxidative degradation takes place much faster than pyrolysis in an inert atmosphere at low temperatures, whereas reaction rates are independent of the medium at high temperatures.[74b] Thermal degradation in air includes the autoxidation of cellulose. The initial step is the abstraction of hydrogen from organic molecules by oxygen. Autoxidation is presumed to be favored at the C1- or C4-position of AGU. This may either lead to the formation of hydroperoxides by the addition of

oxygen or result in β-scission, which could be followed by dehydration or depolymerization.[74b,75b] From the thermogravimetric results and evolution of the degree of polymerization it appears that dehydration is probably the major pathway. In turn, charring reactions are favored.[75b,82]

Reactive Atmosphere

Shindo et al.[83] pyrolyzed cellulose fibers in the presence of HCl vapor. The pyrolysis of cellulose in an HCl atmosphere results in a significantly reduced weight loss compared to a single temperature treatment under nitrogen. Dehydration is catalyzed by HCl, most probably through protonation of the hydroxy groups, and the weight loss takes place over a larger temperature region. To explain the high char residue, Shindo et al. suggested the mechanism that entails the formation of five-membered-ring compounds according to Byrne et al.[84] (Scheme 6). These furan compounds are

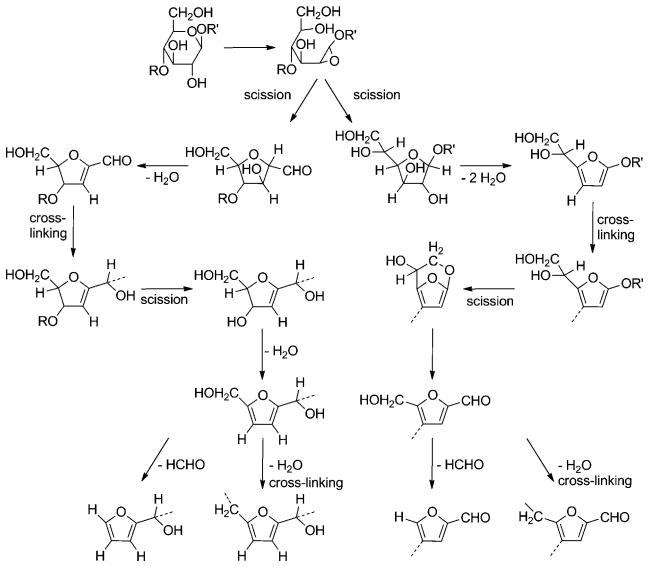

Scheme 6. Pyrolysis mechanism in an HCl gas atmosphere according to Shindo (redrawn from Ref. [83]).

presumed to cross-link before being evaporated.[83] Shindo et al. observed a decrease in the tensile strength of the cellulosic fibers upon heating to 120 °C. This was attributed to the hydrolysis of the glycosidic bonds under these strongly acidic conditions (water desorption from cellulose). Since such a process involves a highly corrosive atmosphere, a practical application appears unlikely.[55d]

Use of Flame Retardants

Flame retardants can either catalyze the removal of the hydroxy groups of cellulose or actually react with them. Catalysts only need to be present in small concentrations and are usually Lewis acids, Lewis bases, or substances that release these substances upon heating. Flame retardants, which react with hydroxy groups, can be cross-linkers such as urea, which stabilize the solid matter.[26f,55d] Other examples are $AlCl_3$, borax, boronic acid, $KHCO_3$, NaH_2PO_4, $ZnCl_2$, NH_4Cl, ammonium phosphates, and ammonium sulfates.[85] For an overview of flame retardants for cellulosic fibers, we refer the reader to the open literature.[66,86]

The impregnation of cellulosic fibers with phosphoric acid, ammonium phosphates, ammonium sulfate, sulfuric acid, and mixtures of phosphoric and boronic acid has been studied for their conversion into activated carbon materials.[81a,87] Morozova and Brezhneva pyrolyzed cellulose fibers after impregnation with a solution of sodium tripolyphosphate.[88] They claimed tensile strengths of 2–4 GPa after carbonization at 700–900 °C by applying heating rates of 2–3 °C min^{-1}. Bhat et al. used a solution of phosphoric acid for impregnation. Stabilization in air up to 380 °C and subsequent carbonization to 1200 °C gave tensile strengths of around 0.6 GPa and moduli of 50 GPa.[89]

Li et al.[90] treated fibers with a solution of $(NH_4)_2SO_4$ and NH_4Cl and studied the gases that evolved during pyrolysis by TG-MS measurements. It could be proved that the early mass loss from the catalyzed system was indeed associated with dehydration. The difference spectrum obtained by subtracting the average MS traces of untreated and treated samples revealed that $(NH_4)_2SO_4$ and NH_4Cl impregnation resulted in an increased formation of CH_4, H_2O, CO, and CO_2 by decreasing the amount of higher molecular weight substances related to tarry products (Figure 17).[90] However, the assign-

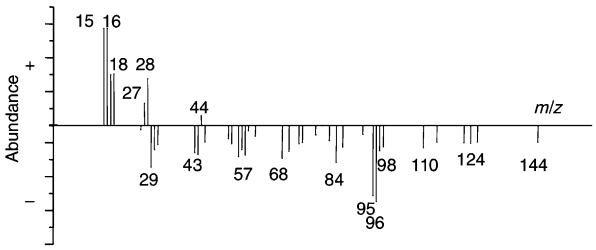

Figure 17. Difference spectrum obtained by subtracting the average MS traces of untreated and treated samples.[90] Reproduced with permission from Elsevier.

ment of the *m*/*z* signals to other pyrolysis products was ambiguous because of the multitude of fragments. Similar TG-MS studies were also carried out by Wu et al. and Liu et al.[78g,91] Statheropoulos and Kyriakou studied the influence of $(NH_4)_2SO_4$ and $(NH_4)_2HPO_4$ on cellulose pyrolysis products by TG-MS.[92] They were able to quantify the MS signals of H_2O and CO_2 by calibration with $KHCO_3$. A chemometric approach was used to identify further pyrolysis products by TG-MS.[93] After stabilization, less tarry products are formed when the fiber is carbonized. An improved thermal stability could be verified by flammability tests.[81a]

Organosilicon Compounds

Plaisantin, Orly, and co-workers used an organosilicon compound dissolved in an organic solvent to impregnate different precursors prior to heat treatment.[94] Significant improvements in CF strengths were achieved even at

relatively high heating rates. The highest values reported for strength and modulus, 1.8 GPa and 100 GPa, respectively, were obtained from a liquid-crystalline precursor yarn[95] impregnated with a mixture of silicon compounds.[94a] The addition of a flame-retardant inorganic salt was also accomplished by impregnating regenerated cellulose fibers with a silicon preparation and subsequently with NH_4Cl. After carbonization at 1200 °C, a CF having a tensile strength of 1.2 GPa and a modulus of 45 GPa was obtained with a carbonization yield of 30 %.[94a] For all the carbonizations without a flame retardant, the carbon yields were only around 16 %.

Lysenco et al.[96] likewise tried to impregnate cellulosic fibers with combinations of organosilicon compounds and a variety of flame retardants. According to their findings, the properties of CFs could be improved by the organosilicon compounds, but when combined with the addition of flame retardants the mechanical properties of the CFs worsened.

Good mechanical properties were also obtained by applying aqueous emulsions of silicon compounds on non-squeezed, nondried high-tenacity precursor fibers. Tensile strengths up to 2.0 GPa and Young's moduli of 62 GPa were obtained after carbonization at 2100 °C. The value of the elongation at break was reported to be 3.2 %.[97] These results were interpreted in a way that silicon compounds are presumed to reduce critical surface defects, which are seen to be responsible for mechanical failure, thereby resulting in better CF properties.[94b] Li et al.[90] treated cellulose fibers with a solution of $(NH_4)_2SO_4$ and NH_4Cl. They observed that aggregation of the salts on the fiber surface upon drying could be suppressed by applying a siloxane pre-polymer solution prior to the addition of the catalyst. The tensile strengths of the CFs were also improved from 0.9 GPa to 1.5 GPa on applying a silicon compound.

2.3.4.2. *Step 2: Carbonization*

At temperatures around 400 °C, pyrolysis ceases and the major chemical reactions are completed. At this temperature, the residue already has a carbon content of about 60–70 %. Carbonization is carried out under an inert gas atmosphere up to temperatures of 900–1500 °C. The release of non-carbon atoms results in a residue forming that consists of more than 95 % carbon.[55d]

The reactions taking place during carbonization are rather complex and difficult to monitor by analytical methods. In principle, the depolymerized, amorphous char, which is formed during pyrolysis, is rearranged and condensed to form polycyclic rings, aromatic structures, and subsequently graphite-like layers. This leads to the formation of a microcrystalline material, which consists of sp^3- and sp^2-hybridized carbon. Carbonization is accompanied by fiber shrinkage, an increase in density, and an increase in tenacity, which is correlated with the formation of the aromatic structure.[55d,80]

2.3.4.3. *Step 3: Graphitization*

Graphitization of carbon is initiated at temperatures between 1500 and 3000 °C. This leads to a carbon content of more than 99 % and a growth of the graphitic layers. Graphitization under stress, so called hot stretching, leads to excellent mechanical properties of the final CF by further improving the orientation of the carbon ribbons along the fiber axis.[54c] Although it may take only seconds,[53b] graphitization is a highly power-consuming process and, therefore, the extent to which it is carried out strongly depends on the field of application of the CF.

2.3.5. *Structure of Cellulose-Based Carbon Fibers*

Useful techniques to study the carbonization of cellulose are infrared spectroscopy (IR) and Raman spectroscopy, as well as solid-state ^{13}C nuclear magnetic resonance (NMR) spectroscopy and X-ray diffraction. FTIR spectroscopy has been widely applied to study chemical composition, molecular conformation, and hydrogen-bonding patterns in cellulose.[98] It can also be used to study the conversion of functional groups during pyrolysis and oxidation reactions.[68,81a,83] Figure 18 shows the attenuated total reflection

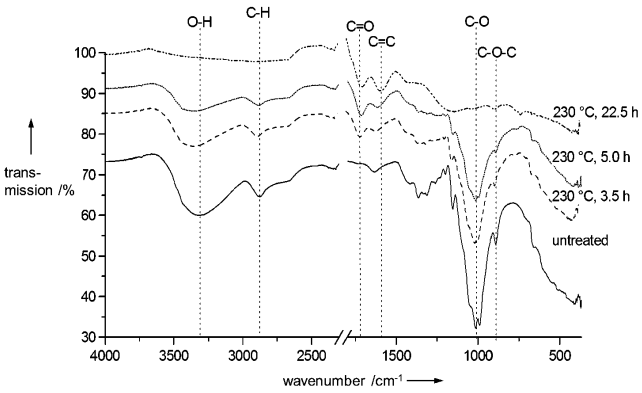

Figure 18. (ATR) FTIR spectra of rayon-type cellulose fibers after heat treatment at 230 °C.

(ATR) FTIR spectra of regenerated cellulose after heat treatment at 230 °C in air for different periods of time. The untreated sample shows characteristic bands of cellulose II type material.[99] Prolonged temperature treatment results in the bands of the O–H stretching vibrations from 3600 to 3100 cm^{-1} vanishing because of the continuous dehydration of cellulose. The C–H stretching vibrations from 3000 to 2800 cm^{-1} also decrease. During oxidation, bands at 1720 cm^{-1} attributed to C=O stretching and 1610 cm^{-1} from C=C stretching are formed. After 22.5 h, the C=O and C=C stretching bands become predominant in the spectrum. The band at 1640 cm^{-1} of the untreated sample is assigned to O–H stretching of absorbed water. The intensities of the C–O and C-O-C stretching bands at 1000 and 900 cm^{-1} become weaker and almost disappear after 22.5 h of heating at 230 °C.

All vibrational modes of cellulose are both IR and Raman active. Consequently, Raman spectroscopy is also used extensively for the characterization of cellulose.[98a,100] Cellulose contains water, which gives very intense IR bands. However, such highly polar bound systems have low polarizabilities and thus, give only weak Raman intensities, which

do not interfere with the cellulose bands. This is a major advantage of the use of Raman spectroscopy for cellulose. Moreover, variations of the refractive index throughout the material are not a problem in Raman spectroscopy because the excitation frequency is far away from any absorption band.[101]

Figure 19 shows Raman spectra for Bocell fibers (regenerated from a solution of phosphoric acid) carbonized at increasingly higher temperatures.[102] The spectrum at the top

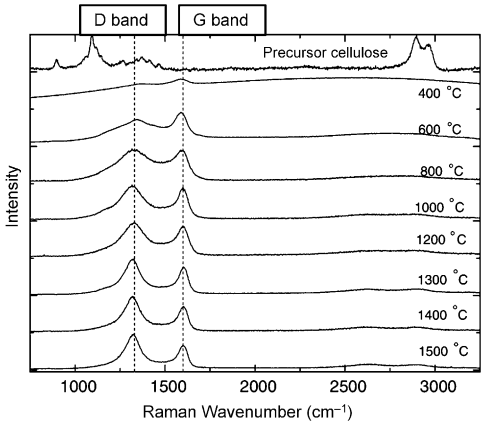

Figure 19. Raman spectra of cellulose carbonized at different temperatures. Reproduced with kind permission from Springer Science and Business Media.[102]

corresponds to untreated cellulose. The typical CF structure is already evident at 400 °C and manifests at higher temperatures. The G and D bands are located at 1600 cm^{-1} and 1350 cm^{-1}, respectively. Whereas the G band is characteristic for sp^2-hybridized carbon in graphite planes and corresponds to the Raman-active vibration modes E_{2g} of the graphite unit cell (the other vibration modes of graphite, $2B_{2g}$, A_{2u}, and E_{1u}, are Raman inactive), the D band is typical of defects.[103] The intensity of the G band increases as the carbonization temperature increases, which can be explained by increasing graphitization at higher temperatures. However, the intensity of the D band remains higher than that of the G band, even at 1500 °C. After heat treatment at 2500 °C, the so-called G′ or 2D band appears at 2700 cm^{-1}, which is an overtone of the D band (Figure 20). The intensity ratio I_D/I_G is used to draw conclusions about the number of defects in graphite materials and the lateral crystal size.[104] The latter increases with temperature (Figure 21).

Solid-state ^{13}C NMR spectroscopy is also a powerful analytical tool for cellulose.[105] Signal intensities can be enhanced by cross-polarization (CP) in solid-state NMR experiments. Magic angle spinning (MAS) is used to overcome signal broadening in the solid-state ^{13}C NMR spectra resulting from chemical shift anisotropy. CP/MAS ^{13}C NMR experiments were used by Pastorova et al.[78c] and Plaisantin et al.[94b,106] to study the chemical changes in cellulose during heat treatment. The CP/MAS ^{13}C NMR spectra of cellulosic fibers treated at different temperatures are illustrated in Figure 22. Typical shifts of the carbon nuclei of AGU in the

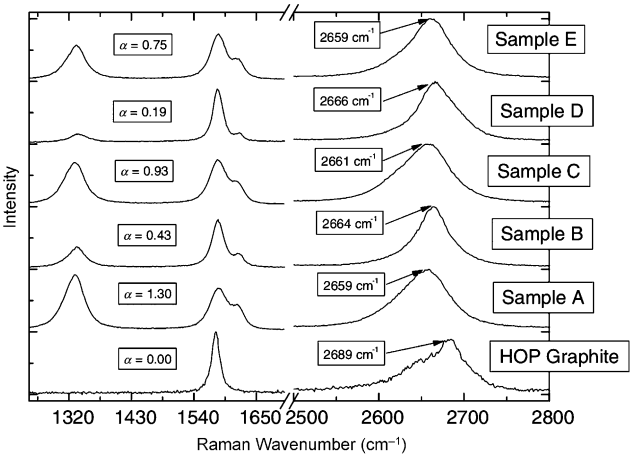

Figure 20. Raman spectra of graphitized fibers.[102] Reproduced with kind permission from Springer Science and Business Media.

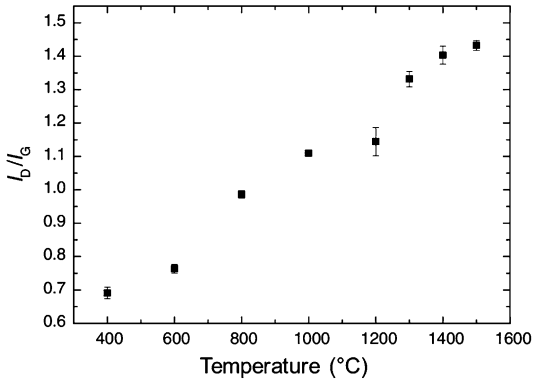

Figure 21. I_D/I_G ratio for fibers carbonized at different temperatures.[102] Reproduced with kind permission from Springer Science and Business Media.

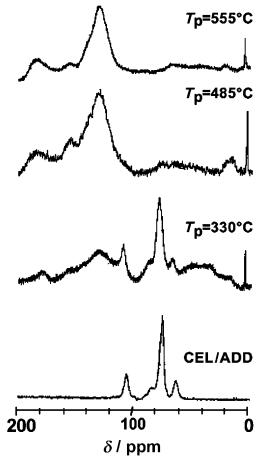

Figure 22. ^{13}C CP/MAS NMR spectra of cellulosic fibers after heat treatment at different temperatures. Reproduced with kind permission from Springer Science and Business Media.[94b]

untreated fiber were observed in the range of $\delta = 60$ to 120 ppm.[105b] Dehydration of AGU was suggested by the formation of additional signals centered at $\delta = 130$ ppm (olefinic carbon) and around $\delta = 170$–180 ppm (carboxyl or

carbonyl groups), while the original signals from cellulose gradually disappeared.

The X-ray diffraction patterns of a regenerated cellulose fiber (Fortisan 36, saponified cellulose acetate) after heat treatment at subsequently higher temperatures are depicted in Figure 23.[68] The oriented crystal structure of cellulose

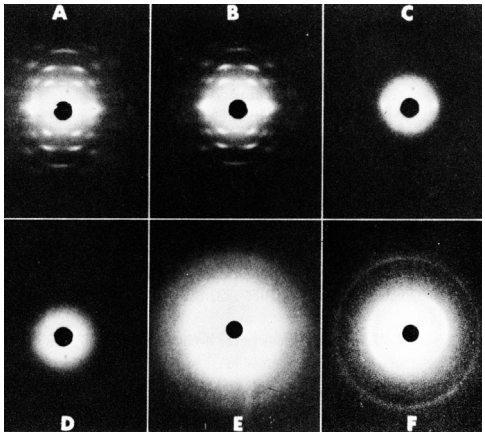

Figure 23. X-ray diffraction patterns during heat treatment of a regenerated cellulose fiber (A) at different temperatures: 245 °C (B), 280 °C (C), 305 °C (D), 900 °C (E), and 2800 °C (F). Reproduced with permission from Elsevier.[68]

remains intact after 12 h at 245 °C. Above this temperature, the degree of crystallinity decreases and the fiber becomes amorphous. From pattern E, the appearance of graphitic structures at 900 °C can be observed. At 2800 °C, a preferred orientation of the graphite layers along the fiber axis can be detected (pattern F).[68] It is important to note that the preferred orientation in the precursor fiber along the fiber axis becomes the preferred orientation in the resulting CFs. To illustrate this, Tang and Bacon made orientation profiles of a highly oriented film from bacterial cellulose before and after graphitization (Figure 24). In the case of the cellulose film, the (101) planes are aligned parallel to the film surface. The film was rocked back and forth and the number of (101) planes, oriented at various angles away from the surface, were recorded. The full width at half maximum of this profile was

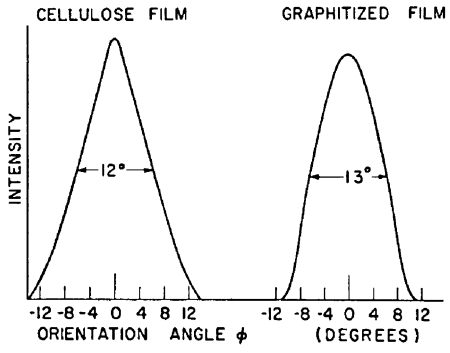

Figure 24. Profile of X-ray scattering intensity versus orientation of the crystal planes relative to the plane of the film sample. Reproduced with permission from Elsevier.[68]

about 12°. For the graphitized sample, the graphite layer plane (002) was used to record the profile. The planes were oriented parallel to the surface and the full width at half maximum was about 13°.[68] This suggested that the graphite planes were derived from the (101) plane of cellulose.

Table 4 lists cellulose-based CFs and their mechanical properties.

Table 4: Cellulose-based CFs and their mechanical properties.

Precursor Material	Diameter	Strength [GPa]	Modulus [GPa]	Elongation [%]	Reference
lyocell	7.5	0.9			[107]
rayon	7.5	0.81			[107]
lyocell		0.49	37.6	1.4	[108]
lyocell filled with 5 wt% carbon black		0.57	48.3	1.2	[108]
rayon		0.82	79.2		[109]
lyocell		0.94	99.7		[109]
lyocell		1.07	96.6		[109]
lyocell		0.40			[110]
rayon "Ural"		0.5–1.2	100		[111]
hydrated cellulose		1.65	97		[112]
rayon		0.944	54.3	1.76	[90]
rayon		1.535	59.8	2.57	[90]
viscose rayon		0.6	50		[89b]
cellulosic fiber		2–4			[88]
cellulose fiber		0.2–0.44		3.0	[113]
sisal fiber		0.8	25		[114]

2.4. Lignin-Based Carbon Fibers

2.4.1. Lignin: Properties and Recovery

Next to cellulose, lignin is the second most abundant biopolymer and the most commonly occurring aromatic biopolymer on Earth. Lignins can be grouped into three types according to their structure: hardwood lignin, softwood lignin, and grass lignin. The structure of these three types differs with the monomer building blocks from which the corresponding lignin is built (Figure 25).

Lignins from annual plants are mainly composed of coumaryl alcohol. Softwood lignin is predominantly based on coniferyl alcohol, while hardwood lignin is mainly composed of coniferyl alcohol and sinapyl alcohol. Additional

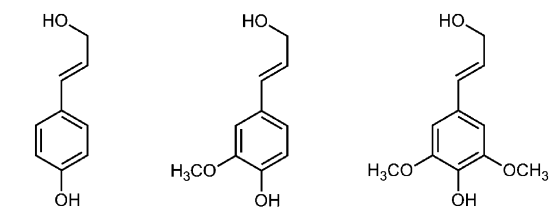

Figure 25. Monomer building blocks of lignin.

functionalities in the structure can be found, depending on the pulping process. Degradation caused by various pulping reagents also varies and results in differently sized lignin fragments and mechanisms of cleavage.[26i] Lignins can be classified into four groups by means of the isolation processes: lignosulfonates from the sulfite pulping process,[26i] kraft lignin from the sulfate pulping or kraft pulping process,[26i] soda lignin,[26i] and organosolv lignin.[26m,n,35b] The sulfate process is, at 85%, the most widely used process for pulp production, and hence for lignin recovery, as well. The sulfite and soda process are both equally applied on an industrial scale. The sulfite process provides lignin fragments up to several 10000 g mol^{-1}, while the other processes generate more degraded lignins with molar masses $\leq$ 10000 g mol^{-1}. The sulfur content of lignosulfonates at up to 8 wt% (mostly sulfonate groups) and the ash content at up to 25 wt% are very high, but kraft lignins also contain sulfur up to 3 wt% in the form of thiols, thioethers, etc. Until now, the organosolv process has not often been realized on a large scale. However, increasing interest in this process is evident, mostly because it provides pure, sulfur-free, in most cases fusible, lignin with low ash content. The diversity of lignins is a big challenge for research and it is thus difficult to develop general procedures for manufacture. Differences in quality, properties, and structures incessantly create new starting conditions.

Lignin has, in contrast to cellulose, not yet been converted into value-added products on a large-scale. A widespread application of lignin is incineration for energy recovery. However, as the increasing oil price is becoming a more and more important issue, the demand for renewable and sustainable resources consequently increases. As a result, the discussion of the sensible use of lignin comes to the fore. Lignins are already used as adhesives[115] and dipersants[116] as well as in thermoplastic materials.[117] Other applications could be the replacement of phenol in phenol-formaldehyde resins,[118] the use as fillers,[119] or as a raw material for chemicals,[120] to mention just a few.[121]

Lignin is also considered to be an alternative, low-cost precursor for the production of CFs.[26l,122] The increasing popularity of lignin is visualized by the steadily growing number of publications on this topic (Figure 26).

Major advantages of this potential CF precursor are related to its high carbon ($\geq$ 60%) content and potentially high carbon yield after carbonization, no exposition of toxic elimination products, such as HCN or nitrous gases, during carbonization, as well as its availability and low costs. For broad applications, CFs must be less expensive and accessible in large quantities, and in the best scenario independent of the oil price. Lignin suits this specification and, therefore, has potential for usage as a CF precursor for automotive and lightweight materials. The use of lightweight materials would result in fuel consumption being decreased or the effectiveness of electro-mobility being increased. Conventional CFs based on PAN-copolymers are too high in price and insufficiently available for this purpose.[123] In 2011, Das determined the life-cycle assessment of a floor pan for both a lignin and textile-grade PAN CF precursor by two different manufacturing processes. According to the investigations, lignin was proposed to be the best CF precursor.[124] Finally, besides the development of lignin-derived high-performance CFs, lignin can also be used as a source of activated CFs.[125]

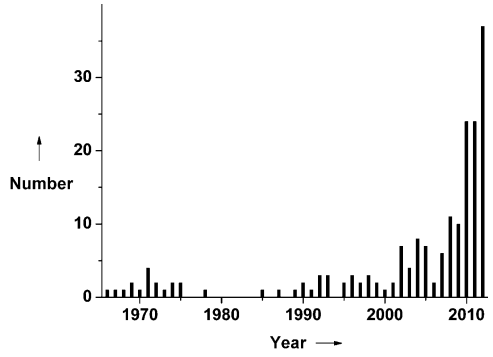

Figure 26. Occurrence of lignin-derived CFs in the literature. Source: ISI Web of Knowledge, Thomson Reuters, July 2013.

2.4.2. *Dry and Wet Spinning*

The first phase in the development and manufacturing of lignin CFs started in the 1960s and 1970s, and was dominated by the Nippon Kayaku Company. The motivation was to establish CFs for applications in which the price had first priority. At that time, fibers were mostly prepared by wet and dry spinning processes. Melt spinning was mentioned, but it was not in the focus of intention because of the lack of fusible lignin or a suitable method of manufacturing. After Otani filed patent applications in 1964 in Japan of a method for producing carbonized materials, intellectual property rights followed in other countries such as in Germany, US, France, etc.[126] The patents comprised of a process for producing carbonized lignin fibers and activated CFs because it was assumed that lignin was particularly suitable for both kinds of fibers. No limitations in the lignin type were mentioned, and alkali-lignin, thiolignin, and lignosulfonate were considered viable lignin types. High-molecular-weight materials such as poly(vinyl alcohol) (PVA), poly(acrylonitrile) (PAN), or viscose were added for the manufacture of wet-spun lignin fibers. Tensile strengths up to 0.8 GPa could be achieved with this method. In 1969, Fukuoka from Nippon Kayaku published a report about these commercially available lignin-derived CFs, which were named Kayacarbon.[127] Mikawa, also from Nippon Kayaku, also discussed this method.[128] The advantages of this method were primarily related to cost efficiency, as well as to the high carbon yields and the fact that no thermostabilization was needed, because of the use of infusible lignin. The applied spinning process entailed the use of alkaline lignosulfonate solutions and PVA followed by dry spinning. Subsequent carbonization could be performed with high heating rates above 30 K min^{-1}, which resulted in CFs with good mechanical properties. Fibers had diameters of 10–16 μm and were claimed to possess tensile strengths of 0.6–1.2 GPa. In 1974, Gould reported on the manufacturing of lignin-derived CFs from a melt-spinning process.[129] Shortly after, Mansmann described in two patents a method for producing CFs from lignin.[130] For this process, lignosulfonate was utilized, preferably in the form of the ammonium salt or

of the free lignosulfonic acid to minimize contamination of the fiber by metal ions. However, manufacture became possible with considerably lower amounts of polymeric additives such as ≤ 5 wt% of poly(ethylene oxide) (PEO) or poly(acrylamide). The use of 0.3–0.5 wt% PEO with a molecular weight of 5000 g mol^{-1} was found to be sufficient for effecting adequate spinnability. With lower molecular weights, the concentration of polymer had to be increased up to a maximum of 5 wt% to achieve equal spinnability. Furthermore, the viscosities of the spinning solutions were tuned and adapted to the spinning process by adjusting the pH value. Tensile strengths up to 0.8 GPa were reported. In the 1970s, the production of lignin-based CFs through these methods was terminated and research activities in this field almost ceased.

2.4.3. *Melt Spinning*

Interest in lignin-based CFs increased again in the early 1990s. At that time, research mainly focused on melt spinning. Therefore, fusible lignins were required and to some extent this could be achieved by tuning the pulping process; in other cases plasticizers were added to the system. However, the melt-spinning process required an additional process factor, that is, thermostabilization. In fact, this is the most essential step to prevent the fusing of the melt-spun fiber during thermal treatment. During the course of thermostabilization, the temperature is kept below the glass transition temperature of lignin, typically below 300 °C, and very slow heating rates are applied in an oxidizing atmosphere, which effects the cross-linking of the lignin moieties. In this way, the fiber shape can be preserved. Clearly, the advantages of melt spinning are related to its simplicity and the fact that no solvent is needed.

Sudo and Shimizu used hydrogenated and thermally treated steam-exploded lignin to obtain a pitch-like material for spinning.[131] Alkaline hydrogenolysis with Raney-Ni as a catalyst results in cleavage of alkyl–aryl ether bonds and the formation of ethylene bridges between aromatic rings. However, both the melting point and the viscosity of the hydrogenated lignin were too low for melt spinning. Heat treatment of the material at 300–350 °C under nitrogen or vacuum improved the viscosity and made the lignin suitable for melt spinning. The pitch-like material could be spun between 155 and 180 °C. Fibers were stabilized up to 210 °C by applying a heating rate of 1–2 K min^{-1} in air, before carbonization at 1000 °C under nitrogen using a heating rate of 5 K min^{-1}. Carbon yields with respect to the starting material were as low as 15.7–17.4%. A tensile strength of 0.66 GPa and a Young's modulus of 40.7 GPa were reported for these fibers. A few years later, Sudo et al. improved his process with respect to energy consumption and carbon yield.[132] Phenolated lignin was used, which was prepared by treatment of the lignin with phenol or creosote at reaction temperatures of 180 to 300 °C. Stabilization of the lignin fiber required thermal treatment at 220–280 °C in a vacuum prior to melt spinning. The mechanical properties of the CFs were nearly the same as those obtained with hydrogenated lignin, and the highest value for the tensile strength was 0.45 GPa; however, the carbon yield could be improved to more than 40%.

In 1995 Uraki et al. reported the preparation of lignin-based CFs from an organosolv lignin, which was obtained by aqueous acetic acid pulping of birch wood.[133] The isolated lignin could be spun without any further modification as some of the hydroxy groups were acetylated during pulping. It turned out that the spinnability increased with an increasing degree of acetylation. In contrast, saponified lignin could not be melt spun into fibers, because the material hardened without melting. Lignin was fractionated into a low- and a high-molecular-weight fraction to allow investigation of the interdependency between spinnability, molecular weight, and polydispersity. The low-molecular-mass fraction had a low melt viscosity and could not be spun into fibers. The high-molecular-mass fraction was no longer fusible and hardened with increasing temperatures. Apparently, the low-molecular-weight fraction acted as a plasticizer in the unfractionated lignin, while the high-molecular-weight fraction provided sufficient viscosity for melt spinning. A high polydispersity index was found to be advantageous. However, spinning for long periods of time was not possible and the obtained fibers had a rough surface and were porous. Subjecting the material to thermal treatment prior to melt spinning led to improvements in terms of spinnability, porosity, and surface. Thermostabilization of the melt-spun fibers was carried out in pure oxygen at 250 °C by applying a heating rate of 0.5 K min^{-1} and a holding time of 1 h at 250 °C. By contrast, the fibers fused together during stabilization in air. Stabilized fibers were carbonized at 1000 °C by using a heating rate of 3 K min^{-1}. CFs obtained by this process showed tensile strengths of 0.36 GPa and a carbon yield of 32.7%. Based on these accomplishments, Uraki et al. investigated a process for preparing activated CFs from softwood and hardwood lignin.[134] In 1998, they presented a method in which melt-spun softwood lignin fibers from acetic acid pulping could be carbonized without thermostabilization.[135] They also compared the fusibility of softwood and hardwood lignin from acetic acid pulping. Hardwood lignin showed sufficient fusibility for melt spinning, because of the partial acetylation during the pulping process, whereas softwood lignin could be converted into a fusible material by removing the infusible fraction. However, the authors did not succeed in converting softwood lignin from a kraft pulping process into a fusible and spinnable material. Thus, the spinning temperature of softwood lignin from acetic acid pulping had to be set to 350–370 °C. This is very high compared to the spinning temperature of hardwood lignin (210 °C). Generally, such a high spinning temperature results in substantial thermal stress to the material. Thermally induced decomposition and cross-linking reactions take place and the material is no longer fusible. However, because of the high spinning temperature applied, thermostabilization became unnecessary, at least for softwood lignin. Therefore, processing without thermostabilization seemed to be an improvement; however, the fiber properties were unsatisfactory. The surface of the fibers was damaged, and the mechanical properties were inferior to that of CFs derived from hardwood lignin. However, fibers derived from hardwood lignin could not be converted into CFs without thermostabilization because of the reduced spinning temperature.

Driven by the low-cost renewable feedstock, the sustainability, the independence from the oil price, and availability, the Oak Ridge National Laboratory (ORNL) entered this field of research in 2001.[136] Since kraft pulping is a widely used process and provides low-cost lignin, Compere et al. selected a softwood kraft lignin as the precursor material. Blends of lignin with different polymers (poly(ethylene) (PE), poly(propylene) (PP), PEO, poly(ethylene terephthalate) (PET)) were melt spun at temperatures between 130 and 260 °C. The fibers were stabilized, carbonized, and graphitized. Powder diffraction data of a lignin-based fiber treated at 2400 °C confirmed the graphitic structure. Scanning electron micrographs showed fibers without holes or pores and a smooth surface. In 2002, Kadla et al. also reported a method for producing lignin-based CFs from lignin–polymer blends. They used organosolv as well as softwood and hardwood kraft lignin. However, the softwood kraft lignin could not be spun into fibers because of the lack of fusibility. Lignin–polymer blends were made using PE, PP, PEO, and PET.[137] The experiments were unsuccessful as the nonpolar polymers PE and PP were immiscible with lignin. The lignin formed core–shell structures with these polymers during extrusion, with the lignin being found in the shell of the fiber and the nonpolar polymer in the core, sometimes in the form of nanofibers.[138] Nevertheless, although such fibers were not suitable for high-performance application, they offered a straightforward access to activated CFs.[139] Melt spinning was carried out below the decomposition temperature: organosolv lignin was melt spun at 155 °C and hardwood kraft lignin at 180 °C. The spinnability of the system was only improved with PEO as a spinning additive, whereas spinning of the lignin/PE blend was nearly impossible. Different heating rates for the stabilization were tested; however, stabilization of the organosolv/PEO fiber could not be accomplished, even with heating rates of 0.2 $K\,min^{-1}$. Generally, the stabilization of hardwood kraft lignin fibers could be achieved more easily. However, the mechanical properties of the CFs were hardly better than those of the CFs prepared from acetic acid pulping lignin. The highest value for the tensile strength obtained was 0.46 GPa. Carbon yields were > 40 %. Shortly after, Kubo and Kadla investigated the interactions in lignin–PVA blends and their spinnability.[140] The melt spinning of pure PVA is challenging, because the melt and decomposition temperature are close to each other.[141] Lignin was used as a plasticizer in this case, and the processability of PVA could be improved. Melt spinning with a high-molecular-weight PVA ($M_w = 93\ kg\,mol^{-1}$) was hardly possible because of the high viscosity of the PVA melt, whereas a relatively low molecular weight PVA ($M_w = 13–23\ kg\,mol^{-1}$) showed good spinning properties within the lignin blend. Macroscopically, the obtained fibers seemed to be homogeneous, but observations under polarized light revealed a heterogeneous structure with both crystalline PVA and amorphous lignin areas. This was confirmed by DSC measurements. However, the crystallinity of PVA could be reduced by blending with lignin, thereby establishing intermolecular interactions. The properties of the obtained fibers were not investigated in detail. In 2004, Kadla and co-workers again investigated the properties of lignin–polymer blends with PP, PVA, PET, and PEO and their intermolecular interactions.[142] Both PEO and PET were highly miscible with lignin, but lignin–PEO blends showed more interactions in the form of intermolecular hydrogen bonds. Consequently, lignin–PEO blends showed the best spinnability and possessed good thermal properties. Experiments with a hardwood kraft lignin also led to good results. A softwood kraft lignin could not be processed in a pure form, but was possible after blending with 50 wt % PEO. Interactions between the softwood blend were weaker than those in the hardwood blend.[143] To address the sustainability, Kubo und Kadla again investigated fibers prepared from hardwood lignin blends with PP and PET. Better results could be achieved with PET because of the immiscibility of lignin and PP. In this case, the heating rate of thermostabilization could be increased from 0.5 $K\,min^{-1}$ for pure lignin to 2 $K\,min^{-1}$ for the blend. Carbon yields decreased with higher polymer contents in the blends, but to an acceptable extent. They obtained CFs with tensile strengths of up to 0.7 GPa and Young's moduli up to 94 GPa with a lignin–PET blend precursor.[144] Based on these developments it was possible to spin multifilaments with 4 to 28 filaments for the first time.

Having proved that lignin can in principle be used as a CF precursor, both the process and the properties of the final CFs had to be further optimized. Thus, the quality of the precursor and its purification were addressed. As a rule of thumb, the ash content of the precursors should be less than 1000 ppm and the sulfur content should be as low as possible. These specifications for the precursor were, in particular, discussed by Compere et al.[145] In 2005, Compere reported the best mechanical properties so far. This report deals with the evaluation of soda hardwood lignin as a CF precursor.[146] Single filaments of lignin–PET blend fibers were carbonized at 1200 °C and reached tensile strengths up to 1.03 GPa with a Young's modulus up to 109 GPa. However, holes and pores in the final CF and changes in the material as a consequence of the residence time in the extruder remained challenging.

In 2007, Eckert described the possibility to melt spin and carbonize acetylated softwood lignin.[147] Another method for processing softwood lignin was presented by Warren in which softwood and hardwood lignin were blended. In this case, the fusible hardwood lignin acted as a plasticizer.[123a] Alternative stabilizing methods beyond the existing thermal processes for stabilization were discussed. Treatment with electron beams, UV radiation, or plasma were discussed, but no significant progress could be made.[148] Baker and co-workers found big differences when performing rheological studies on several lignins. The differences in the rheological behavior correspond to differences in the spinnability and thermal resistance. Lignin reacts sensitively to thermal stress through cross-linking reactions, which is expressed in gradually increasing viscosity. Unfortunately, the properties of lignin melts from untreated lignin samples were not constant.[149] This issue could, however, be eliminated by using purified lignin, which was prepared by extracting lignin with organic solvents.[150] This lignin provides constant viscosities at 150 °C for 60 min. In contrast, an increase in viscosity was observed during frequency measurements of the same lignin at 210 °C in air, whereas measurements under nitrogen led only to a slight increase in viscosity.[151] However, this lignin showed good

spinnability and the melting temperature decreased from 200 to 130 °C as a result of the purification. However, the low spinning temperature leads to a lower thermostabilization. The fusing of fibers could only be prevented by applying very low heating rates of less than 0.05 K min^{-1}.[122b] Better spinning properties of lignin melt were obtained, as relative low spinning temperatures and suitable constant viscosities for spinning lead to difficulties in thermostabilization. Very slow heating rates had to be applied to prevent the fibers from fusing together.[152] A further approach for optimizing the system was to add carbon nanotubes to the precursor material. Melt-spun fibers with up to 10 wt % carbon nanotubes showed better mechanical properties compared to the pure lignin fibers. However, the properties of the resulting CFs were not specified.[149b,153] In 2012, Eberle claimed tensile strengths of 1.2 GPa and a Young's modulus of 83 GPa for a CF prepared from softwood lignin.[154] Baker et al. reported on the successful melt spinning of solvent-extracted fractions of softwood kraft lignin. They simulated the oxidative thermostabilization and carbonization by thermogravimetric analysis and obtained different behavior during the thermostabilization of the fractionated lignins. The lignin fraction with the highest glass transition temperature could be stabilized with the highest heating rate.[155]

Patents from Toho Tenax and Lignol Innovations cover a wide range of potential CF precursors by claiming as many modifications of lignin as possible. However, the advantages of these systems were not presented clearly.[156] Another patent of Toho Tenax described the analytical properties of a lignin precursor system.[157] In 2011, Luo et al. reported on lignin-based CFs from a modified kraft pulping process, but the properties of the final CFs were inferior by far to the state of the art CFs.[158] Qin and Kadla investigated a pyrolytic lignin that was extracted from bio-oil as a precursor. After optimization of the pretreatment, the spinning process, and the thermostabilization, CFs with tensile strengths of 0.37 GPa and Young's moduli up to 36 GPa were presented. The mechanical properties were thus in the same range as those of CFs derived from conventional lignin precursors.[159] Qin and Kalda also found that organoclay loadings below 1 wt % improved the mechanical properties of CFs by 12 %.[160] Sevastyanova et al. investigated the reinforcement of CFs from organosolv lignin with organoclay.[161] Nordström further investigated the plasticizing effect of hardwood lignin on softwood lignin and could obtain dense and smooth lignin fibers from these blends.[162] The CFs had a tensile strength of 0.3 GPa and a Youngs modulus of 30 GPa.[26k,163] In 2012, Awal and Sain presented rheological investigations on soda hardwood lignin and blends with PEO. They also succeeded in processing this precursor into fibers.[164] Prauchner et al. presented bio-pitch as a potential CF precursor. This lignin- and pitch-like precursor was obtained by the pyrolysis and condensation of eucalyptus wood and mainly consisted of lignin monomer units.[165] After thermal pretreatment, the pitch-like material was melt spun, stabilized, and carbonized. Unfortunately, the mechanical properties of the resulting CFs were not satisfactory, with tensile strengths of ≤ 0.13 GPa and Young's moduli < 14 GPa being found.[166]

As a consequence of the lack of progress in the manufacturing of lignin CFs and the awareness of the complexity of the feedstock, purification methods and analytical investigations came to the fore.[167] Several investigations revealed the complexity of lignin materials.[168]

In the early days of lignin-based CF research, PAN was already mentioned as a possible spinning additive.[126] Since 2011, lignin–PAN blends again appeared in the literature as precursors for CF manufacturing. Seo et al. reported a lignin–PAN blend that was processed by electrospinning and consequently not accessible on a large scale.[169] A few publications on the manufacture of CFs from such a blend material appeared; however, the blends were processed by wet spinning.[170] Lehmann et al. also mentioned the use of cellulose and cellulose derivatives as spinning additives.[171]

The electrospinning of lignin was also investigated; however, in most cases fibers could not be formed without additives and rather beaded structures were obtained.[169,172] Hosseinaei and Baker were able to make carbon nanofiber mats without additives. The fibers have smooth surfaces without defects. They used softwood kraft lignin, which they purified by solvent extraction prior to electrospinning.[173]

2.4.4. *Structural Investigations of Lignin-Based Carbon Fibers*

In 1974, Johnson and Tomizuka investigated the structure of lignin- and pitch-based CFs and found that lignin-based fibers did not possess any preferred orientation.[174] A lignin-derived CF that carbonized at 1500 °C showed properties comparable to those of PAN-derived CFs heat treated at 400–600 °C. The lignin-based CFs possess a low degree of orientation and cross-linking as well as pores and heterogeneities in the fine structure of the fiber. These heterogeneities appeared as areas with a higher degree of graphitization, which formed by the action of inorganic impurities acting as graphitization catalysts. This resulted in density fluctuations and, therefore, a decreased strength of the material. In 1975, Johnson et al. reinvestigated the fine structure of lignin-derived CFs in detail.[36c] They used CFs prepared by a dry-spinning process with PVA as a plasticizer and carbonized at 1500 °C and 2000 °C. Differently shaped areas with a higher degree of graphitization could again be identified by scanning electron microscopy. In addition, X-ray diffraction (XRD) patterns were analyzed to determine the degree of orientation and value of L_c. Generally, lignin-based CFs carbonized at 2000 °C were poorly oriented. Tomizuka and Johnson investigated microvoids in lignin- and pitch-based CFs by means of XRD.[175] The microvoids found in lignin-based CFs were partially comparable to microvoids in pitch-based CFs. However, in lignin-based CFs, bigger voids were also found, and their size and shape were much more complicated to determine. In 1993, Davé et al. analyzed lignin fibers in substances with liquid-crystalline phases. They compared the results to lignin model compounds and pitch.[176] Difficulties in the examination of mesophases of natural lignin resulted from inhomogeneous carbonization. At that temperature, where mesophases could best be observed, carbonized particles already appeared. It was, therefore, assumed that the inhomogeneous melting behavior

of lignin prevents any improved tensile strength of the final material. Rodriguez-Mirasol et al. investigated carbonized kraft lignins in terms of their ash content at different carbonization temperatures (1400–2800 °C) by using XRD, Raman spectroscopy, scanning electron microscopy (SEM), and N_2 adsorption.[177] N_2 adsorption measurements showed reduced specific surface areas with increasing temperature. The X-ray diffractograms showed increased peak intensities at higher temperatures, whereas the half width decreased as a result of an increasing thickness L_c of the graphite-like crystals. The spacing between the planes was reduced with increasing temperature. Raman measurements also confirmed the presence of more and more ordered graphitic structures at elevated temperatures, which were comparable to carbon materials obtained from other precursors such as PAN and pitch. The reactivity of carbonized lignin towards oxygen, with a conversion of up to 40 %, was similar to that of graphite. At higher conversions, carbonized lignin showed lower oxidation resistance. Rodriguez-Mirasol et al. assumed that the core of the carbonized lignin material consists of turbostratic carbon. To confirm whether impurities of lignin precursors act as graphitization catalysts, as observed by the research group of Johnson,[36c] lignin precursors with different ash contents were analyzed by XRD and their oxidation resistances were determined. The increasing structural order with more inorganic impurities was verified by XRD, oxidation resistance, and SEM measurements. As evident from SEM studies, the differences in structure were already generated at relative low temperatures. Baker investigated lignin-derived CFs by XRD and compared the results to those obtained with a commercially available PAN-based T-300 CF. The diffractogram of lignin-based CFs carbonized at 2100 °C was similar to that of T-300 CF.[149b] Consequently, the low mechanical strength of lignin CF is not related to the quality of the graphite crystallites, but to their orientation. Thus, in contrast to PAN-based CFs, the graphite crystallites have little preferential orientation along the fiber axis (Figure 27).[151]

Prauchner et al. reported on structural conversions during the carbonization of an eucalyptus tar pitch material.[178] This material was obtained by pyrolysis and condensation and consisted mainly of lignin monomer units. XRD measurements showed properties similar to lignin, however, an ordered structure was observed at low temperatures (from 600 °C) as a result of the better mobility of the smaller molecules. Davé et al. reported on a similar behavior with regards to liquid-crystalline phases observed with lignin model compounds. A general important issue in the production of CFs is their thermostabilization. Braun et al. investigated the thermostabilization in more detail.[179] The process was monitored at heating rates of 0.11 to 1.0 $K\,min^{-1}$ by means of elemental analysis, TGA, XPS, FTIR spectroscopy, solid-state NMR spectroscopy, and DSC. An increasing oxygen content and the formation of carbonyl and carboxyl groups was observed. At higher temperatures, the number of aromatic protons decreased and more C–C bonds formed. An optimum heating rate could be predicted for the investigated lignin from a continuous heating transformation diagram. According to the constructed diagram, it should be possible to hold the glass transition temperature above the currently applied temperature by applying a heating rate of 0.06 $K\,min^{-1}$. Experiments revealed that fiber fusion can be prevented by using heating rates of 0.2 $K\,min^{-1}$. Foston et al. used NMR spectroscopy to monitor the demethoxylation and the appearance of carbonyl and carboxyl structures during stabilization, which were presumed to be formed by the generation of ester and anhydride groups through cross-linking reactions. At higher temperatures, a lower number of carbonyl and carboxyl structures was observed, but the fractions of uncondensed and condensed aryl carbon atoms increased.[180] Brodin and co-workers investigated the chemical processes taking place during the pyrolysis of lignin between 200 and 700 °C and deduced the reactions that were occurring from the results obtained by GC/MS equipped with a pyrolyzer.[122a] They compared the pyrolysis products of native lignin and of lignin thermally treated in air and nitrogen. They detected a lower mass loss for a sample thermally treated in air compared to a sample treated similarly under nitrogen. The methylation of lignin partially produced the corresponding methylated degradation products, however, the same mass losses occurred, while the glass transition temperature decreased. The oxidative stabilization of lignin was further investigated to identify the influence of the heating rate, final temperature of stabilization, and holding time. Brodin and co-workers also discussed the mass losses during stabilization and carbonization as well as the glass transition temperatures. Changes in the temperature programs lead to different behavior in terms of mass losses at the different stages of heat treatment. In the case when stabilization was performed with slow heating rates to high temperatures, contiguous to the lignin decomposition temperature, with additionally long holding times at the final stabilization temperature, the lignin showed an increased mass loss during stabilization treatment. In the case of milder conditions, that is, higher heating rates, a lower final temperature, and shorter holding times at the final stabilization temperature, the lignin showed a reduced mass loss in comparison to that when the stabilization treatment was carried out under harsher conditions. Carbon yields after carbonization were higher in the case when harsher conditions were applied during stabilization and lower with mild stabilization conditions. Monitoring of the glass transition

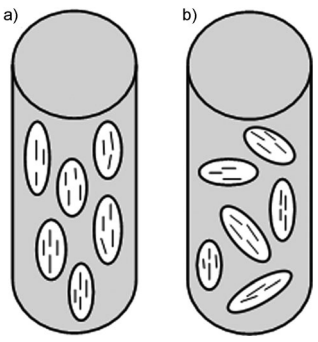

Figure 27. Degree of orientation of graphite-type crystallites along the fiber axis in a) PAN-based and b) lignin-based CFs (according to Baker et al.).[151]

temperatures showed the different stabilization times for hardwood and softwood lignin. A shift of the glass transition to higher temperatures could be observed for relatively long periods of time during the stabilization of hardwood lignin. In the case of softwood lignin, no glass transition temperature could be measured after a short period of time, because softwood lignin was no longer fusible, because of completed cross-linking reactions during the stabilization.[181] Through optimization of the holding time, Brodin and co-workers were able to stabilize lignin fibers in the absence of oxygen and without the formation of fused fibers. This clearly reveals the possibility of a single-step process. The holding time had to be adjusted from 80 to 255 min when 5–10 wt % hardwood lignin was added to softwood lignin. However, the stabilization times could be reduced to 45 or 105 min, respectively, when the stabilization was carried out in air.[182]

2.5. Poly(ethylene) (PE) Based Carbon Fibers

Early investigations on the carbonization of PE started in 1972. PE powder was chlorinated for stabilization and carbonization purposes, and clearly demonstrated the possibility to convert PE into aromatic structures.[183] A process of producing CFs from PE was first disclosed in a US patent.[184] To reach high carbon yields, the PE must be treated chemically to substitute hydrogen by heteroatoms so as to stabilize the carbon skeleton of the polymer for carbonization. Sulfur turned out to be an appropriate heteroatom, because pure oxygen degrades the PE at higher temperatures. A strong oxidizing agent, for example, sulfuric acid, oleum, or chlorosulfonic acid, is needed to remove the hydrogen from the carbon backbone and to add the sulfur atom in a suitable way to the carbon backbone because of the high binding energy of the C–H bonds. To achieve this sulfonation, melt-spun PE fibers were immersed in chlorosulfonic acid, sulfuric acid, fuming sulfuric acid, or a mixture thereof at 80 °C. The carbonization of the resulting precursor fiber was carried out by heating between 600 and 3000 °C; tension could also be applied to the fiber during the heating. Carbonization yields were as high as 75 % and, with the application of tension, the elastic modulus and tensile strength were 139 GPa and 2.5 GPa, respectively.

In the early 1990s, Dunbar et al.[185] disclosed a method for producing CFs from a synthetic PE precursor that yielded fair tenacity and good tensile modulus by using highly oriented and highly crystalline UHWMPE fibers. The approach was similar to the one used by Horikiri et al.,[184] except that stabilization times were longer and graphitization temperatures were higher (between 2000 and 3000 °C). Zhang et al.[186] also used highly oriented PE fibers and investigated the effects of time, temperature, tension, and the sulfonation medium on the properties of the final CFs. They compared both partially and highly oriented PE precursors, and showed that the wet acid stabilization time decreases with the use of only partially oriented PE (LLDPE); unfortunately the properties of the CFs also worsened. This again points towards a situation where the orientation of the crystallites of the progenitor fiber carries over into the orientation of the graphitic crystallites of the final CF.

Despite these drawbacks, the increasing prices of PAN-based precursors have resulted in renewed attention to the field of PE-based CFs. In 2004, HEXCEL obtained good results with a PE precursor on a pilot scale. They constructed a pilot plant in which PE could be treated with sulfuric acid (Figure 28).[187] LLDPE was used for better spinnability in

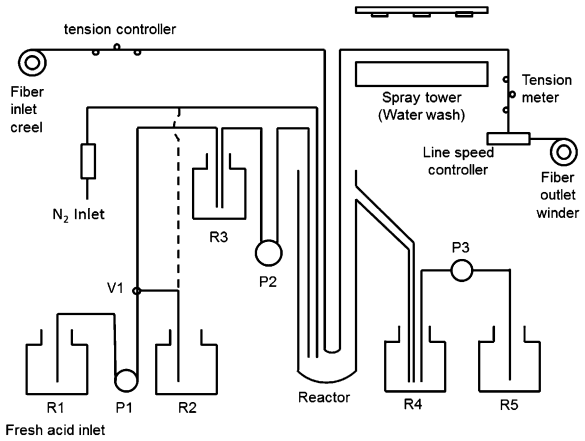

Figure 28. HEXCEL pilot line for the stabilization of PE precursors, with acid reservoirs R1–R5 and pumps P1–P3 used for continuous refreshing of the sulfuric acid in the reactor.[187] Reproduced with permission from SAMPE.

melt spinning and because of its better reactivity in wet acid treatment (concentrated sulfuric acid). Sulfuric acid concentrations of at least 97 wt % are necessary to obtain high carbon yields (Figure 29). The best carbon yields were around 65 %, with tensile strengths up to 1.54 GPa and Young's moduli up to 134 GPa (although in another trial). The reaction was carried out under nitrogen since small amounts of water from air generally prevent good stabilization.

In recent years, ORNL improved the wet acid sulfonation method for PE precursors by using a LLDPE precursor.[188] ORNL used a complex bicomponent spinning method to

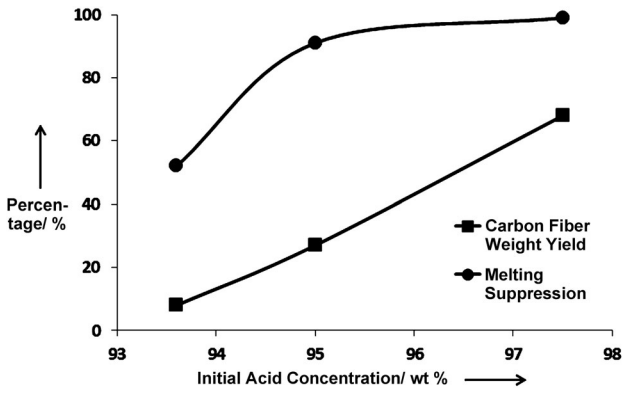

Figure 29. Dependency of melting suppression (fiber fusing) and carbon yield on the concentration of sulfuric acid.[187] Reproduced with permission from SAMPE.

obtain the necessary PE precursor filament diameter. In this method, a matrix of PLA was employed, which was re-dissolved after spinning in THF at 50 °C to obtain the remaining PE filaments. These were sulfonated at 70 °C in 20 wt % fuming sulfuric acid and then carbonized (Figure 30). No information on the PE used or about the mechanical data of the CFs was given by the authors.

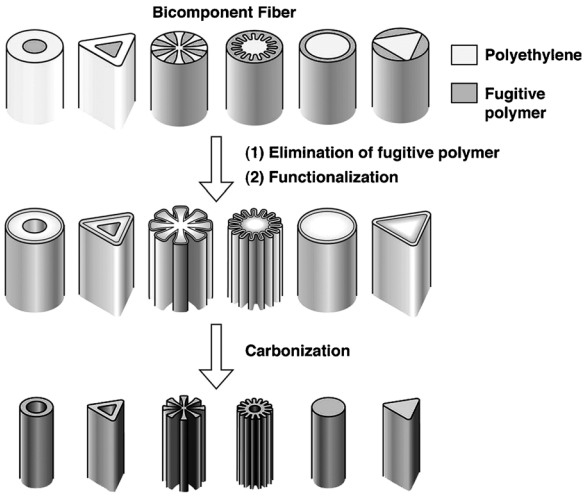

Figure 30. Principle processing path for the preparation of patterned CFs from PLA/PE precursors by sulfonation and carbonization.[188] Reproduced with permission from Wiley.

2.6. Other Synthetic High-End Precursors

Apart from the precursors discussed so far, numerous other, less-common sources for CFs deserve to be mentioned. Thus, CFs have been prepared from Saran, a poly(vinylidene chloride)-poly(vinyl chloride) copolymer.[189] Tensile strengths up to 0.24 GPa and Young's moduli up to 28 GPa have been reported for the final CF. Thermal decomposition of the initial fiber and formation of graphitic units was followed by both IR spectroscopy and XRD. A patent filed by Sumitomo Chem. Co. in 1972 describes the use of poly-(styrene) (PS), chlorinated PS, and poly(acenaphthylene)-based fibers as progenitors to CFs (Figure 31). Oxidative stabilization was achieved by chlorosulfination, sulfonation, nitration, or treatment with SO_3. Carbon yields up to 82.5 % were realized; however, no values for the tensile strength or the modulus of the final CFs were given.[190] Melt-spun poly(butadiene) (PBD, Figure 31) fibers prepared from highly crystalline syndiotactic (*st*) PBD with a vinyl content of at least 85 % were cross-linked by the action of Lewis acids and subsequently treated with molten sulfur or a sulfur-containing solution. This treatment resulted in the dehydrogenation of PBD. CFs were formed by a subsequent heat treatment up to 3000 °C.[191] Tensile strengths and Young's moduli of 2 and 400 GPa, respectively, have been reported for these CFs.[192] By contrast, atactic BPD fibers prepared by a similar approach showed a tensile strength of only 1.2 GPa and a modulus around 70 GPa.[191] These results clearly point to the importance of preorganization of the polymer chains prior to any cross-linking/oxidative stabilization and carbonization.

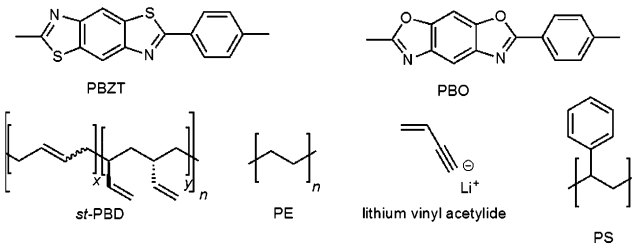

Figure 31. Structure of CF precursors.

In 1968, Coal Ind. Ltd. filed a patent in which the production of CFs from phenol/hexamine and from phenol/formaldehyde/ammonia is described.[193] The tensile strengths and Young's moduli of the final CFs were reported to be 2.1 and 69 GPa, respectively.[194] Economy and Lin reported on an activated CF prepared from highly cross-linked phenolic precursors and their use for the removal of iodine.[195] Celanese Inc. claimed the production of CFs from polyamide 6.6 as well as from an aromatic polyamide prepared from terephthalic acid and hexamethylene-1,6-diamine.[196] The tensile strengths and Young's moduli reported for CFs prepared from the aromatic polyamide were 0.7 and 69 GPa, respectively. Clearly, the use of aromatic precursors, here terephthalic acid, accounts for the formation of CFs with a high content of aromatic (graphitic) units, which favor high Young's moduli.

In 1989, Murakami filed a patent in which the use of polyaromatic fiber progenitors, that is, of poly(phenylene-oxadiazole), poly(benzothiazole)s, poly(benzobisthiazole), poly(benzoxazole), poly(benzobisoxzole), and poly(thiazole), for CF production were described.[193b] With these progenitors, 100 % graphitization was claimed at $T \geq 2800$ °C, thereby suggesting that precursors with a high degree of aromatization such as the ones used facilitate the formation of graphitic structures at elevated temperature. Furthermore, the use of polyaromatic, stiff-chain precursors such as poly(*p*-phenylene benzobisthiazole) (PBZT, Figure 31), allows the generation of CFs with a high Young's modulus.[197] PBZT-fibers with diameters of 20 μm were obtained by dry-jet wet spinning. Oxidative stabilization followed by carbonization resulted in elastic moduli up to 200 GPa. In contrast to PBZT fibers, poly(*p*-phenylenebenzobisoxazole) (PBO, Figure 31) fibers can be converted into CFs without any oxidative stabilization.[198] Upon thermal treatment, similar to PAN-derived fibers, the tensile strength of the PBO-derived carbon fibers displays a maximum around 1500 °C, while the tensile modulus increases up to at least 2000 °C. XRD measurements indicate a conversion from a highly oriented state into an amorphous one around 600 °C. At $T = 1600$ °C, a turbostratic carbon structure develops, which is in accordance with the maximum tensile strength at this temperature. Newell and Edie stated that the reduced tensile strength of PBO-derived CFs is related to flaws in the parent PBO fibers.[199] Consequently, any improvement in the spinning process for PBO fibers improves the tensile strength of the final CF. More interesting, rapid heating turned out to improve the tensile strength of the final fiber. This finding was attributed to the

fact that the graphite crystallites that form are smaller in diameter when rapid heating is applied and to the finding that the evolution of nitrogen occurred after formation of the graphite crystallites. Clearly, the damage to the fiber during the release of nitrogen is much smaller when small crystallites are converted into the final CF structure. An in-depth investigation of the kinetics of the carbonization and graphitization of PBO fibers revealed an activation energy of $(318 \pm 25)\ kJ\,mol^{-1}$ for the thermal initiation of free radicals.[200] Spacing between individual graphene planes was reduced with increasing temperature. The energy for graphitization was found to be $(502 \pm 71)\ kJ\,mol^{-1}$. Notably, carbonized PBO fibers were found to possess a more developed long-range order than CFs produced from other progenitors, for example, from PAN or pitch. Small- and wide-angle X-ray scattering (SAXS and WAXS) studies on PBO-derived CFs complemented by transmission electron microscopy (TEM) provided further insight into the development of the final CF structure.[201] Kaburagi et al. reported on the formation of carbon layers extending along the fiber axis. The interlayer spacing d_{002} was 0.3355 nm and was thus very close, if not identical, to the theoretical value for graphite ($d_{002} = 0.335$ nm). In terms of crystallite sizes, values for L_c and L_a of > 100 nm were reported.[201a] The authors also emphasized that the PBO-derived CFs were highly oriented and graphitized. Lázló and co-workers suggested that the preferential preorganization of the individual polymer chains in the PBO fibers leads to a multiscale orientation that is close to the lamellar nanostructure of graphitizable carbon atoms.[201b] This preorganization is apparently essential for structure evolution. At 900 °C, graphene-type structures with their *c*-axes perpendicular to the domain axis are present. Holes, resulting from the shrinkage of the parent PBO polymer along the axis, exist between these domains. The shrinking that occurs upon carbonization is not uniform; instead, independent carbonized sections are formed. After heating to 2000 °C, a compact, lamellar nanostructure is formed, which is, however, still imperfect. Nonetheless, this lamellar structure provides a sufficiently robust template to allow the remaining structure to coalesce and graphitize with the same orientation.[202] After heating to 2700 °C, the longitudinal packing becomes denser, the graphitization proceeds, the structure is mostly lamellar, and the fibrils are up to 50 nm thick. Notably, the preferential axial orientation of the graphitic layers is a result of the internal fibril structure, which is itself dependent on the draw axis of the PBO fiber. Vásquez-Santos et al. also investigated the effect of additional phosphoric acid on structure formation during the carbonization of PBO fibers.[203] A comparably weak effect was found, which is not surprising, in view of the fact that PBO fibers contain substantial residual amounts of poly(phosphoric acid) from wet spinning. Finally, Vásquez-Santos et al. prepared activated CFs from PBO by chemical activation with phosphoric acid. Specific surface areas up to $1.250\ m^2\,g^{-1}$ could be realized.[204] In an alternative approach, CO_2 was used as an activator, which resulted in specific surface areas up to $943\ m^2\,g^{-1}$.[205]

Researchers at General Electric proposed a continuous process in which melt-spun poly(acetylene)/phenol dipropargyl ether blends from poly(*m*-diethynylbenzene) or poly(*p*-diethynylbenzene) were converted into CFs.[206] Dichlorobenzene or pyridine was used as a plasticizer. Tensile strengths of drawn and carbonized fibers were around 2.3 GPa and a modulus of 390 GPa was obtained.

Pennings and co-workers prepared poly(vinylacetylene) from lithium vinyl acetylide (Figure 31) by anionic polymerization and subjected the polymer to melt spinning.[207] Oxidative stabilization allowed the carbon yield to be increased to 62 %. Cyclization of the pendant alkyne moieties, similar to the process occurring in PAN-derived CFs, was shown to occur around 230 °C. No information on a CF prepared from this progenitor was provided.

Finally, CFs prepared form polyimides need to mentioned, unfortunately, substantial information on the parent polymer is not provided.[208]

3. Structure and General Precursor Requirements

In contrast to other allotropic forms of carbon, such as graphite and diamond, the structure of CFs is rather complex.[209] A main structural motif of a CF is the so-called turbostratic carbon (Figure 32) The crystallites are composed of more- or less-bent layers with sp^2-hybridized carbon atoms.

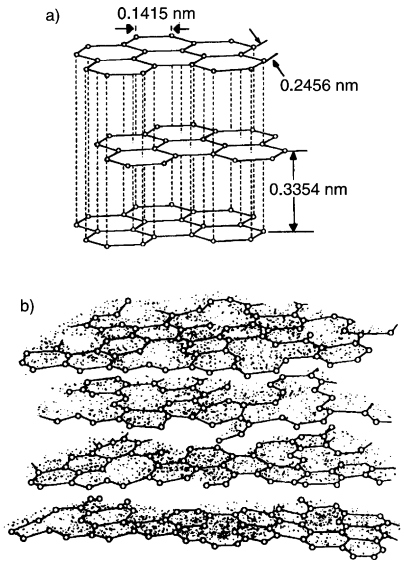

Figure 32. Three-dimensional graphite (a) and turbostratic carbon structure (b).[210] Reproduced with permission from Cambridge University Press.

The crystallites are defined by their length L_a, their thickness L_c, the interlayer distance d_{002} between the carbon layers, and the mean orientation of the crystallites, with 0 for a fully non-oriented carbon and 1 (100 %) for a (theoretically) perfect oriented fiber.

As outlined earlier, a polymeric precursor has to fulfill many requirements to be applicable for the production of CFs. This includes spinnability and orientation. To achieve acceptable mechanical values in terms of tensile strength and

Young's modulus (stiffness), at least 70–80% of the polymer chains of the precursor must have the same orientation. For high-modulus CFs, typically >80% of the polymer chains must have the same orientation. The resulting modulus solely depends on this orientation, not on the underlying precursor system.

Another important point is related to stabilization. Thus, for carbonization, the precursor fiber may not melt and any fusion of single filaments of the precursor fiber has to be avoided. As an additional effect, the presence of heteroatoms such as oxygen and nitrogen stabilizes the carbon backbone of the precursor polymer, and this results in both the carbon yield and the quality of the resulting CFs subsequently being increased. Finally, the carbon yield is an issue. As the thermal treatment uses a lot of electrical energy, the mass loss during conversion of the precursor into the CF has to be minimized.

In terms of polymer structure, some rules of thumb apply for a CF precursor polymer:[211]

a) Linear or branched alkyl chains are not stable during carbonization. Cross-linking by chemical or radiation methods typically does not change this behavior. Examples are poly(ethylene), poly(propylene), and poly(styrene), which do not carbonize without chemical modification.
b) The precursor should have a high content of double bonds and/or aromatic groups as part of the main chain at the beginning of the carbonization. If double bonds or aromatic groups are not present from the very beginning as in, for example, pitch, the precursor polymer must be able to undergo aromatization through cyclization or cross-linking of the polymer chains in early states of the carbonization.
c) In polymer chains containing aromatic groups, the aromatic rings should be connected by not more than one carbon atom. Example: -Ar-CH_2-Ar-CH_2-….
d) Heteroatoms in the side groups (X = O, N, P, S, Cl) stabilize alkyl chains and aromatic groups in polymer chains during carbonization.

- Heteroatoms in form of side groups stabilize longer alkyl chains: Example: lignin, but this does not apply to PVA.
- Heteroatoms in aromatic groups increase the carbonization yield. Example: (stabilized) PAN or poly(furfurylalcohol).
- Oxygen in aromatic compounds, for example, phenolic groups, increases the carbon yield. Examples: lignin and phenolic resins.

e) The aromatic structure and the preferred orientation in the precursor fiber must exist at the beginning of the carbonization phase. Even high-temperature treatment of non-oriented carbon does not result in a better orientation.

The prepared CFs have a carbon structure made of turbostratic, bent carbon layers of more- or less-oriented and ordered carbon crystallites. In the early days, the term "pregraphitic" was used.[212] The bending of the carbon layers increases the interlayer distance, which is 0.335 nm in perfect graphite.[1] Both the size and structure of the turbostratic carbon layers depend on the precursor polymer and the maximum heat-treatment temperature applied during carbonization and graphitization (>2000 °C). Fitzer et al. investigated the development of the mean interlayer distance of some typical precursor systems made from PAN and pitch depending on the maximum heat-treatment temperature (Figure 33). As can be seen, PAN-based CFs cannot reach interlayer distances less than 0.344 nm, even at temperatures as high as 2800 °C. The carbon structure of PAN-based CFs remains turbostratic.[6]

The crystallites grow with increasing maximum heat treatment (Figure 34); this growth depends on the preorientation of the carbon layers. An amorphous or any kind

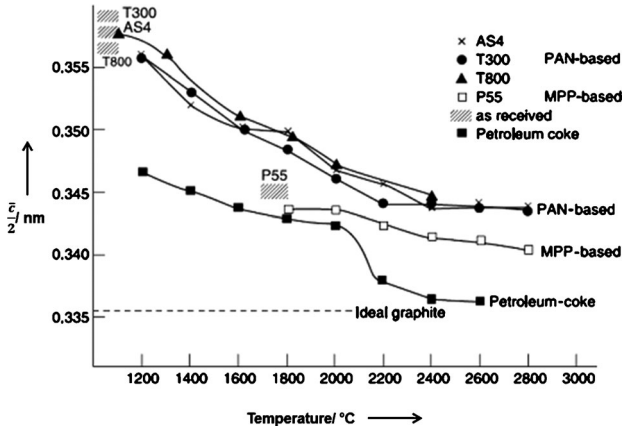

Figure 33. Mean interlayer distance of PAN- and pitch-based CFs depending on the maximum heat-treatment temperature.[213] Reproduced with permission from Elsevier.

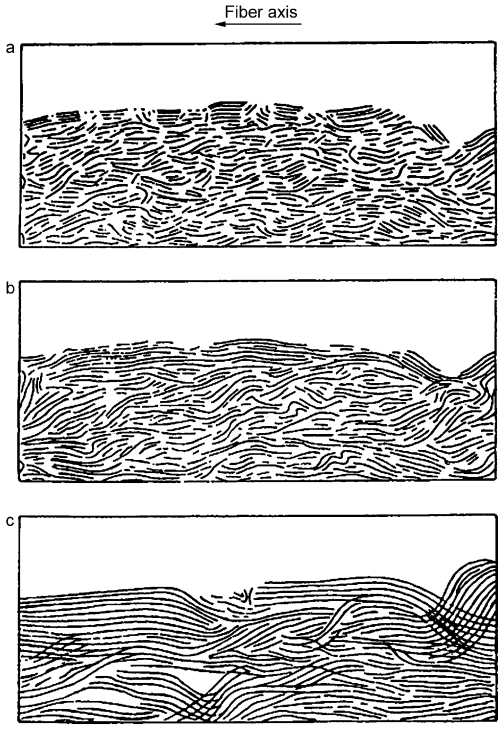

Figure 34. Model for the development of carbon layer structures from TEM studies. a) 1000 °C, b) 1500 °C, c) 2500 °C.[215]

of poorly oriented precursor will not develop larger carbon crystallites even at very high graphitization temperatures. Instead, glassy carbon[214] with very small crystallites will result.[211]

The mechanical properties of CFs increase with increasing temperature during carbonization. Notably, the type of precursor is of utmost importance. Mesophase pitch-derived CFs show a very different increase in the tensile strength and modulus depending on the heat treatment temperature compared to PAN-derived CFs (Figure 35). PAN-derived

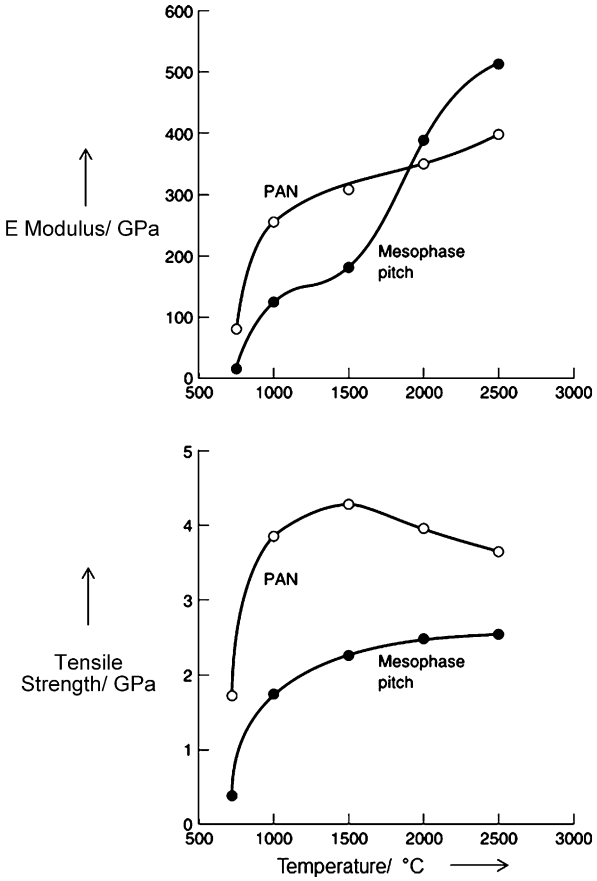

Figure 35. Correlation of Young's modulus (above) and tensile strength (below) for CFs made from PAN and pitch precursor systems.[51] Reproduced with permission from IUPAC.

CFs reach a maximum in tensile strength at around 1500 °C, while pitch-derived CFs show a sharp increase in strength below 1500 °C, but to a lower degree than PAN-derived fibers. There is no decrease in the tensile strength with increasing graphitization temperatures. The Young's modulus of PAN-derived fibers increases linearly, but slowly with increasing temperature. Pitch-derived CFs need at least 2000 °C to show higher Young moduli, but can reach much higher moduli than PAN-derived CFs at high graphitization temperatures.

The different behavior is related to the size, structure, and orientation of the carbon crystallites. The dependency of the length of the crystallites L_c on the maximum processing temperature is shown in Figure 36. L_c is, in general, higher for pitch-derived CFs and increases linearly with temperature.

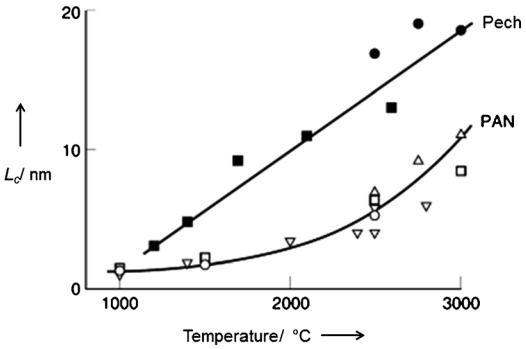

Figure 36. Plots of L_c versus the maximum process temperature for pitch-based CFs (solid symbols) and PAN-based CFs (open symbols).[216] Reproduced with permission from Springer.

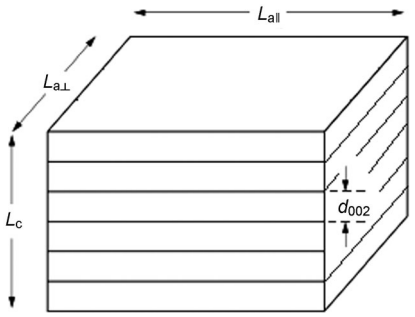

Figure 37. Schematic representation of carbon crystallites inside a CF, showing L_a (parallel to the fiber axis = "length" of crystallites), L_a (perpendicular to the fiber axis ("width"), L_c ("depth" of crystallites), and d_{002} (mean distance of carbon layers). Redrawn from Ref. [217].

Figure 37 gives an illustration of the different values, $L_{a\parallel}$ (parallel to fiber axis), $L_{a\perp}$ (perpendicular to the fiber axis), L_c, and d_{002}, used to describe a crystallite. Figure 38 shows the crystallite size $L_{a\parallel}$ and $L_{a\perp}$ versus L_c for pitch- and PAN-derived CFs. The crystallite "length" $L_{a\perp}$ perpendicular to the fiber axis is similar for both precursor systems. The crystallite "length" $L_{a\parallel}$ parallel to the larger fiber axis is different for

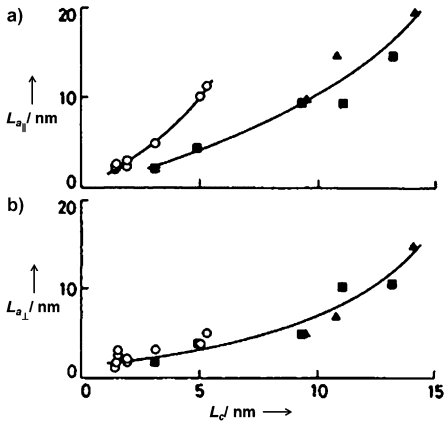

Figure 38. Plots of a) L_a (parallel to the fiber axis) and b) L_a (perpendicular to the fiber axis) versus L_c at the maximum process temperature for pitch- (solid symbols) and PAN-based CFs (open symbols). Reproduced with permission from Springer.

PAN- and pitch-derived CFs. The crystallite length is larger in pitch systems because of the high pre-orientation of the polycyclic arenes in the mesophase pitch precursor.

Figure 39 shows the volume fraction of carbon crystallites v_c, of noncrystalline carbon v_a, and the volume fraction of microvoids v_p versus the L_c of pitch- and PAN-derived CFs. Clearly, the crystallinity v_c is independent of the precursor system. Together, v_c, v_a, and v_p add up to 100 vol%. The

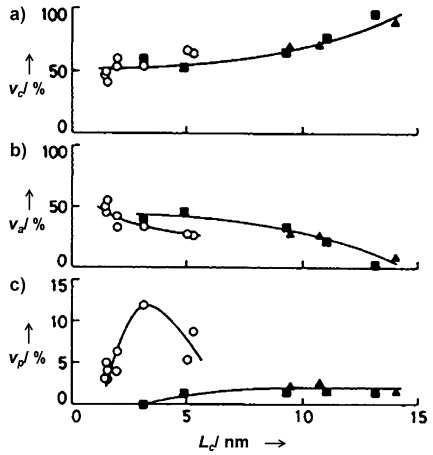

Figure 39. Plots of a) v_c, b) v_a, and c) v_p versus L_c of pitch-derived CFs (solid symbols) and PAN-derived CFs (open symbols). Reproduced with permission from Springer.

amount of microvoids is much larger in the case of PAN- than pitch-derived CFs. From Figures 36 and 37 one can estimate an optimum carbonization temperature of around 1500 °C to achieve the highest strength for PAN-derived CFs with L_c dimensions of 3–5 nm. According to Figure 39c, such a high-tenacity fiber will contain about 5–10 vol% microvoids, with an even larger amount (10–15 vol%) of microvoids in earlier stages of the carbonization, that is, at lower temperatures. As a consequence of the higher disordering of the turbostratic carbon and the microvoids, PAN-derived CFs only have a density (Figure 40) of typically 1.8 g cm^{-3}. The density of pitch-derived CFs is in a typical range of 2.0 to 2.15 g cm^{-3}, depending on the maximum processing temperature.

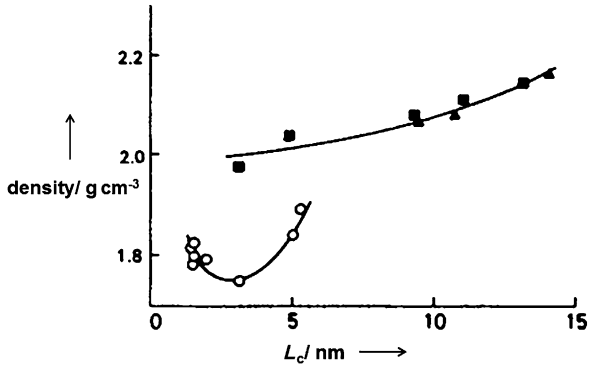

Figure 40. Density of CFs versus L_c of pitch- (solid symbols) and PAN-derived CFs (open symbols). Reproduced with permission from Springer.

The orientation factor f as a function of the crystallite "length" parallel to the fiber axis (Figure 41) is largely independent of the precursor system used. This fits the finding that the Young's modulus depends on the orientation of the crystallites, but not on the precursor system.

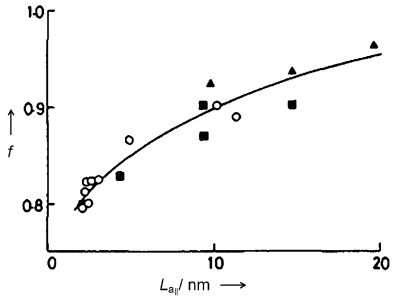

Figure 41. Orientation factor f versus L_a (parallel to fiber axis) for pitch- (solid symbols) and PAN-derived CFs (open symbols). Reproduced with permission from Springer.

4. Models for the CF Structure and Morphology

Unlike the two-dimensional form of carbon, graphene,[218] which is also a substructure of CFs, the structure and morphology of a CF is complex. The crystallite dimensions L_a, L_c, and d_{002} depend on the method of measurement and are not well-defined in a highly oriented carbon phase. The crystallite sizes can be measured by WAXS, Raman spectroscopy (Figure 42), or TEM.

A typical single graphene plane of a CF is shown in Figure 43. There are some vacancy cluster defects visible in the plane, thus limiting the maximum tensile strength of the CF. As stated before, the turbostratic carbon layers are more or less bent, which is essential for the transfer of mechanical loads onto and within the CF to reach high tensile strengths.[1,220]

Another model (Figure 44) defines the crystallites with the length L_a and the depth L_c as intersections of endless fibrils of stacked carbon layers, with voids in between the fibrils.[221] Figure 45 describes the orientation φ (0–100%) and the crystallite depth L_c inside this model of an endless carbon fibril of stacked carbon layers. Both values are a statistical mean value of the intersections of the carbon fibrils. A similar model representation was discussed by Johnson (Figure 46) in a more detailed description of penetrating carbon structures.[222]

A model developed by Diefendorf et al. (Figure 47) shows CF fibrils without interlinkages or voids.

High-modulus CFs, heat-treated above 2000 °C, develop a higher-ordered structure called 3D carbon. This structure development becomes clearly visible by Raman spectroscopy, where it shows up as new band at 2700 cm^{-1}.[224]

A model of such a 3D structure with interlinked crystallinity was also discussed by Johnson et al. (Figure 48).

Some additional features have to be discussed over the length scale of the entire CF. Larger voids from the spinning processes and loss of material during carbonization have to be

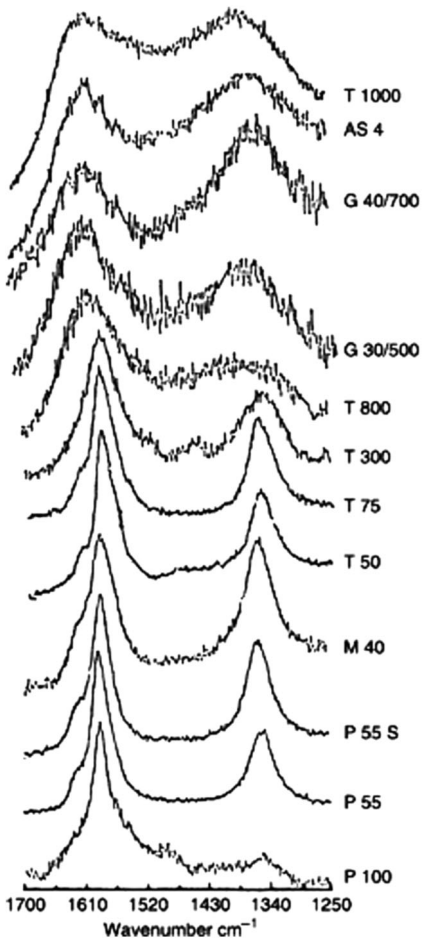

Figure 42. Raman signals of commercially available pitch- and PAN-derived CFs.[219] Reproduced with permission from Elsevier.

Figure 43. Drawing of a model graphene layer in a CF showing vacancy defects.[221] Reproduced with permission from Maney Publishing.

taken in consideration. Additionally, a CF typically has a core–shell structure with more graphitized carbon at the surface and more interlinked carbon structures in the core. Barnett and Norr presented a model (Figure 49) with a comprehensive representation of all the macroscale features important for the properties of CFs.

Two alternative models show a more in-detail representation of CF features. Figure 50 shows features typical for PAN-derived CFs. Important are the voids in these fibers, which result in typical densities for high-tensile CFs in the range of 1.75 to 1.80 g cm^{-3} (and even higher densities for high-modulus fibers, which are structurally closer to a perfect graphite crystal structure with a density of 2.26 g cm^{-3}).

The same author proposed a more detailed model representation (Figure 51) that shows the core–shell structure of a PAN-derived CF. This core–shell structure is typical for PAN-based CFs formed as an artifact from the coagulation process,

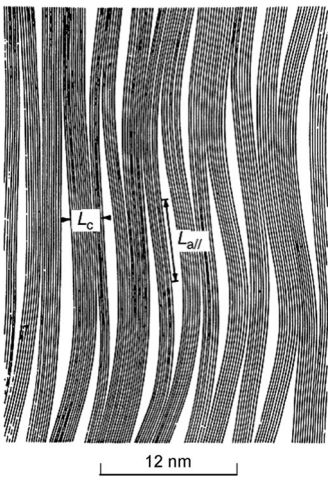

Figure 44. Schematic representation of the cross-section of PAN-derived CFs with L_a and L_c as intersections of endless fibrils of carbon.[221,223] Reproduced with permission from Maney Publishing.

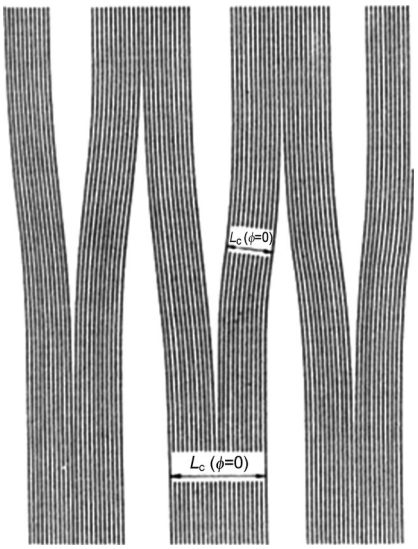

Figure 45. Detailed representation of the cross-section of PAN-derived CFs with L_c and the orientation ϕ as intersections of endless fibrils of carbon.[221] Reproduced with permission from Maney Publishing.

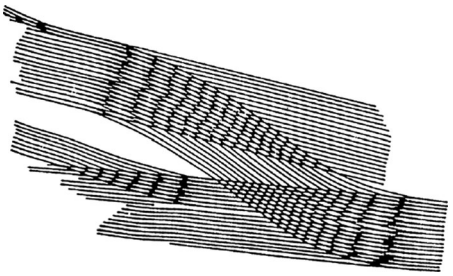

Figure 46. Interlinking carbon structures and voids in a CF.[222] Reproduced with permission from IOPScience.

which prefers the separation by a polymer "skin". This skin forms in case steep concentration gradients between the solvent and the coagulation bath exist.

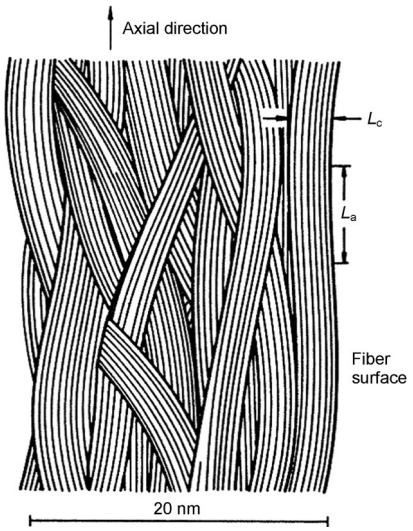

Figure 47. Ribbon structure model for CFs.[55b] Reproduced with permission from the Society of Plastic Engineers.

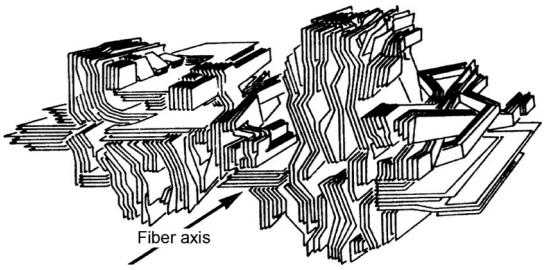

Figure 48. Model of a 3D-carbon structure of a high-modulus CF with interlinked crystallinity. Reproduced with kind permission from Ref. [225].

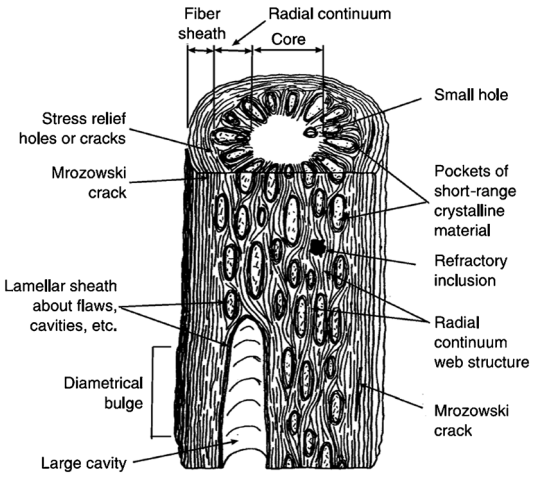

Figure 49. Structural model with macroscale features for PAN-derived high-modulus CFs.[226] Reproduced with permission from Maney Publishing.

5. Conclusions and Prospectives

Despite the fact that CFs have been around for quite a while, the synthesis of CFs with tailored tensile strength/high modulus fibers from a precursor is still an unaccomplished task. This is mostly related to a lack of understanding of how the structure, that is, polymer orientation, crystallinity, crystallite size, and orientation of a given precursor polymer translates into the structure of the final CF. Moreover, the impact of the CF structure, again in terms of crystallinity, crystallite dimensions, orientation, nature, and amount of defects, amount of sp^2 and sp^3 hybridization of the carbon atoms, etc., on the tensile strength, E modulus, conductivity, etc. is far from being fully understood. Only if the structure and structure formation of CFs are understood on a molecular level will tailored fibers be accessible and the currently high production costs reduced to a minimum. Although there has been a continuous growth of CF production over the last few years, large-volume applications of CFs, for example, in the automotive industry, have been impeded by the high fiber costs and the lack of techniques for the high-speed fabrication of composites. However, current investigations and future developments might well change the market and establish

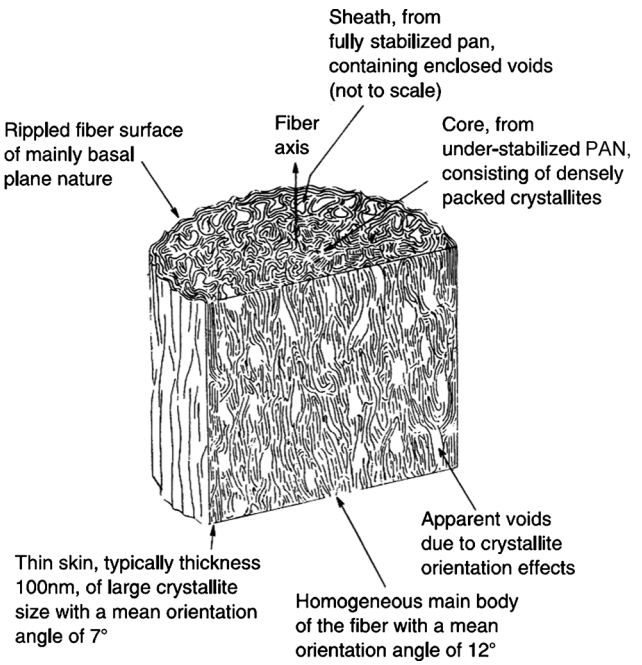

Figure 50. Representation of some of the features of a PAN-derived high-modulus CF.[215]

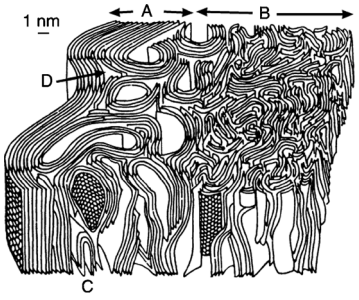

Figure 51. Microstructure of a PAN-derived CF. A: skin region, B: core region, C: a hairpin defect, D: a wedge disclination.[227] Reproduced with permission from the Society of Chemical Industry/London.

Table 5: Global annual CF consumption (in tons) and future trends.[5b,c]

Sector	2006	2008	2010	2011	2016	2020
aerospace	6500	7500	9800	7000	13100	19700
industrial	12800	15600	17500	29800	68500	120000
consumer goods	5900	6700	7000	9000	10800	13300
total	25200	29800	34200	45800	92400	153000

CFs as a mass product similar to other synthetic fibers or even metals. The actual and predicted future global consumption of CFs is summarized in Table 5.

With an increasing use of CFs for wind power and in the automotive sector, the demand for CFs in the coming five years is expected to at least double. In the medium term, alternative raw materials for CFs must be identified and implemented. Not only the automotive industry but also the construction industry, power industry, and mechanical engineering will require such novel, low-cost fibers when switching to new materials in price-sensitive products and renewable energies. Renewable raw materials such as biopolymers or polymers from biogenic sources are especially interesting sources of CFs. Therefore, worldwide research projects for the investigation of biogenic CFs have been initiated. These fibers do not yet compete with PAN-derived CFs, but provide new markets for CFs through their high availability and low production costs. However, as already outlined, any development of such alternative precursors to obtain useful CFs in terms of tensile strength and modulus (stiffness) requires an immense knowledge of the underlying chemistry. Today's modern analytical tools and modeling methods are a prerequisite to carry such fiber developments through to success.

Received: July 15, 2013
Published online: March 25, 2014

[1] P. Morgan, *Carbon Fibers and Their Composites*, CRC, Boca Raton, **2005**.
[2] S. Horikiri, J. Iseki, M. Minobe (Sumitomo Chemical Co., Ltd.), DE2404962A1, **1974**.
[3] Z. Xu, H. Sun, X. Zhao, C. Gao, *Adv. Mater.* **2013**, *25*, 188 – 193.
[4] a) H.-W. Liang, J.-W. Liu, H.-S. Qian, S.-H. Yu, *Acc. Chem. Res.* **2013**, *46*, 1450 – 1461; b) Z.-Y. Wu, C. Li, H.-W. Liang, J.-F. Chen, S.-H. Yu, *Angew. Chem.* **2013**, *125*, 2997 – 3001; *Angew. Chem. Int. Ed.* **2013**, *52*, 2925 – 2929; c) L.-F. Chen, Z.-H. Huang, H.-W. Liang, Q.-F. Guan, S.-H. Yu, *Adv. Mater.* **2013**, *25*, 4746 – 4752; d) H.-S. Qian, S.-H. Yu, L. Luo, J. Gong, L. Fei, X. Liu, *Chem. Mater.* **2006**, *18*, 2102 – 2108; e) H.-W. Liang, L. Wang, P.-Y. Chen, H.-T. Lin, L.-F. Chen, D. He, S.-H. Yu, *Adv. Mater.* **2010**, *22*, 4691 – 4695; f) H.-W. Liang, W.-J. Zhang, Y.-N. Ma, X. Cao, Q.-F. Guan, W.-P. Xu, S.-H. Yu, *ACS Nano* **2011**, *5*, 8148 – 8161; g) P. Chen, H.-W. Liang, X.-H. Lv, H.-Z. Zhu, H.-B. Yao, S.-H. Yu, *ACS Nano* **2011**, *5*, 5928 – 5935; h) H.-W. Liang, X. Cao, W.-J. Zhang, H.-T. Lin, F. Zhou, L.-F. Chen, S.-H. Yu, *Adv. Funct. Mater.* **2011**, *21*, 3851 – 3858; i) L.-F. Chen, X.-D. Zhang, H.-W. Liang, M. Kong, Q.-F. Guan, P. Chen, Z.-Y. Wu, S.-H. Yu, *ACS Nano* **2012**, *6*, 7092 – 7102; j) H.-W. Liang, Q.-F. Guan, Z. Zhu, L.-T. Song, H.-B. Yao, X. Lei, S.-H. Yu, *NPG Asia Mater.* **2012**, *4*, e19; k) L.-F. Chen, Z.-H. Huang, H.-W. Liang, W.-T. Yao, Z.-Y. Yu, S.-H. Yu, *Energy Environ. Sci.* **2013**, *6*, 3331 – 3338; l) H.-W. Liang, Q.-F. Guan, L.-F. Chen, Z. Zhu, W.-J. Zhang, S.-H. Yu, *Angew. Chem.* **2012**, *124*, 5191 – 5195; *Angew. Chem. Int. Ed.* **2012**, *51*, 5101 – 5105.
[5] a) J. B. Donnet, R. C. Bansal, *Carbon Fibers*, Marcel Dekker, New York, **1990**, pp. 1 – 145; b) in Lucintel Report: Growth Opportunities in Carbon Fibre Market 2010 – 2015, **2010**; c) in *Composites World's annual Carbon Fibre 2011 conference*, Washington, DC, **2011**; d) R. J. Diefendorf, E. Fitzer, M. Heym, *Chem. Ing. Tech.* **1976**, *48*, 765 – 774; e) K. J. Hüttinger, *Adv. Mater.* **1990**, *2*, 349 – 355.
[6] M. K. Jain, A. S. Abhiraman, *J. Mater. Sci.* **1987**, *22*, 278 – 300.
[7] A. Shindo in *Report of the Government Industrial Research Institute*, Osaka, Japan, **1961**.
[8] a) S. R. Sandler, *Polymer Synthesis*, Academic Press, New York/London, **1974**; b) Y. Ashina, I. Oshima, K. Sekine (Nitto Chemical Industry Co., Mitsubishi Rayon Co.), US3701761, **1972**; c) R. Bacon, *Trans. Faraday Soc.* **1946**, *42*, 140 – 155; d) M. Bero, T. Rosner, *Makromol. Chem.* **1970**, *136*, 1 – 10; e) B. von Falkai, R. Bonart, *Synthesefasern — Grundlagen, Technologie, Verarbeitung und Anwendung*, Chemie, Weinheim, **1981**; f) P. Fritzsche, J. Ulbricht, *Faserforsch. Textiltechn.* **1963**, *14*, 320; g) P. Fritzsche, J. Ulbricht, *Faserforsch. Textiltech.* **1964**, *15*, 93; h) G. A. Gabrielyan, Z. A. Rogovin, *J. Text. Inst.* **1964**, *55*, 26; i) J. M. Grim, *Chem. Abstr.* **1952**, *46*, 7822; j) M. Lewin, *Handbook of Fiber Chemistry*, CRC, Boca Raton, **2007**; k) L. H. Peebles, *J. Appl. Polym. Sci.* **1973**, *17*, 113; l) J. A. Price, W. M. Thomas, J. J. Padbury, *Chem. Abstr.* **1953**, *47*, 670; m) V. E. Shashoua in *Preparative Methods of Polymeric Chemistry*, *Vol. 2* (Eds.: W. R. Sorenson, T. W. Campbell), Wiley Interscience, New York, **1968**, p. 235; n) W. K. Wilkinson, *Macromol. Symp.* **1966**, *2*, 78; o) R. B. Parker, B. V. Mokler (Kalvar Corporation), US3161511, **1964**; p) D. W. Chaney (American Viscose Corporation), US2537031, **1951**; q) W. G. Schmidt, (Courtaulds, Ltd.), GB796294, **1958**; r) J. Czajlik, T. Földes-Berezsnic, F. Tüldös, S. Szasacs, *Eur. Polym. J.* **1978**, *14*, 1059 – 1066; s) D. Feldman, *Mater. Plast.* **1966**, *3*, 25; t) H. Kiuchi, *Chem. Abstr.* **1964**, *61*, 7107; u) H. Blades (Union Rheinische Braunkohlen Kraftstoff), DE2219703A1, **1962**; v) E. L. Kropa (Old Greenwich Con.), US2356767, **1944**; w) H. Miyama, N. Harumiya, A. Takeda, *J. Polym. Sci. Part A* **1972**, *10*, 943; x) I. G. Murgulescu, T. Oncescu, I. I. Vlagiu, *Chem. Abstr.* **1972**, *77*, 75804; y) L. H. Peebles, *J. Polym. Sci. Part A* **1965**, 341; z) C. E. Schildknecht, *Vinyl and related polymers*: *their preparations*, *properties*, *and applications in rubbers*, *plastics*, *fibers*, *and in medical and industrial arts*, Wiley, New York, **1952**; aa) J. Szafko, E. Turska, *Makromol. Chem.* **1972**, *156*, 297 – 310; ab) W. M. Thomas, *Fortschr. Hochpolym.-Forsch.* **1961**, *2*, 401; ac) W. K. Wilkinson (E. I. du Pont, Del. Wilmington), US3087919, **1963**; ad) J. Szafko, E. Turska, *Makromol. Chem.* **1972**, *156*, 311 – 320.
[9] A. Ziabicki, *Fundamentals of Fibre Formation*: *The Science of Fibre Spinning and Drawing*, Wiley, London, **1976**.
[10] E. Frank, F. Hermanutz, M. R. Buchmeiser, *Macromol. Mater. Eng.* **2012**, *297*, 493 – 501.
[11] D. D. L. Chung, *Carbon Fiber Composites*, Butterworth-Heinemann, Newton, **1994**.
[12] J.-S. Tsai, C.-H. Lin, *J. Appl. Polym. Sci.* **1991**, *43*, 679.
[13] a) M. Kibayashi, Y. Matsuhisa, A. Okuda, K. Yamasaki (Toray Industries, Inc.), US20020009588A1, **2002**; b) R. J. Anders, W. Sweeny (E. I. du Pont), US2837500, **1958**; c) T. Otani, T. Setsuie, K. Yoshida (Mitsubishi Rayon Co., Ltd.), US4695415A, **1987**; d) Y. Nishihara, Y. Furuya, M. Toramaru (Mitsubishi Rayon Co.), JP63275714 A, **1987**; e) Y. Kai, M. Kuboyama (Asahi Chemical), JP02139425 A, **1990**; f) A. Hajikano, T. Yamamoto, T. Kubota (Mitsubishi Rayon Co.), JP04240220 A, **1992**; g) A. Hajikano, S. Hayashi, T. Yamamoto, K. Aoki (Mitsubishi Rayon Co.), JP05132813A, **1993**; h) D. E. Stuetz, K. H. Gump (Celanese Corporation), GB1264026,

1969; i) E. Fitzer, D. J. Müller, *Makromol. Chem.* **1971**, *144*, 117; j) N. Grassie, R. McGuchan, *Eur. Polym. J.* **1972**, *8*, 257; k) G. Henrici-Olivé, S. Olivé, *Adv. Polym. Sci.* **1983**, *51*, 36; l) T. Yoshinori, O. Hiroshi (Mitsubishi Toasty Chemical Inc.), JP6215329 A, **1987**; m) K. Morita, T. Mizushima, H. Kitagawa, H. Sakai (Toray Industries Inc.), GB1254166, **1969**; n) T. Hiramatsu, T. Higuchi, S. Mitsui (Toray Industries Inc.), JP58214534A, **1983**; o) S. Takeda, A. Tsunoda (Toray Industries Inc.), JP58214521 A, **1983**; p) O. Haruo, O. Masahi, T. Hiroyoshi (Toray Industries Inc.), JP59168128A, **1984**; q) S. Yamane, T. Higuchi, K. Yamasaki (Toray Industries Inc.), EP 223199, **1987**; r) Y. Matsuhisa, K. Ono, T. Hiramatsu (Toray Industries Inc.), JP 0214012 A, **1990**; s) J. Yamazaki, M. Shirakata, Y. Adachi (Toray Industries Inc.), JP0364514 A, **1991**; t) M. Kobayashi, N. Takada (Toray Industries Inc.), JP 04333620 A, **1993**; u) T. Hiramatsu, T. Higuchi, S. Mitsui (Toray Industries Inc.), JP58214526 A, **1983**; v) T. Iharaki, S. Yoshino (Asahi Chemical Industry), JP61119712 A, **1986**; w) T. Ogawa, E. Wakita, T. Kobayashi (Asahi Kasei Kogyo KK), GB1435447, **1974**; x) L. Y. Park, D. Ofer, R. R. Schrock, M. S. Wrighton, *Chem. Mater.* **1992**, *4*, 1388; y) K. Imai, H. Senchi (Nikkiso Co Ltd.), JP61289132A, **1982**; z) G. Moutaud, J.-P. Loiseau, D. Desmicht (Le Carbone Lorraine), GB1280850, **1969**; aa) S. Kishimoto, S. Okazaki (Japan Exlan Co Ltd.), US4009248 A, **1977**; ab) K. Tominari, T. Ishimoto (Mitsui Petrochemicals Ind. Ltd.), JP 58191704 A, **1984**; ac) O. Takeji, F. Takashi, K. Tadao (Mitsubishi Rayon Co., Ltd.), JP59125912, **1984**; ad) Y. Imai, Y. Tasaka, S. Nakatani, N. Fukahori (Mitsubishi Rayon Co Ltd.), JP60151317 A, **1985**; ae) Y. Imai, Y. Tasaka, S. Nakatani, N. Fukahori, (Mitsubishi Rayon Co., Ltd.), JP60151317, **1985**; af) S. Sasaki, Y. Imai, S. Nakatani, T. Kobayashi (Mitsubishi Rayon Co. Ltd.), JP 62231027 A, **1987**; ag) Y. Imai, M. Nakatani, Y. Tanuku, H. Yoneyama (Mitsubishi Rayon Co., Ltd.), US5051216A, **1991**; ah) H. D. Mackenzie, F. Reeder (Courtaulds Ltd.), GB944217, **1963**; ai) R. Moreton, H. P. McLonghlin (Ed.: R. A. Establishment); aj) N. V. Platonova, I. B. Klimenko, V. I. Grachev, G. A. Kiselev, *Vysokomol. Soedin. Ser. A* **1988**, *30*, 1056; ak) G. A. Kiselev, I. S. Rabinovich, A. A. Lysenko, O. I. Sorokina, M. L. Syrkina, E. S. Roskin, G. S. Makarevich (Leningrad Institute of Textile and Light Industry, USSR; All-Union Scientific-Research Institute of Synthetic Fibers), SU1065509A1, **1984**.

[14] a) S. Hirotaka, K. Hiroaki (Teijin Ltd.), JP2006016482, **2006**; b) H. Kuwahara, H. Suzuki, S. Matsumura (Teijin Limited), US7338997 B2, **2008**; c) C. D. Warren, F. L. Paulauskas, F. S. Baker, C. C. Eberle, A. Naskar in *Proceedings of the SAMPE Fall Technical Conference*, Memphis, TN, USA, **2008**; d) H. Dasarathy, W. C. Schimpf, T. Burleson, S. B. Smith, C. W. Herren, A. C. Frame, P. W. Heatherly in *Proceedings of the International SAMPE Technical Conference*, Baltimore, MD, USA, **2002**; e) P. Bajaj, D. K. Paliwal, A. K. Gupta, *J. Appl. Polym. Sci.* **1998**, *67*, 1647 – 1659.

[15] a) G. P. Daumit, Y. S. Ko, C. R. Slater, J. G. Venner, C. C. Young, M. M. Zwick (Basf Aktiengesellschaft), US4933128 A, **1990**; b) G. P. Daumit, Y. S. Ko, C. R. Slater, J. G. Venner, C. C. Young (Basf Aktiengesellschaft), US4921656A, **1990**; c) G. P. Daumit, Y. S. Ko, C. R. Slater, J. G. Venner, C. C. Young (Basf Aktiengesellschaft), US4935180A, **1990**.

[16] D. Ingildeev, F. Hermanutz, K. Bredereck, F. Effenberger, *Macromol. Mater. Eng.* **2012**, *297*, 585 – 594.

[17] H. Blades (Du Pont), US3767756, **1972**.

[18] S. Yamane, T. Higuchi, K. Yamazaki (Toray Industries Inc.), JP 621178818, **1986**.

[19] a) V. Gröbe, K. Meyer, *Faserforsch. Textiltech.* **1969**, *467*; b) J. P. Craig, J. P. Knudsen, V. F. Holland, *Text. Res. J.* **1962**, *32*, 435 – 448.

[20] S. Hartig, E. Peter, W. Dohrn, *Lenzinger Ber.* **1973**, *35*, 17.

[21] a) J. P. Knudsen, *Text. Res. J.* **1963**, *33*, 13; b) G. Duwe, G. Mann, A. Gröbe, *Faserforsch. Textiltech.* **1966**, *17*, 142; c) H. Takeda, Y. Nukushima, *Kogyo Kagaku Zasshi* **1964**, *67*, 626; d) A. Gröbe, G. Mann, *Faserforsch. Textiltech.* **1966**, *17*, 315.

[22] M. Takahashi, M. Watanabe, *Sen-I Gakkaishi* **1960**, *16*, 7.

[23] a) S. Uchida (Japan Exclan Co Ltd.), JP62299509 A, **1987**; b) Y. Nishihara, Y. Furuya, M. Toramaru (Mitsubishi Rayon Co., Ltd.), JP 63275713 A, **1988**; c) D. Zenke, D. Geiß, J. Beckmann, P. Weigel (Akademie der Wissenschaften der DDR), DD 279275, **1990**; d) R. Kashani-Shirazi (Hoechst Aktiengesellschaft), EP0645479A1, **1987**; e) M. Cerf, D. Colombie, T. D. N'Zudie (Hunton & Williams LLP), US2004/0068069A1, **1988**; f) Y. Nishihara, K. Nishimura (Mitsubishi Rayon Co., Ltd.), JP 05239712 A, **1993**.

[24] a) Y. Funakoshi, Y. Maeda (Matsushita Electric Ind. Co. Ltd.), JP60018334, **1985**; b) Y. Shiromoto, A. Okuda, S. Mitsui (Toray Ind. Inc.), JP 58214520 A, **1983**.

[25] W. Watt, W. Johnson, *Nature* **1975**, *257*, 210 – 212.

[26] a) X. Huang, *Materials* **2009**, *2*, 2369 – 2403; b) R. C. Houtz, *J. Text. Res.* **1950**, *20*, 786 – 801; c) J. Schurz, *J. Polym. Sci.* **1958**, *28*, 438 – 439; d) A. Standage, R. Matkowski, *Eur. Polym. J.* **1971**, *7*, 775 – 783; e) H. N. Friedlander, L. H. Peebles, J. Brandrup, J. R. Kirby, *Macromolecules* **1968**, *1*, 79 – 86; f) P. J. Goodhew, A. J. Clarke, J. E. Bailey, *Mater. Sci. Eng.* **1975**, *17*, 3 – 30; g) A. J. Clarke, J. E. Bailey, *Nature* **1973**, *243*, 146 – 150; h) J. E. Bailey, A. J. Clarke, *Chem. Ber.* **1970**, *6*, 484 – 489; i) J. Lora in *Monomers, Polymers and Composites from Renewable Resources*, Elsevier, Amsterdam, **2008**, pp. 225 – 241; j) D. A. Baker, T. G. Rials, *J. Appl. Polym. Sci.* **2013**, *130*, 713 – 728; k) Y. Nordström, R. Joffe, E. Sjöholm, *J. Appl. Polym. Sci.* **2013**, *130*, 3689 – 3697; l) F. S. Baker, N. C. Gallego, D. A. Baker, in *DOE FY 2009 Progress Report for Lightweighting Materials, Part 7A.*, **2009**; m) J. Sundquist, in *Papermaking Science and Technologie*, *Book 6B*, *Chemical Pulping*, *Vol. 6B* (Eds.: J. Gullichsen, C.-J. Fogelholm), Finnish Paper Engineers' Association and TAPPI, Helsinki **1999**, pp. 411 – 427; n) X. Pan, C. Arato, N. Gilkes, D. Gregg, W. Mabee, K. Pye, Z. Xiao, X. Zhang, J. Saddler, *Biotechnol. Bioeng.* **2005**, *90*, 473 – 481.

[27] a) M. M. Coleman, G. T. Sivy, *Carbon* **1981**, *19*, 133 – 155; b) G. T. Sivy, M. M. Coleman, *Carbon* **1981**, *19*, 127 – 131.

[28] a) V. Raskovic, S. Marinkovic, *Carbon* **1975**, *13*, 535 – 538; b) J. B. Donnet, P. Ehrburger, *Carbon* **1977**, *15*, 143 – 152.

[29] a) N. Grassie, J. N. Hay, *J. Polym. Sci. Part A* **1962**, *56*, 189; b) E. Fitzer, M. Heine, G. Jacobsen, *International Symposium on Carbon*, Toyohashi, **1982**.

[30] S. M. White, J. E. Spruiell, F. L. Paulauskas in *Proceedings of the International SAMPE Technical Conference*, **2006**.

[31] J. Dietrich, P. Hirt, H. Herlinger, *Eur. Polym. J.* **1996**, *32*, 617.

[32] F. L. Paulauskas, T. L. White, J. E. Spruiell in *Proceedings of the International SAMPE Technical Conference*, **2006**.

[33] J. S. Tsai, *Text. Res. J.* **1994**, *64*, 772 – 774.

[34] V. Raskovic, S. Marinkovic, *Carbon* **1978**, *16*, 351 – 357.

[35] a) J. Bromley in *International Conference on Carbon Fibers, their Composites and Applications*, London, **1971**; b) A. Johansson, O. Aaltonen, P. Ylinen, *Biomass* **1987**, *13*, 45 – 65.

[36] a) Z. Wangxi, L. Jie, W. Gang, *Carbon* **2003**, *41*, 2805 – 2812; b) D. O'Neil, *Int. J. Polym. Mater.* **1979**, *7*, 203 – 218; c) D. J. Johnson, I. Tomizuka, O. Watanabe, *Carbon* **1975**, *13*, 321 – 325.

[37] K. Morita, Y. Murata, A. Ishitani, K. Murayama, T. Ono, A. Nakajima, *Pure Appl. Chem.* **1986**, *58*, 455 – 468.

[38] a) I. Shimada, T. Takahagi, M. Fukuhara, K. Morita, A. Ishitani, *J. Polym. Sci. A* **1986**, *24*, 1989 – 1995; b) G. T. Sivy, B. Gordon, M. M. Coleman, *Carbon* **1983**, *21*, 573 – 578; c) S. P. Varma, B. B. Lal, N. K. Srivastava, *Carbon* **1976**, *14*, 207 – 209.

[39] T. Takahagi, I. Shimada, M. Fukuhara, K. Morita, A. Ishitani, *J. Polym. Sci. A* **1986**, *24*, 3101 – 3107.

[40] D. M. Riggs, R. J. Shuford, R. W. Lewis, *Graphite fibers and composites*, Van Nostrand Reinhold, New York, **1982**.
[41] J. D. Brooks, G. H. Taylor, *Chem. Phys. Carbon*, *Vol. 4* (Ed.: P. L. Walker, Jr.), Marcel Dekker, New York, **1995**.
[42] L. H. Peebles, *Carbon Fibers*: *Formation*, *Structure*, *and Properties*, CRC, Boca Raton, **1995**, pp. 29 – 30.
[43] K. Okuda, *Trans. Mater. Res. Jpn.* **1990**, 119 – 139.
[44] S. Otani, A. Oya, *Progress of pitch based carbon fiber in Japan*, American Chemical Society, Washington, DC, **1986**.
[45] D. D. Eddie, R. J. Diefendorf, *Carbon fibre manufacturing*, William Andrew, Park Ridge, **1993**.
[46] I. Mochida, Y. Sone, Y. Korai, *Carbon* **1985**, *23*, 175 – 178.
[47] S. Otani, A. Oya, in Proc Japan-US CCM III Jpn Soc Compos Mater, **1986**.
[48] T. Hamada, T. Nishida, Y. Sajiki, M. Matsumoto, M. Endo, *J. Mater. Res.* **1987**, *2*, 850 – 857.
[49] J. E. Zimmer, J. L. White, *Adv. Liq. Cryst.* **1982**, *5*, 157 – 213.
[50] J. D. Buckley, D. D. Edie, *Carbon-Carbon Materials and Composites*, William Andrew, Park Ridge, **1993**.
[51] T. Matsumoto, *Pure Appl. Chem.* **1985**, *57*, 1553 – 1562.
[52] T. A. Edison (Edison, Thomas A.), US223898, **1880**.
[53] a) C. E. Ford, C. V. Mitchell (Union Carbide Corp.), DE1130419, **1962**; b) C. E. Ford, C. V. Mitchell (Union Carbide Corp.), US3107152, **1963**.
[54] a) R. Bacon, W. A. Schalamon, *Carbon* **1968**, *6*, 211; b) R. Bacon, W. A. Schalamon, *High temperature resistant fibers from organic polymers*, *Vol. 9* (Ed.: J. Preston), Interscience, New York, **1969**, pp. 285 – 292; c) R. Bacon, W. A. Schalamon (Union Carbide Corp.), US3716331, **1973**; d) R. Bacon, G. E. Cranch (Union Carbide Corp), US3305315, **1967**.
[55] a) R. Bacon in *Chem. Phys. Carbon*, *Vol. 9* (Eds.: P. L. Walker, P. A. Thrower), Marcel Dekker, New York, **1973**, pp. 1 – 102; b) R. J. Diefendorf, E. Tokarsky, *Polym. Eng. Sci.* **1975**, *15*, 150 – 159; c) J. B. Donnet, *Carbon Fibers*, Marcel Dekker, New York, **1984**; d) A. A. Konkin in *Handbook of Composites*, *Vol. 1* of *Strong Fibres* (Eds.: W. Watt, B. V. Perov), Elsevier Science, Amsterdam, **1985**, pp. 275 – 325; e) S. Chand, *J. Mater. Sci.* **2000**, *35*, 1303 – 1313; f) X. Huang, *Materials* **2009**, *2*, 2369 – 2403; g) A. Dumanlı, A. Windle, *J. Mater. Sci.* **2012**, *47*, 4236 – 4250.
[56] J. W. S. Hearle, *J. Polym. Sci.* **1958**, *28*, 432 – 435.
[57] a) K. Bredereck, F. Hermanutz, *Rev. Prog. Color. Relat. Top.* **2005**, *35*, 59 – 75; b) M. G. Northolt, H. Boerstoel, H. Maatman, R. Huisman, J. Veurink, H. Elzerman, *Polymer* **2001**, *42*, 8249 – 8264.
[58] J. Dyer, G. C. Daul, *Fiber Chemistry*, *Vol. 4* (Eds.: M. Lewin, E. M. Pearce), Marcel Dekker, New York, **1985**, pp. 910 – 1000.
[59] L. M. J. Kroon-Batenburg, J. Kroon, M. G. Northolt, *Polym. Commun.* **1986**, 290 – 292.
[60] T. Röder, J. Moosbauer, G. Kliba, S. Schlader, G. Zuckerstätter, H. Sixta, *Lenzinger Ber.* **2009**, *87*, 98 – 105.
[61] W. A. Sisson, *Text. Res. J.* **1960**, *30*, 153 – 170.
[62] D. Ingildeev, F. Effenberger, K. Bredereck, F. Hermanutz, *J. Appl. Polym. Sci.* **2012**, 4141 – 4150.
[63] F. R. Barnet, M. K. Norr, *Composites* **1976**, *7*, 93 – 99.
[64] a) R. P. Swatloski, S. K. Spear, J. D. Holbrey, R. D. Rogers, *J. Am. Chem. Soc.* **2002**, *124*, 4974 – 4975; b) R. P. Swatloski, R. D. Rogers, J. D. Holbrey (University of Alabama; PG Res. Foundation Inc), WO03029329, **2003**; c) F. Hermanutz, F. Gähr, E. Uerdingen, F. Meister, B. Kosan, *Macromol. Symp.* **2008**, *262*, 23 – 27.
[65] R. J. Sammons, J. R. Collier, T. G. Rials, J. E. Spruiell, S. Petrovan, *J. Appl. Polym. Sci.* **2012**, 951 – 957.
[66] B. K. Kandola, A. R. Horrocks, D. Price, G. V. Coleman, *J. Macromol. Sci. Polym. Rev.* **1996**, *36*, 721 – 794.
[67] D. Shen, R. Xiao, S. Gu, K. Luo, *RSC Adv.* **2011**, *1*, 1641 – 1660.
[68] M. M. Tang, R. Bacon, *Carbon* **1964**, *2*, 211 – 214.
[69] F. J. Kilzer, A. Broido, *Pyrodynamics* **1965**, 151 – 163.
[70] A. Broido in *Thermal uses and properties of carbohydrates and lignins* (Eds.: F. Shafizadeh, K. V. Sarkanen, D. A. Tillman), Academic Press, New York, **1976**, pp. 19 – 36.
[71] C. Fairbridge, R. A. Ross, S. P. Sood, *J. Appl. Polym. Sci.* **1978**, *22*, 497 – 510.
[72] P. H. Brunner, P. V. Roberts, *Carbon* **1980**, *18*, 217 – 224.
[73] F. Shafizadeh in *Wood chemicals*, *a future challenge*, *Vol. 28 – 1* (Ed.: T. E. Timell), Wiley, New York **1975**, pp. 153 – 174.
[74] a) A. G. W. Bradbury, Y. Sakai, F. Shafizadeh, *J. Appl. Polym. Sci.* **1979**, *23*, 3271 – 3280; b) F. Shafizadeh, A. G. W. Bradbury, *J. Appl. Polym. Sci.* **1979**, *23*, 1431 – 1442.
[75] a) J. L. Banyasz, S. Li, J. L. Lyons-Hart, K. H. Shafer, *J. Anal. Appl. Pyrolysis* **2001**, *57*, 223 – 248; b) V. Mamleev, S. Bourbigot, J. Yvon, *J. Anal. Appl. Pyrolysis* **2007**, *80*, 151 – 165.
[76] F. Shafizadeh, Y. Z. Lai, *J. Org. Chem.* **1972**, *37*, 278 – 284.
[77] a) F. Shafizadeh, *J. Anal. Appl. Pyrolysis* **1982**, *3*, 283 – 305; b) F. Shafizadeh, W. F. DeGroot, *Thermal uses and properties of carbohydrates and lignins* (Eds.: F. Shafizadeh, K. V. Sarkanen, D. A. Tillman), Academic Press, New York **1976**, pp. 1 – 18.
[78] a) P. Zhu, S. Sui, B. Wang, K. Sun, G. Sun, *J. Anal. Appl. Pyrolysis* **2004**, *71*, 645 – 655; b) Y.-C. Lin, J. Cho, G. A. Tompsett, P. R. Westmoreland, G. W. Huber, *J. Phys. Chem. C* **2009**, *113*, 20097 – 20107; c) I. Pastorova, R. E. Botto, P. W. Arisz, J. J. Boon, *Carbohydr. Res.* **1994**, *262*, 27 – 47; d) D. Fabbri, G. Chiavari, S. Prati, I. Vassura, M. Vangelista, *Rapid Commun. Mass Spectrom.* **2002**, *16*, 2349 – 2355; e) D. Fabbri, S. Prati, I. Vassura, G. Chiavari, *J. Anal. Appl. Pyrolysis* **2003**, *68 – 69*, 163 – 171; f) A. E. S. Green, M. Zanardi, *Int. J. Quantum Chem.* **1998**, *66*, 219 – 227; g) Q. Liu, C. Lv, Y. Yang, F. He, L. Ling, *Thermochim. Acta* **2004**, *419*, 205 – 209; h) P. M. Molton, T. F. Demmitt, "Reaction mechanisms in cellulose pyrolysis: a literature review": http://www.osti.gov/bridge/servlets/purl/7298596/, **1977**; i) A. D. Pouwels, G. B. Eijkel, J. J. Boon, *J. Anal. Appl. Pyrolysis* **1989**, *14*, 237 – 280.
[79] C. B. Cross, D. R. Ecker, O. L. Stein (Union Carbide Corp.), US3116975, **1964**.
[80] R. Bacon, M. M. Tang, *Carbon* **1964**, *2*, 221 – 225.
[81] a) I. Karacan, T. Soy, *J. Mater. Sci.* **2013**, *48*, 2009 – 2021; b) S. E. Ross, *Text. Res. J.* **1968**, *38*, 906 – 913; c) R. F. Schwenker, E. Pacsu, *Ind. Eng. Chem.* **1958**, *50*, 91 – 96.
[82] J. Rychlý, M. Strlič, L. Matisová-Rychlá, J. Kolar, *Polym. Degrad. Stab.* **2002**, *78*, 357 – 367.
[83] A. Shindo, Y. Nakanishi, I. Soma, *Applied Polymer Symposia*, *Vol. 9* (Ed.: J. Preston), Interscience, New York **1969**, pp. 271 – 284.
[84] G. A. Byrne, D. Gardiner, F. H. Holmes, *J. Appl. Chem.* **1966**, *16*, 81 – 88.
[85] a) W. K. Tang, W. K. Neill, *J. Polym. Sci. Part C* **1964**, *6*, 65 – 81; b) A. Basch, M. Lewin, *Text. Res. J.* **1975**, *45*, 246 – 250; c) J. B. Tomlinson, C. R. Theocharis, *Carbon* **1992**, *30*, 907 – 911.
[86] E. D. Weil, S. V. Levchik, *J. Fire Sci.* **2008**, *26*, 243 – 281.
[87] a) F. Zeng, D. Pan, N. Pan, *J. Inorg. Organomet. Polym. Mater.* **2005**, *15*, 261 – 267; b) D.-Y. Kim, Y. Nishiyama, M. Wada, S. Kuga, *Cellulose* **2001**, *8*, 29 – 33.
[88] A. A. Morozova, Y. V. Brezhneva, *Fibre Chem.* **1997**, *29*, 31 – 35.
[89] a) G. Bhat, K. Akato, W. Hoffman, *Proceedings of the Fiber Society Spring Conference*, St. Gallen, **2012**; b) K. Akato, Masters thesis, University of Tennessee Knoxville (US-TN), **2012**.
[90] H. Li, Y. Yang, Y. Wen, L. Liu, *Compos. Sci. Technol.* **2007**, *67*, 2675 – 2682.
[91] a) Q. Wu, N. Pan, K. Deng, D. Pan, *Carbohydr. Polym.* **2008**, *72*, 222 – 228; b) Q. Liu, C. Lv, Y. Yang, F. He, L. Ling, *J. Mol. Struct.* **2005**, *733*, 193 – 202.

[92] M. Statheropoulos, S. A. Kyriakou, *Anal. Chim. Acta* **2000**, *409*, 203 – 214.
[93] A. Pappa, K. Mikedi, N. Tzamtzis, M. Statheropoulos, *J. Anal. Appl. Pyrolysis* **2003**, *67*, 221 – 235.
[94] a) P. Olry, H. Plaisantin, S. Loison, R. Pailler (Snecma Propulsion Solide), US2002182139, **2002**; b) H. Plaisantin, R. Pailler, A. Guette, M. Birot, J.-P. Pillot, G. Daude, P. Olry, *J. Mater. Sci.* **2006**, *41*, 1959 – 1964.
[95] P. Villaine, C. Janin (Michelin Recherche et Technique S.A.), US4839113, **1985**.
[96] A. A. Lysenko, I. A. Piskunova, O. V. Astashkina, *Fibre Chem.* **2003**, *35*, 189 – 192.
[97] P. Olry, C. Soumailles, R. Pailler, S. Loison, R. Konig, A. Guette (Snecma Propulsion Solide), WO 2006/061386, **2006**.
[98] a) J. Blackwell, P. D. Vasko, J. L. Koenig, *J. Appl. Phys.* **1970**, *41*, 4375 – 4379; b) J. Mann, H. J. Marrinan, *J. Polym. Sci.* **1958**, *32*, 357 – 370; c) C. Y. Liang, R. H. Marchessault, *J. Polym. Sci.* **1959**, *37*, 385 – 395; d) R. H. Marchessault, *Pure Appl. Chem.* **1962**, *5*, 107 – 130; e) A. J. Michell, *Carbohydr. Res.* **1993**, *241*, 47 – 54; f) T. Kondo, *Cellulose* **1997**, *4*, 281 – 292.
[99] a) J. Široký, R. Blackburn, T. Bechtold, J. Taylor, P. White, *Cellulose* **2010**, *17*, 103 – 115; b) F. Carrillo, X. Colom, J. J. Suñol, J. Saurina, *Eur. Polym. J.* **2004**, *40*, 2229 – 2234.
[100] a) R. H. Atalla, R. E. Whitmore, C. J. Heimbach, *Macromolecules* **1980**, *13*, 1717 – 1719; b) K. Schenzel, S. Fischer, *Cellulose* **2001**, *8*, 49 – 57.
[101] J. H. Wiley, R. H. Atalla, *Carbohydr. Res.* **1987**, *160*, 113 – 129.
[102] K. Kong, L. Deng, I. Kinloch, R. Young, S. Eichhorn, *J. Mater. Sci.* **2012**, *47*, 5402 – 5410.
[103] M. A. Pimenta, G. Dresselhaus, M. S. Dresselhaus, L. G. Cancado, A. Jorio, R. Saito, *Phys. Chem. Chem. Phys.* **2007**, *9*, 1276 – 1290.
[104] a) A. C. Ferrari, *Solid State Commun.* **2007**, *143*, 47 – 57; b) A. C. Ferrari, J. Robertson, *Phys. Rev. B* **2000**, *61*, 14095 – 14107.
[105] a) R. H. Atalla, D. L. Vanderhart, *Science* **1984**, *223*, 283 – 285; b) R. H. Atalla, J. C. Gast, D. W. Sindorf, V. J. Bartuska, G. E. Maciel, *J. Am. Chem. Soc.* **1980**, *102*, 3249 – 3251; c) C. A. Fyfe, R. L. Dudley, P. J. Stephenson, Y. Deslandes, G. K. Hamer, R. H. Marchessault, *J. Macromol. Sci. Polym. Rev.* **1983**, *23*, 187 – 216.
[106] H. Plaisantin, R. Pailler, A. Guette, G. Daudé, M. Pétraud, B. Barbe, M. Birot, J. P. Pillot, P. Olry, *Compos. Sci. Technol.* **2001**, *61*, 2063 – 2068.
[107] a) Q. Wu, D. Pan, *Text. Res. J.* **2002**, *72*, 405 – 410; b) Q.-L. Wu, S.-Y. Gu, J.-H. Gong, D. Pan, *Synth. Met.* **2006**, *156*, 792 – 795.
[108] H. Zhang, L. Guo, H. Shao, X. Hu, *J. Appl. Polym. Sci.* **2006**, *99*, 65 – 74.
[109] S. Peng, H. Shao, X. Hu, *J. Appl. Polym. Sci.* **2003**, *90*, 1941 – 1947.
[110] J. K. Park, J. Y. Lee, Y. G. Won, D. H. Cho (Agency for Defence Development), US2010/0285223A1, **2010**.
[111] Sohim, "Rayon based carbon fibers": http://www.sohim.by/en/catalog/carbon, **2013**.
[112] L. P. Kobets, I. S. Deev, *Compos. Sci. Technol.* **1998**, *57*, 1571 – 1580.
[113] T. Fukuda, N. Ishizaki, S. Iwahori, M. Shimada (Toyobo Co. Ltd.), JP3969268, **1976**.
[114] M. Zhang, S. Zhu, H. Zeng, Y. Lu, *Angew. Makromol. Chem.* **1994**, *222*, 147 – 163.
[115] N. Shiraishi in *Lignin*, *Vol. 397* (Eds.: W. G. Glasser, S. Sarkanen), American Chemical Society, Washington, DC, **1989**, pp. 488 – 495.
[116] T. Aso, K. Koda, S. Kubo, T. Yamada, I. Nakajima, Y. Uraki, *J. Wood Chem. Technol.* **2013**, *33*, 286 – 298.
[117] a) H. Naegele, J. Pfitzer, E. Naegele, E. R. Inone, N. Eisenreich, W. Eckl, P. Eyerer, *Chemical Modification*, *Properties and Usage of Lignin*, Kluwer Academic/Plenum, **2002**, pp. 101 – 119; b) Y. Li, J. Mlynar, S. Sarkanen, *J. Polym. Sci. Part B* **1997**, *35*, 1899 – 1910; c) H. Naegele, N. Eisenreich, J. Pfitzer, P. Elsner, E. Inone, W. Eckl, P. Eyerer (Fraunhofer-Gesellschaft zur Foerderung der Angewandten Forschung e.V., Germany.), DE19852029A1, **2000**; d) H. Naegele, P. Elsner, J. Pfitzer, W. Eckl, P. Eyerer, N. Eisenreich (Fraunhofer-Gesellschaft zur Foerderung der Angewandten Forschung e.V., Germany.), DE19852033A1, **2000**.
[118] P. M. Cook, T. Sellers in *Lignin*, *Vol. 397* (Eds.: W. G. Glasser, S. Sarkanen, American Chemical Society, Washington, DC, **1989**, pp. 324 – 333.
[119] W. Thielemans, E. Can, S. S. Morye, R. P. Wool, *J. Appl. Polym. Sci.* **2002**, *83*, 323 – 331.
[120] P. Azadi, O. R. Inderwildi, R. Farnood, D. A. King, *Renewable Sustainable Energy Rev.* **2013**, *21*, 506 – 523.
[121] J. H. Lora, W. G. Glasser, *J. Polym. Environ.* **2002**, *10*, 39 – 48.
[122] a) G. Gellerstedt, E. Sjoeholm, I. Brodin, *Open Agric. J.* **2010**, *4*, 119 – 124; b) D. A. Baker, N. C. Gallego, F. S. Baker, *J. Appl. Polym. Sci.* **2012**, *124*, 227 – 234.
[123] a) C. D. Warren, "Future Lower Cost Carbon Fiber for Autos: International Scale-up & What is needed": http://www.speautomotive.com/SPEA_CD/SPEA2008/pdf/k/K2.pdf, **2008**; b) C. D. Warren, F. L. Paulauskas, F. S. Baker, C. C. Eberle, A. Naskar, *SAMPE J.* **2009**, *45*, 24 – 36.
[124] S. Das, *Int. J. Life Cycle Assess.* **2011**, *16*, 268 – 282.
[125] a) F. S. Baker (UT-Battelle, LLC), US20070142225A1, **2007**; b) S. Kubo, T. Yoshida, J. F. Kadla, *J. Wood Chem. Technol.* **2007**, *27*, 257 – 271; c) Q. Shen, T. Zhang, W.-X. Zhang, S. Chen, M. Mezgebe, *J. Appl. Polym. Sci.* **2011**, *121*, 989 – 994; d) K. Babel, K. Jurewicz, *Carbon* **2008**, *46*, 1948 – 1956.
[126] S. Otani, Y. Fukuoka, K. Sasaki (Nippon Kayaku Co., Ltd.), US3461082, **1969**.
[127] Y. Fukuoka, *Jpn. Chem. Q.* **1969**, *5*, 63 – 66.
[128] S. Mikawa, *Chem. Econ. Eng. Rev.* **1970**, *2*, 43 – 46.
[129] A. M. Gould (G. B. Tools and Components Exports Ltd.), GB1358164A, **1974**.
[130] a) M. Mansmann (Farbenfabriken Bayer AG), DE2118488A, **1972**; b) M. Mansmann (Bayer AG), US 3723609, **1973**.
[131] a) K. Sudo, K. Shimizu (Forestry Experiment Station), JP62110922A, **1987**; b) K. Sudo, K. Shimizu, *J. Appl. Polym. Sci.* **1992**, *44*, 127 – 134.
[132] a) K. Sudo, K. Shimizu, N. Nakashima, A. Yokoyama, *J. Appl. Polym. Sci.* **1993**, *48*, 1485 – 1491; b) K. Sudo, K. Shimizu (Forestry and Forest Products Research Institute, Ministry of Agriculture, Forestry and Fisheries), US5344921, **1993**.
[133] Y. Uraki, S. Kubo, N. Nigo, Y. Sano, T. Sasaya, *Holzforschung* **1995**, *49*, 343 – 350.
[134] a) Y. Uraki, S. Kubo, H. Kurakami, Y. Sano, *Holzforschung* **1997**, *51*, 188 – 192; b) Y. Uraki, A. Nakatani, S. Kubo, Y. Sano, *J. Wood Sci.* **2001**, *47*, 465 – 469.
[135] S. Kubo, Y. Uraki, Y. Sano, *Carbon* **1998**, *36*, 1119 – 1124.
[136] A. L. Compere, W. L. Griffith, C. F. Leitten, Jr., J. T. Shaffer, *Int. SAMPE Tech. Conf.* **2001**, 1306 – 1314.
[137] a) J. F. Kadla, S. Kubo, R. A. Venditti, R. D. Gilbert, A. L. Compere, W. Griffith, *Carbon* **2002**, *40*, 2913 – 2920; b) J. F. Kadla, S. Kubo, R. D. Gilbert, R. A. Venditti, *Chemical Modification*, *Properties*, *and Usage of Lignin*, Kluwer Academic/Plenum, **2002**, p. 121.
[138] J. F. Kadla, S. Kubo, R. A. Venditti, R. D. Gilbert, *J. Appl. Polym. Sci.* **2002**, *85*, 1353 – 1355.
[139] J. F. Kadla, R. D. Gilbert, R. A. Venditti, S. Kubo (North Carolina State University), US20030212157A1, **2003**.
[140] S. Kubo, J. F. Kadla, *Biomacromolecules* **2003**, *4*, 561 – 567.
[141] T. Tanigami, L.-H. Zhu, K. Yamaura, S. Matsuzawa, *Sen'i Gakkaishi* **1994**, *50*, 53 – 61.

[142] a) S. Kubo, R. D. Gilbert, J. F. Kadla, *Natural Fibers, Biopolymers, and Biocomposites* (Eds.: A. K. Mohanty, M. Misra, L. T. Drzal), CRC, Boca Raton, **2005**, pp. 671 – 697; b) J. F. Kadla, S. Kubo, *Compos. Part A* **2004**, *35*, 395 – 400.

[143] a) S. Kubo, J. F. Kadla, *Macromolecules* **2004**, *37*, 6904 – 6911; b) S. Kubo, J. F. Kadla, *J. Appl. Polym. Sci.* **2005**, *98*, 1437 – 1444.

[144] S. Kubo, J. F. Kadla, *J. Polym. Environ.* **2005**, *13*, 97 – 105.

[145] A. L. Compere, W. L. Griffith, C. F. Leitten, Jr., S. Petrovan, *SAMPE Conf. Proc.* **2004**, 2246 – 2254.

[146] A. L. Compere, "Evaluation of Lignin from Alkaline-Pulped Hardwood Black Liquor": http://www.ornl.gov/info/reports/2005/3445605475900.pdf, **2005**.

[147] R. C. Eckert (Weyerhaeuser Company), WO 2009/002784 A1, **2008**.

[148] T. L. White, F. L. Paulauskas, T. S. Bigelow (UT-Battelle, LLC), US7824495B1, **2010**.

[149] a) N. C. Gallego, D. A. Baker, F. S. Baker, *SAMPE Conf. Proc.* **2009**, 1 – 6; b) F. S. Baker, "Low Cost Carbon Fiber from Renewable Resources": http://www1.eere.energy.gov/vehiclesandfuels/pdfs/merit_review_2010/lightweight_materials/lm005_baker_2010_o.pdf, **2010**.

[150] a) D. A. Baker, N. C. Gallego, F. S. Baker, "Carbon Fiber Production from a Kraft Hardwood Lignin": http://www.thefibersociety.org/httpdocs/Assets/Past_Meetings/BooksOfAbstracts/2008_Fall_Abstracts.pdf, **2008**; b) D. A. Baker, D. P. Harper, J. J. Bozell, "Rapid Manufacture of Carbon Fiber from Organosolv Lignins": http://www.thefibersociety.org/httpdocs/Assets/Past_Meetings/BooksOfAbstracts/2011_Fall_Abstracts.pdf, **2011**.

[151] F. S. Baker, N. C. Gallego, D. A. Baker, *SAMPE Conf. Proc.* **2010**, 1 – 16.

[152] D. A. Baker, F. S. Baker, N. C. Gallego, "Thermal Engineering of Lignin for Low-cost Production of Carbon Fiber": http://www.thefibersociety.org/httpdocs/Assets/Past_Meetings/BooksOfAbstracts/2009_Fall_Abstracts.pdf, **2009**.

[153] F. S. Baker, D. A. Baker, P. A. Menchhofer (UT-Battelle, LLC), US20110285049A1, **2011**.

[154] C. Eberle, "Carbon Fiber From Lignin": http://www.cfcomposites.org/PDF/Breakout_Cliff.pdf, **2012**.

[155] D. A. Baker, D. P. Harper, T. G. Rials, "Carbon Fiber from Extracted Commercial Softwood Lignin": http://www.thefibersociety.org/httpdocs/Assets/Past_Meetings/BooksOfAbstracts/2012_Fall_Abstracts.pdf, **2012**.

[156] a) B. Wohlmann, M. Woelki, A. Ebert, G. Engelmann, H.-P. Fink (Toho Tenax Europe GmbH; Fraunhofer-Gesellschaft zur Foerderung der Angewandten Forschung e.V.), WO2010081775A1, **2010**; b) A. Berlin (Lignol Innovations Ltd.), WO2011097721A1, **2011**.

[157] B. Wohlmann, M. Woelki, S. Stuesgen (Toho Tenax Europe GmbH), WO2012038259A1, **2012**.

[158] J. Luo, J. Genco, B. Cole, R. Fort, *BioResources* **2011**, *6*, 4566 – 4593.

[159] W. Qin, J. F. Kadla, *J. Appl. Polym. Sci.* **2012**, *126*, 203 – 212.

[160] W. Qin, J. F. Kadla, *Ind. Eng. Chem. Res.* **2011**, *50*, 12548 – 12555.

[161] O. Sevastyanova, W. Qin, J. F. Kadla, *J. Appl. Polym. Sci.* **2010**, *117*, 2877 – 2881.

[162] a) E. Sjoeholm, G. Gellerstedt, R. Drougge, I. Brodin (Innventia AB; Nordstroem, Ylva), WO2012112108A1, **2012**; b) Y. Nordström, I. Norberg, E. Sjoeholm, R. Drougge, *J. Appl. Polym. Sci.* **2013**, *129*, 1274 – 1279.

[163] Y. Nordström, Ph.D. thesis, Luleå University of Technology (SE), **2012**.

[164] A. Awal, M. Sain, *J. Appl. Polym. Sci.* **2013**, *129*, 2765 – 2771.

[165] M. J. Prauchner, V. M. D. Pasa, C. Otani, S. Otani, S. M. C. de Menezes, *J. Appl. Polym. Sci.* **2004**, *91*, 1604 – 1611.

[166] M. J. Prauchner, V. M. D. Pasa, S. Otani, C. Otani, *Carbon* **2005**, *43*, 591 – 597.

[167] a) I. Brodin, E. Sjoeholm, G. Gellerstedt, *Holzforschung* **2009**, *63*, 290 – 297; b) A. L. Compere, W. L. Griffith, *Biofuels, Vol. 581* (Ed.: J. R. Mielenz), Humana, New York, **2009**, pp. 185 – 212.

[168] a) S. E. Harton, S. V. Pingali, G. A. Nunnery, D. A. Baker, S. H. Walker, D. C. Muddiman, T. Koga, T. G. Rials, V. S. Urban, P. Langan, *ACS Macro Lett.* **2012**, *1*, 568 – 573; b) Y. Uraki, Y. Sugiyama, K. Koda, S. Kubo, T. Kishimoto, J. F. Kadla, *Biomacromolecules* **2012**, *13*, 867 – 872; Biomacromolecules; c) A. K. Sangha, L. Petridis, J. C. Smith, A. Ziebell, J. M. Parks, *Environ. Prog. Sustainable Energy* **2012**, *31*, 47 – 54; d) L. Petridis, R. Schulz, J. C. Smith, *J. Am. Chem. Soc.* **2011**, *133*, 20277 – 20287.

[169] D. K. Seo, J. P. Jeun, H. B. Kim, P. H. Kang, *Rev. Adv. Mater. Sci.* **2011**, *28*, 31 – 34.

[170] a) P. J. Bissett, C. W. Herriott (Weyerhaeuser NR Company), US20120003471A1, **2012**; b) S. P. Maradur, C. H. Kim, S. Y. Kim, B.-H. Kim, W. C. Kim, K. S. Yang, *Synth. Met.* **2012**, *162*, 453 – 459; c) M. O. Seydibeyoglu, *J. Biomed. Biotechnol.* **2012**, 1 – 8; d) G. Husman, "Development and Commercialization of a Novel Low-Cost Carbon Fiber": http://www1.eere.energy.gov/vehiclesandfuels/pdfs/merit_review_2012/lightweight_materials/lm048_husman_2012_o.pdf, **2012**.

[171] A. Lehmann, H. Ebeling, H.-P. H. Fink (Fraunhofer-Gesellschaft zur Förderung der Angewandten Forschung e.V.), EP2524980A1, **2012**.

[172] a) M. Lallave, J. Bedia, R. Ruiz-Rosas, J. Rodríguez-Mirasol, T. Cordero, J. C. Otero, M. Marquez, A. Barrero, I. G. Loscertales, *Adv. Mater.* **2007**, *19*, 4292 – 4296; b) R. Ruiz-Rosas, J. Bedia, M. Lallave, I. G. Loscertales, A. Barrero, J. Rodriguez-Mirasol, T. Cordero, *Carbon* **2010**, *48*, 696 – 705; c) I. Dallmeyer, F. Ko, J. F. Kadla, *J. Wood Chem. Technol.* **2010**, *30*, 315 – 329.

[173] O. Hosseinaei, D. A. Baker, "Electrospun Carbon Nanofibers from Kraft Lignin": http://www.thefibersociety.org/httpdocs/Assets/Past_Meetings/BooksOfAbstracts/2012_Fall_Abstracts.pdf, **2012**.

[174] D. J. Johnson, I. Tomizuka, *Plast. Polym. Conf. Suppl.* **1974**, *6*, 20 – 24.

[175] I. Tomizuka, D. J. Johnson, *Yogyo Kyokai Shi* **1978**, *86*, 186 – 192.

[176] V. Davé, A. Prasad, H. Marand, W. G. Glasser, *Polymer* **1993**, *34*, 3144 – 3154.

[177] J. Rodríguez-Mirasol, T. Cordero, J. J. Rodríguez, *Carbon* **1996**, *34*, 43 – 52.

[178] M. J. Prauchner, V. M. D. Pasa, N. D. S. Molhallem, C. Otani, S. Otani, L. C. Pardini, *Biomass Bioenergy* **2005**, *28*, 53 – 61.

[179] J. L. Braun, K. M. Holtman, J. F. Kadla, *Carbon* **2005**, *43*, 385 – 394.

[180] M. Foston, G. A. Nunnery, X. Meng, Q. Sun, F. S. Baker, A. Ragauskas, *Carbon* **2013**, *52*, 65 – 73.

[181] I. Brodin, M. Ernstsson, G. Gellerstedt, E. Sjoeholm, *Holzforschung* **2012**, *66*, 141 – 147.

[182] I. Norberg, Y. Nordstroem, R. Drougge, G. Gellerstedt, E. Sjoeholm, *J. Appl. Polym. Sci.* **2013**, *128*, 3824 – 3830.

[183] F. Villeurbanne, *J. Polym. Sci.* **1972**, *16*, 2991 – 3002.

[184] S. Horiki, J. Iseki, M. Minobe (Sumitomo Chemical Co.), US4070446, **1978**.

[185] J. J. Dunbar, G. C. Weedon, T. Y. T. Tam (Allied-Signal, Inc.), WO9203601A2, **1992**.

[186] a) D. Zhang, *Proc. Am. Soc. Compos. Tech. Conf.* **1992**, *7*, 249 – 257; b) S. G. Bhat, D. Zhang, *Miner. Met. Mater. Soc.* **1993**, 475 – 485; c) D. Zhang, S. G. Bhat, *Mater. Manuf. Processes* **1994**, *9*, 221 – 235; d) D. Zhang, Q. Sun, *Proc. Am. Soc. Compos. Tech. Conf.* **1999**, 995 – 1003.

[187] C. A. Leon y Leon, W. C. Schimpf, B. C. Hansen, C. W. Herren, A. Frame, P. W. Heatherley in *International SAMPE Technical Conference*, **2002**.
[188] M. A. Hunt, T. Saito, R. H. Brown, A. S. Kumbhar, A. K. Naskar, *Adv. Mater.* **2012**, *24*, 2386 – 2389.
[189] E. A. Boucher, R. N. Cooper, D. H. Everett, *Carbon* **1970**, *8*, 597 – 605.
[190] H. Yokota, A. Kobayashi, J. Horikawa, A. Miyashita (Sumitomo Chem. Co.), GB1406378, **1975**.
[191] A. Nagasaka, H. Ashitaka, Y. Kusuki, D. Oda, T. Yoshinaga (UBE Industries), US4131644, **1978**.
[192] a) H. Ashitaka, Y. Kusuki, S. Yamamoto, Y. Ogata, A. Nagasaka, *J. Appl. Polym. Sci.* **1984**, *29*, 2763 – 2776; b) H. Ashitaka, H. Ishikawa, H. Ueno, A. Nagasaka, *J. Polym. Sci. Polym. Chem. Ed.* **1983**, *21*, 1853 – 1860.
[193] a) A. Shindo, R. Fujii, I. Souma (Agency of Industrial Science and Technologie, Tokyo), US 3427120, **1969**; b) M. Murakami (Research development Coorporation of Japan, Mitsushita Elec. Ind.), US 4876077, **1989**.
[194] a) K. Kawamura, G. M. Jenkins, *J. Mater. Sci.* **1970**, *5*, 262 – 267; b) K. Kawamura, G. M. Jenkins, *J. Mater. Sci.* **1972**, *7*, 1099 – 1112.
[195] J. Economy, R. Y. Lin, *Appl. Polym. Symp.* **1976**, *29*, 199 – 211.
[196] J. G. Santangelo (Celanese Corp.), US 3547584, **1970**.
[197] H. Jiang, P. Desai, S. Kumar, A. S. Abhiraman, *Carbon* **1991**, *29*, 635 – 644.
[198] a) J. A. Newell, D. K. Rogers, D. D. Edie, C. C. Fain, *Carbon* **1994**, *32*, 651 – 658; b) S. Purkayashta, P. Pandian, K. B. Dinesh, R. Shinde, N. R. Yelle, N. B. Timble, *Man-Made Fiber Year Book* **2010**, 25 – 27.
[199] J. A. Newell, D. D. Edie, *Carbon* **1996**, *34*, 551 – 560.
[200] J. A. Newell, D. D. Edie, E. L. Fuller, Jr., *J. Appl. Polym. Sci.* **1996**, *60*, 825 – 832.
[201] a) Y. Kaburagi, K. Yokoi, A. Yoshida, Y. Hishiyama, *Tanso* **2005**, *217*, 111 – 114; b) M. B. Vázquez-Santos, A. Martínez-Alonso, J. M. D. Tascón, J.-N. Rouzaud, E. Geissler, K. László, *Carbon* **2011**, *49*, 2960 – 2970.
[202] M. B. Vázquez-Santos, A. Martínez-Alonso, J. M. D. Tascón, J.-N. Rouzaud, C. rochas, E. Geissler, K. László, *J. Alloys Compd.* **2012**, *536*, S464 – S468.
[203] M. B. Vázquez-Santos, A. Martínez-Alonso, J. M. D. Tascón, *J. Anal. Appl. Pyrolysis* **2012**, *95*, 68 – 74.
[204] M. B. Vázquez-Santos, F. Suárez-García, A. Martínez-Alonso, J. M. D. Tascón, *Langmuir* **2012**, *28*, 5850 – 5860.
[205] a) M. B. Vázquez-Santos, M. Beatriz, A. Martínez-Alonso, J. M. D. Tascón, *Carbon* **2008**, *46*, 825 – 828; b) M. B. Vázquez-Santos, A. Castro-Muñiz, A. Martínez-Alonso, J. M. D. Tascón, *Microporous Mesoporous Mater.* **2008**, *116*, 622 – 626.
[206] a) D. E. Sliva, Q. G. Selley (General Electrics Co.), US3928516, **1975**; b) C. Krutchen (General Electrics Co.), US3852235, **1974**.
[207] A. Mavinkurve, S. Visser, A. J. Pennings, *Carbon* **1995**, *33*, 757 – 761.
[208] H. M. Ezekiel, R. G. Spain, *J. Polym. Sci. Part C* **1967**, *19*, 249 – 265.
[209] M. S. Dresselhaus, G. Dresselhaus, K. Sugihara, I. L. Spain, H. A. Goldberg, *Graphite Fibers and Filaments*, Springer, Berlin/Heidelberg, **1988**.
[210] W. P. Hoffman, W. C. Hurley, P. M. Liu, T. W. Owens, *J. Mater. Res.* **1991**, *6*, 1685 – 1694.
[211] G. M. Jenkins, K. Kawamura, *Polymeric Carbons: Carbon Fibre, Glass and Char*, Cambridge University Press, New York, **1976**.
[212] E. Fitzer, *Makromol. Chem. Rapid Commun.* **1982**, *3*, 357 – 364.
[213] E. Fitzer, *Carbon* **1989**, *27*, 621 – 645.
[214] a) E. Fitzer, *Angew. Chem.* **1980**, *92*, 375 – 386; *Angew. Chem. Int. Ed. Engl.* **1980**, *19*, 375 – 385; b) H. Böder, E. Fitzer, *Naturwissenschaften* **1970**, *57*, 29 – 36.
[215] S. C. Bennett, Ph.D. thesis, University of Leeds (UK), http://etheses.whiterose.ac.uk/1034/1/uk_bl_ethos_518543.pdf, **1976**.
[216] A. Takaku, M. Shioya, *J. Mater. Sci.* **1990**, *25*, 4873 – 4879.
[217] S. C. Bennett, D. J. Johnson, *Carbon* **1979**, *17*, 25 – 39.
[218] a) L. Chen, Y. Hernandez, X. Feng, K. Müllen, *Angew. Chem.* **2012**, *124*, 7758 – 7773; *Angew. Chem. Int. Ed.* **2012**, *51*, 7640 – 7654; b) K. K. Baldridge, J. S. Siegel, *Angew. Chem.* **2013**, *125*, 5546 – 5548; *Angew. Chem. Int. Ed.* **2013**, *52*, 5436 – 5438; c) A. H. C. Neto, F. Guinea, N. M. R. Peres, K. S. Novoselov, A. K. Geim, *Rev. Mod. Phys.* **2009**, *81*, 109; d) A. C. Ferrari, J. C. Meyer, V. Scardaci, C. Casiraghi, M. Lazzeri, F. Mauri, S. Piscanec, D. Jiang, K. S. Novoselov, S. Rioth, A. K. Geim, *Phys. Rev. Lett.* **2006**, *97*, 187401; e) A. K. Geim, K. S. Novoselov, *Nat. Mater.* **2007**, *6*, 183; f) J. Wu, W. Pisula, K. Müllen, *Chem. Rev.* **2007**, *107*, 718 – 747; g) S. Yang, R. E. Bachman, X. Feng, K. Müllen, *Acc. Chem. Res.* **2013**, *46*, 116 – 128; h) S. B. Yang, X. L. Feng, L. Wang, K. Tang, J. Maier, K. Müllen, *Angew. Chem.* **2010**, *122*, 4905 – 4909; *Angew. Chem. Int. Ed.* **2010**, *49*, 4795 – 4799; i) L. Zhi, K. Müllen, *J. Mater. Chem.* **2008**, *18*, 1472; j) Y. Zhu, D. K. James, J. M. Tour, *Adv. Mater.* **2012**, *24*, 4924 – 4955.
[219] E. Fitzer, F. Rozploch, *Carbon* **1988**, *26*, 594 – 595.
[220] W. Ruland, *J. Polym. Sci. Part C* **1969**,*28*, 143 – 151.
[221] A. Fourdeaux, R. Perret, W. Ruland, in Proceedings of the Internantional Conference on Carbon Fibres, their Composites and Applications: Plastics and Polymer Conf. Supplement, **1971**, 57 – 67.
[222] D. J. Johnson, *J. Phys. D* **1987**, *20*, 286 – 291.
[223] L. Fischer, W. Ruland, *Colloid Polym. Sci.* **1980**, *258*, 917 – 922.
[224] a) F. Tuinstra, J. L. Koenig, *J. Chem. Phys.* **1970**, *53*, 1126; b) R. J. Nemanich, S. A. Solin, *Solid State Commun.* **1977**, *23*, 417 – 420; c) R. Tsu, H. J. Gonzalez, C. I. Hernandez, *Solid State Commun.* **1978**, *27*, 507 – 510.
[225] D. Crawford, D. J. Johnson, *J. Microsc.* **1971**, *94*, 51 – 62.
[226] F. R. Barnett, M. K. Norr in International Conference on Carbon Fibres, their Composites and Applications, **1974**.
[227] S. C. Bennett, D. J. Johnson in 5th London Internantional Carbon and Graphite Conference, London, **1978**.